

## River erosion, landslides and slope development in Göta River

A study based on bathymetric data and general limit equilibrium slope stability analysis

*Master of Science Thesis in the Master's Programme Geo and Water Engineering*

**DANIEL MILLET**

Department of Civil and Environmental Engineering  
Division of GeoEngineering

*Geotechnical Engineering Research Group*

CHALMERS UNIVERSITY OF TECHNOLOGY

Göteborg, Sweden 2011

Master's Thesis 2011:131



# River erosion, landslides and slope development in Göta River

A study based on bathymetric data and general limit equilibrium  
slope stability analysis

*Master of Science Thesis in the Master's Programme Geo and Water Engineering*

DANIEL MILLET

Department of Civil and Environmental Engineering

*Division of GeoEngineering*

*Geotechnical Engineering Research Group*

CHALMERS UNIVERSITY OF TECHNOLOGY

Göteborg, Sweden 2011

River erosion, landslides and slope development in Göta River

A study based on bathymetric data and general limit equilibrium slope stability analysis

*Master of Science Thesis in the Master's Programme Geo and Water Engineering*

DANIEL MILLET

© DANIEL MILLET 2011

Examensarbete / Institutionen för bygg- och miljöteknik,  
Chalmers tekniska högskola 2011:131

Department of Civil and Environmental Engineering  
Division of GeoEngineering  
Geotechnical Engineering Research Group  
Chalmers University of Technology  
SE-412 96 Göteborg  
Sweden  
Telephone: + 46 (0)31-772 1000

Cover:

Topographic data generated in ArcGIS of Göta River close to Ekbacken, and slope profile Ekbacken\_4 based on bathymetric data from 2003 and 2009, see Chapter 6 for further information.

Chalmers Reproservice / Department of Civil and Environmental Engineering  
Göteborg, Sweden 2010

River erosion, landslides and slope development in Göta River  
A study based on bathymetric data and general limit equilibrium slope stability  
analysis

*Master of Science Thesis in the Master's Programme Geo and Water Engineering*

DANIEL MILLET

Department of Civil and Environmental Engineering

Division of GeoEngineering

Geotechnical Engineering Research Group

Chalmers University of Technology

## ABSTRACT

There can be many different triggers and combinations of factors that set off a clay landslide. One of those factors is river erosion, which through the removal of soil material causes changes in the stress distribution in the adjoining soil. These changes might be large enough to unsettle the static equilibrium that makes a slope stable, and subsequently cause a slope failure and landslide. Even though river erosion generally is regarded as a major factor when it comes to landslides along Göta River, relatively little is known about how the river erosion more precisely affects the geometry of a slope profile, and how these geometric changes affect the slope stability factor of safety. This thesis examines the characteristics of the river erosion in Göta River, including estimations of erosion rates over time, by analysing and comparing geophysical and bathymetric data from 2003 and 2009. The bathymetric data has also been used in conjunction with a topographic land model in a geographical information system to study and classify different types of slope geometries along the river. Based on previous geotechnical field investigations at two locations along the river, a couple of different slopes were modelled in the geotechnical software Slope/W to determine how the slope stability factor of safety varies with the established characteristic erosion in this thesis. The method used in the slope stability calculations was the general limit equilibrium (GLE) method. The different elements in this thesis span many disciplines within earth science and engineering. Hence the result can be seen as an example of how different data, methods (such as the use of geographical information systems and geophysical data) and disciplines have been combined to produce a general theory on the geomorphologic development of slopes in Göta River, and in particular how the river erosion affects the geometry and stability of the slopes in the river. One of the more specific results in this thesis show how river erosion in Göta River mainly occurs along trenches on the river bottom and along the slope toe, and that the erosion is localized and unevenly distributed and seemingly not a direct function of the hydraulic shear stress caused by the water flow. This is in contrast to some previous notions based on turbidity measurements where the river erosion has been thought of as a more uniform process occurring all over the river bed, which leads both to over- and underestimation of erosion rates depending on the location.

Key words: Erosion, sediment transport, landslides, quick clay, slope stability, river geomorphology, Göta River (Göta Älv), general limit equilibrium method, GIS (geographical information systems), DEM (digital elevation model), river bathymetry, side-scan, backscatter, geohazards



# Contents

ABSTRACT	I
CONTENTS	III
PREFACE	VI
NOTATIONS	VII
ABBREVIATIONS AND ACCRONYMS	VIII
1 INTRODUCTION	1
1.1 Project background	1
1.2 Purpose	1
1.3 Method	2
1.4 Limitations	2
2 EROSION AND SEDIMENT TRANSPORT	3
2.1 River erosion	3
2.1.1 The main erosion processes in rivers	4
3 SLOPE STABILITY ANALYSIS WITH SLOPE/W	5
3.1 Basic static principles	5
3.2 Basic statics applied on geotechnical slope stability	6
3.2.1 General Limit Equilibrium method	7
3.2.2 Early methods	10
3.2.3 Morgenstern-Price	10
3.3 Soil strength models	10
3.3.1 Drained analysis	11
3.3.2 Undrained analysis	11
3.3.3 Combined analysis	12
3.4 Concluding remarks	13
3.4.1 The factor of safety	13
4 GÖTA RIVER	15
4.1 Geology	17
4.2 Morphology	18
4.2.1 Wave induced erosion and river banks	19
4.3 Erosion of river bottom	21
4.3.1 Summary of Göta River geology and morphology	22
5 TOPOGRAPHIC, GEOPHYSICAL AND HYDRAULIC DATA USED IN STUDY	23
5.1 Topographic and bathymetric data	23

5.1.1	The 2003-2009 bathymetric dataset	25
5.2	Additional sonar data	26
5.2.1	Backscatter	26
5.2.2	Side scan	27
5.3	Hydraulic shear stress data	28
5.4	Comments	29
6	OBSERVATIONS OF EROSION AND SEDIMENT TRANSPORT PROCESSES AND PATTERNS	30
6.1	Sand dunes and ripples along the bottom	30
6.2	Propeller induced bottom erosion	31
6.3	Possible subaquatic landslide at Ekbacken	32
7	STUDY OF SLOPES	35
7.1	Sampling and extraction of slope profiles	35
7.2	Analysis and classification of slope profiles	36
7.2.1	Trollhättan – Lilla Edet	36
7.2.2	Lilla Edet - Kungälv	39
7.3	Connection between classes and river geometry	40
8	CASE STUDY OF SLOPES AND EROSION AT OLD LANDSLIDES	42
8.1	Agnesberg	42
8.1.1	Slope profiles	42
	48	
8.1.2	Geotechnical conditions and parameters	49
8.1.3	Erosion	50
8.2	Ballabo	58
8.2.1	Slope profiles	58
	61	
8.2.2	Geotechnical conditions and parameters	61
8.2.3	Erosion	63
9	RESULTS FROM SLOPE STABILITY CALCULATIONS	68
9.1	Agnesberg slopes	68
9.1.1	Comments	69
9.2	Ballabo slopes	71
9.2.1	Ballabo South: erosion of assumed old landslide mass	71
9.2.2	Ballabo South: current erosion	77
9.2.3	Ballabo North	79
9.2.4	Comments	80
10	FINAL CONCLUSIONS AND SUMMARY OF RESULTS	81
10.1	Characterization of erosion	81



10.2	Quantification of erosion	83
10.3	Erosion and the slope stability factor of safety	84
10.4	Slope profiles and geomorphology	86
10.4.1	General theory on development of slope profiles	87
10.5	Comparison to similar study in Italy 2009	89
11	DISCUSSION	91
11.1	Erosion and GIS	91
11.2	Slope stability calculations	92
11.3	Preventive measures	92
11.4	Quantification of erosion	93
12	REFERENCES	95

## Preface

This project has been carried out at the Swedish Geotechnical Institute (SGI) in Gothenburg, Sweden, during the fall semester of 2010 and spring semester of 2011. Supervisor for the project has been Victoria Svahn, head of Landslide Risk Engineering and Head of Research Council at SGI, and PhD candidate at Chalmers University of Technology, Department of Civil and Environmental Engineering, Division of GeoEngineering. The project has been carried out as a desktop study, involving data from previous geotechnical field investigations and multibeam echo soundings in Göta River. This project can be regarded as part of Victoria's and Prof. Göran Sällfors's general research on slope stability, as well as a part of the broader research and investigations carried out by SGI within the frame of the Göta River Project. A project which aims to map and assess the risks connected to landslides in the Göta River Valley in the light of future climate change.

I would like to thank Victoria and Göran for presenting me with this opportunity and especially Victoria for showing great patience throughout the project and providing me with all the tools and resources necessary to carry out the work and deepening my knowledge within geotechnics and slope stability. I would also like to thank Mats Öberg (SGI) for helping me with the management of the large amount of GIS data used in this study, as well as Håkan Persson (SGI) for the joint work analysing the data and the general discussions and input of knowledge on issues related to erosion. I'm also very appreciative of all the staff at the SGI Gothenburg office for accommodating me and making me feel very at home for the duration of the work!

My final thanks go out to my family and dear friend Sara Persson who has given me tremendous support in many ways throughout my studies at Chalmers, particularly in the final stages helping me finish this master thesis!

Gothenburg, September 2011

Daniel Millet

## NOTATIONS

$A$	Cross sectional area [ $\text{m}^2$ ]
$F$	Factor of safety
$F_k$	Factor of safety for combined analysis
$F_c$	Factor of safety for undrained analysis
$F_F$	Force factor of safety
$F_M$	Moment factor of safety
$F_f$	Friction force [N]
$F_n$	Normal force [N]
$F_p$	Force along plane [N]
$S_m$	Shear force mobilized at the base of each slice [Pa]
$c$	Cohesion [Pa]
$c'$	Effective cohesion [Pa]
$m$	Mass [kg]
$g$	Gravitational acceleration coefficient [ $\text{m/s}^2$ ]
$s$	Shear strength [Pa]
$\tau_{mob}$	Mobilized shear stress [Pa]
$\tau_f$	Available shear strength due to friction [Pa]
$\tau_{fu}$	Undrained shear strength [Pa]
$\theta$	Angle of plane [ $^\circ$ ]
$\mu$	Coefficient of friction
$\gamma$	Unit weight of soil [ $\text{N/m}^3$ ]
$\theta'$	Effective angle of internal friction [ $^\circ$ ]

## ABBREVIATIONS AND ACCRONYMS

DEM	Digital Elevation Model
GIS	Geographical Information System
GLE	General Limit Equilibrium
GWL	Ground Water Level
LIDAR	Light Detection and Ranging
MMA	Marin Miljöanalys AB
SGI	Swedish Geotechnical Institute
SGU	Swedish Geological Survey
SMHI	Swedish Meteorological and Hydrological Institute





# 1 Introduction

This master thesis investigates a matter that is very closely linked to, and often the cause of landslides; erosion. Erosion is one of the most important geological processes that shape the surface of the earth. There are many types of erosion; however, the focus of this work is on erosion caused by rivers. Erosion of river banks has been documented and researched for a long time. It is also clear that erosion of river banks often is the cause of both small and major landslides. There is however a lack of knowledge of how the erosion of the subaquatic slopes of the river bank looks like and how this erosion should be modelled, and in turn, how this erosion relates to a decrease of slope stability. This thesis is an attempt to fill this gap through literature studies, characterization of slopes and erosion and slope stability case studies along sections of Göta River in western Sweden.

## 1.1 Project background

The county of Västra Götaland in Sweden, which contains the Göta River Valley is the most landslide prone area in Sweden. The earliest documented landslide in Göta River occurred around the year 1150. This was a massive landslide covering a land area of about 60 hectares, reaching back over 1.5 km from the shoreline. Since then about 10 other landslides of relatively large proportions have been documented, and in the last 60 years a total of 15 people have been killed due to landslides. In addition to these large documented landslides, there are many yearly occurrences of smaller landslides of different character in and close to the river (Göta älvs Vattenvårdförbund, 2006).

Since the 1960s, the government agency SGI (Swedish Geotechnical Institute) has had the responsibility to oversee and monitor landslide hazards and risks in Sweden. Naturally, the Göta River Valley has been central in much of this work, and the SGI office in Gothenburg as well as the Geotechnical Research Group at Chalmers University of Technology has devoted a lot of time investigating and studying the behaviour of the clays in this region.

In 2009 SGI was commissioned with the task to perform an extensive mapping and landslide risk assessment of the entire Göta River. This was in part prompted because of possibilities of a larger water discharge and runoff into the river due to climate change (SGI, 2011). This thesis project is closely linked with, and touches on many of the same topics and areas as the Göta River commission. It was however initiated as a part of research conducted at the division of GeoEngineering at Chalmers University of Technology.

## 1.2 Purpose

The aim of this thesis was to carry out a study and analysis of slope profiles in Göta River and characterize and analyse the river erosion in Göta River based on multibeam echo soundings carried out in the river in the years of 2003 and 2009. The main purpose for this was to model a number of slopes in the geotechnical software Slope/W and apply the characterized erosion as a geometric parameter, and thereby being able to express the slope stability factor of safety as a function of the case

specific erosion. All of this would then result in a discussion and theory regarding the relationship between erosion, landslides and slope development in Göta River.

### **1.3 Method**

This thesis has been performed as a desktop study, carried out at the office of the Swedish Geotechnical Institute in Gothenburg, and in part in cooperation with the staff at this office. In addition to literature studies the analysis work related to the study of slope profiles and erosion has been carried out using the geographical information system suite ArcView. A variety of large datasets have been used for this, mostly geophysical multibeam data, using the internal databases at the Swedish Geotechnical Institute. For the evaluations of slope stability the software Slope/W 2007 has been used and the geotechnical parameters used to model the slopes came from of pre-existing geotechnical field investigations along Göta River.

### **1.4 Limitations**

All of the investigations and studies carried out in this thesis are based around studying Göta River in Sweden. Therefore this work has to be viewed within the geological context of this area, which can be described as deep glacial and postglacial cohesive soils deposited in a rift valley, in which Göta River has formed as a result of the glacial rebound throughout the last 12 000 years.

As the target group of this thesis is assumed to have basic knowledge of geotechnical engineering, the thesis does not contain any in-depth explanation of- or theory on basic geotechnical concepts and parameters. Also, ArcView has been used extensively in this thesis, but the thesis does not contain any in-depth theory of geographical information systems in general. For more insight and knowledge on geographical information systems and geotechnical engineering the reader is advised to study basic literature and online resources available free of charge at [www.swedgeo.com](http://www.swedgeo.com) (Swedish Geotechnical Institute) and [www.esri.com](http://www.esri.com) (Environmental Systems Research Institute, the software developer behind ArcView).



## 2 Erosion and sediment transport

The central theme in this study is the relationship between erosion and slope stability. The first two chapters of this thesis therefore presents some of the basics of erosion and sediment transport, as well as basics regarding slope stability and a more detailed description of the method used to calculate the slope stability factor of safety used in this thesis.

The term erosion can most simply be described as a process in which material is removed from the surface of the earth. This material is then transported and at some point deposited at another location. There are many different types of erosion processes, ranging from freeze and thaw erosion, chemical erosion such as the gradual dissolving of lime stone subjected to acids, human activities like farming to bioerosion caused by burrowing animals. The most important natural forces behind erosion are the forces created by wind and water, including ice, which are the main factors that have shaped the natural landscape around us. The erosion processes involving water and wind are a direct function of the kinetic energy and the shear force caused by the wind or water on a surface. The force of gravity can also be viewed as a main factor behind erosion. Something which of course is the main force acting on and driving a landslide, which in turn can be seen as one of the most dramatic forms of erosion which transports soil material from a higher to lower elevation.

### 2.1 River erosion

The focus of this thesis is of course on the erosion caused by the water in a river. The flowing water and surface waves in a river subjects the surrounding ground surfaces to several different types of eroding actions caused by the different types of movements of the water. Simply put, if the shear forces from the water becomes higher than the shear force that can be mobilized between the soil particles, the soil particles will begin to move. At low forces the particles are only rearranged, but if the forces are strong enough they are lifted by the water and transported as long as the forces of the current are strong enough. When the forces of the current aren't strong enough to carry the particles they are deposited on the river bed. In addition to the shear forces between the particles themselves the stability, or erosion resistance, of the soil particles depend on their density, shape and grading, compactness of the bottom material and the angle of the bottom surface. Most resistant to erosion are cohesion soils where the particles are hold together by electrochemical forces. Therefore, the formulas to describe the forces in play during erosion processes are different for friction and cohesive soils (Rankka and Rydell, 2005; Andersson et al, 2008). The so called *Hjulström's diagram* however, see Figure 1, very effectively shows the relationship between flow velocity, particle grain size and the transport state of the sediment. As seen in the diagram, the particle grain size that is most easily eroded is around 0.2-0.3 mm, which is fine sand. For grain sizes smaller than that, silt and clay, erosion requires a higher flow velocity to occur.

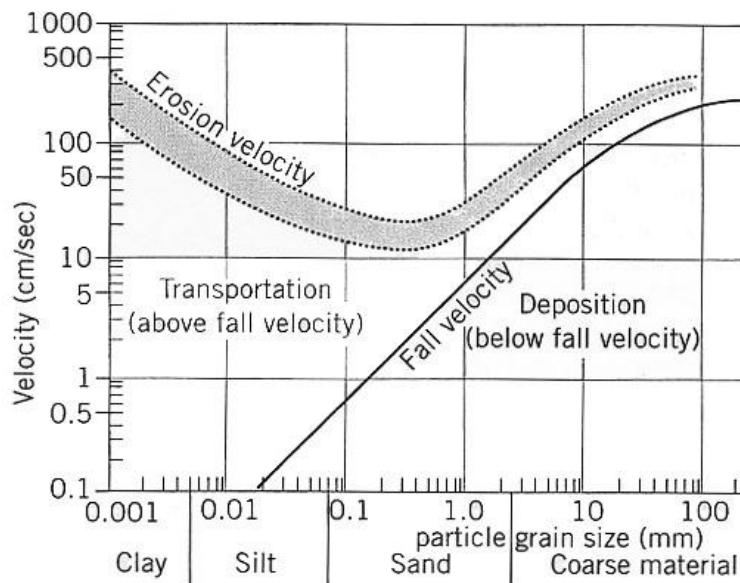


Figure 1 Hjulström's curve (Geography Department of Lord Wandsworth College, 2011).

### 2.1.1 The main erosion processes in rivers

The main types of natural river erosion and corresponding terms are described below:

- *Hydraulic, or fluvial, erosion*- the direct shear force from linear flowing water transport the soil particles. As described by Hjulström's diagram above.
- *Abrasion, or corassion*- particles transported along the river bed surface acts as a grinding material, often described as a sand papering action. This kind of action can also be caused by river ice moving along the river bank.
- *Attrition*- soil or rocks being moved along the river and colliding with other material, subsequently breaking into smaller pieces.
- *Evorsion, or pothole erosion*- which can be regarded as a combination of hydraulic erosion and corassion where rotating, whirling water or a vortex containing soil material or rocks grinds the bottom in a rotating and stationary action causing what can be described as potholes in the river bed.
- *Wave erosion*- erosion of river banks caused by water waves. These waves are most often caused by wind or ship traffic, but can for example also be caused by the release of water from dams etc.

(Jenssen and Tesaker, 2009; Lawrence, 1995)

The different interactions between rivers and surrounding soil, can of course be described in more complex ways, involving the physics of both solid and fluid mechanics. But overall the processes and terms described above are well sufficient for the scope of this thesis.

### 3 Slope stability analysis with Slope/W

The target group of this thesis is expected to have a general theoretical knowledge of geotechnical engineering and a basic knowledge of different soil parameters etc. This theoretical chapter will therefore only deal with the fundamentals of the actual slope stability analysis and the specific methods used in the software for the slope stability calculations in this thesis.

The software used in this study, Slope/W 2007, is part of a larger geotechnical, hydro geological and environmental engineering software suite called GeoStudio 2007. The basis of all the methods used in Slope/W is the general limit equilibrium method (GLE), which is a formulation brought forward by professor D.G Fredlund in the 1970's to collect all the existing methods of assessing slope stability in one theoretical basket. All of these methods are in turn based on the perhaps more well-known term "method of slices", referring to when you divide a potential sliding mass into slices for calculation of the stability of that mass.

#### 3.1 Basic static principles

The basic principle behind the method of slices for assessing the slope stability factor of safety is simple statics. The body situated on an incline in Figure 2 is subjected to gravity which gives a downward force of  $F_w = m \cdot g$ . Dividing  $F_w$  into a force normal to the plane and into a force parallel to the plane one gets  $F_n = m \cdot g \cdot \cos \theta$  and  $F_p = m \cdot g \cdot \sin \theta$ .

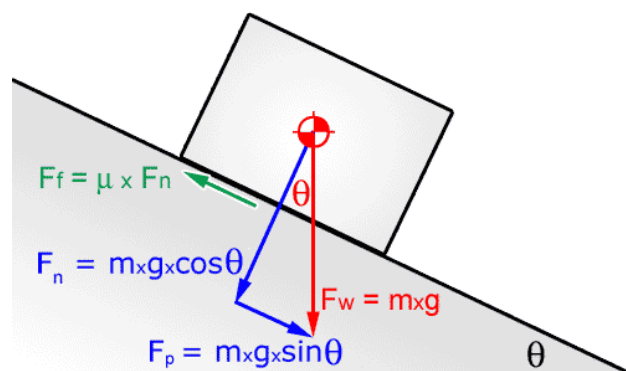


Figure 2 Sliding body with the mass  $m$  on a plane with inclination  $\theta$ .

In a general sense, friction is the force that converts the energy when two surfaces move relative to each other. In the case in Figure 2 friction is the force acting along and resisting the relative motion of the two solid surfaces between the plane and the body. The friction force is not a fundamental force itself, and is therefore found empirically depending on the materials involved and the type of friction. In this case above, dry friction between two solids, the friction force is defined as  $F_f = \mu \cdot F_n$  where the coefficient of friction  $\mu$  is an empirically determined property of the involved materials. Hence  $F_f$  is directly resisting the force  $F_p$  on the body. If the inclination of the plane,  $\theta$ , and coefficient of friction  $\mu$  is such that  $F_p$  is larger than  $F_f$ , then the body would slide down the plane.

Assigning an area  $A$  to the bottom surface of the body and dividing  $F_p$  with this area equals what is called the mobilized shear stress  $\tau_{mob}$ . Similarly dividing  $F_f$  with  $A$  gives the maximum shear stress available,  $\tau_f$ :

$$\tau_{mob} = \frac{F_p}{A} = \frac{m \cdot g \cdot \sin \theta}{A} \qquad \tau_f = \frac{F_f}{A} = \frac{\mu \cdot m \cdot g \cdot \cos \theta}{A} \qquad \left[ \frac{kg \cdot \frac{m}{s^2}}{m^2} = Pa \right]$$

By using the mobilized shear stress and the available shear strength the factor of safety can then be defined as:

$$F = \frac{\tau_f}{\tau_{mob}}$$

This means that the factor of safety is the ratio between available shear strength and the mobilized shear stress. When  $F = 1$ , the body in the case above will slide down the plane, and vice versa; when  $F > 1$  the friction will keep the body in place.

The factor of safety could of course in this case be directly calculated using the two forces parallel to the plane without converting them it into shear forces. The reason for converting them into shear forces is because of the relation to the strength of soil, which is expressed as shear strength.

Having knowledge about the coefficient of friction, the slope angle and the mass of the body in Figure 2 is sufficient to calculate the different forces, strengths and ultimately the factor of safety. The example is a simplistic figure which is statically determinable.

### 3.2 Basic statics applied on geotechnical slope stability

When it comes to soil slopes and their factor of safety, the basic principle is the same as in the previous example of a body on a sloping plane but the static situation and conditions naturally are not as simple.

First of all, the shape and geometry differs from the example in Figure 2. Real life slope stability problems usually does not consist of a box shaped soil body sliding along a plane. Although there might in theory exist such a case, or similar, involving soil and rock material it was early observed that most deep landslides in cohesive soils follow a circular slip surface, as opposed to the straight slip surface along the plane in Figure 2. This means that the angle  $\theta$  is not constant along the entire slip surface. In Figure 3 a conceptual 3D drawing of such a slip surface can be seen as a soil mass is sliding into a river, as is the case for landslides into Göta River.

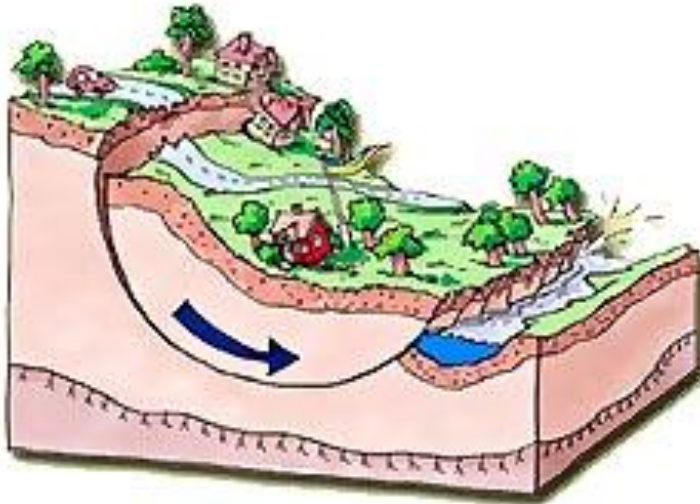


*Figure 3 Conceptual drawing of typical landslide with a circular slip surface on a river bank (SGI, 2011).*

Secondly, the material or soil properties along the slip surface are normally not constant along the slip surface. Analogues to the basic static example, one could imagine the coefficient of friction not being constant along the slip surface. As neither the angle  $\theta$  nor the material properties are constant one cannot directly apply the equations in the example for a whole slip surface.

A third issue is of course that the slip surface in soil is unknown, and solving a slope stability problem is basically an iterative process by which one has to calculate several slip surfaces. This is of course not a big problem when using software such as Slope/W which can process thousands of slip surfaces in a matter of seconds on a normal computer of today's standard. There are also numerous methods in Slope/W for specifying and defining different slip surfaces.

### **3.2.1 General Limit Equilibrium method**

A natural way to deal with these issues to be able to calculate a factor of safety, is to divide the slip surface into slices, where slip surface angle and soil properties are constant for each slice.

Some basic assumptions for the use of this approach are:

- The slip and failure surface is assumed rather than determined by analysis.
- A plain strain 2D condition is assumed, meaning 3D effects are ignored.
- The sliding mass is assumed to move as a rigid block, i.e. movements are only taking place along the slip surface itself.
- The shear stress is uniformly mobilized along the slip surface at the same time.

Together with the method of slices these assumptions make it possible to model a slope stability limit equilibrium problem with a circular slip surface as follows:



Summation of moment of all slices around the axis point where  $W$  is the slice weight,  $kW$  denotes a horizontal seismic force,  $D$  represents an external point load and  $A_L$  and  $A_R$  the external water forces:

$$\sum Wx - \sum S_m R + \sum kW e \pm \sum Dd \pm \sum Aa = 0$$

Substituting for  $S_m$  then makes it possible to formulate the factor of safety as a moment factor of safety,  $F_M$ :

$$F_M = \frac{\sum (c' \beta R + (N - u \beta) R \tan \phi')}{\sum Wx + \sum kW e \pm \sum Dd \pm \sum Aa}$$

The key parameter in this expression is the normal force  $N$  which is derived from summing the vertical forces on each slice:

$$(X_L - X_R) - W + N \cos \alpha + S_m \sin \alpha - D \sin \omega = 0$$

Substituting for  $S_m$  once more and rearranging the terms yields the expression:

$$N = \frac{W + (X_L - X_R) - \frac{(c' \beta R \sin \alpha + u \beta \sin \alpha \tan \phi')}{F} + D \sin \omega}{\cos \alpha + \frac{\sin \alpha \tan \phi'}{F}}$$

What now becomes apparent is that the expression of  $F_M$  is nonlinear as  $N$  is also a function of  $F$  which is the same as the moment equilibrium factor of safety when solving for moment equilibrium. This is solved through an iterative process.

$N$  is also dependant on  $X_L$  and  $X_R$  which are interslice shear forces. Interslice forces, both normal  $E$  and shear  $X$ , is a key concept in the GLE method and are as mentioned required to calculate the normal force  $N$  at the base of each slice. The following empirical equation express the relationship between the interslice forces:

$$X = E \lambda f(x)$$

The function  $f(x)$  is called the interslice force function where  $x$  refers to each slice from left to right of the slip surface and is an arbitrary function one has to specify, and  $\lambda$  denotes the percentage of this function to be used. Summing all the forces for each slice, knowing that the left interslice normal force  $E_L$  is zero, yields an expression for  $E_R$  which involves  $S_m$  and subsequently  $F$ . Through the interslice force equation it is then possible to also express  $X$  from this, however those expressions are also depending on the factor of safety and are also part of the iterative solution processes.

As a starting value for the iteration processes,  $N$  is calculated by simply neglecting interslice shear and normal forces summing all the forces in the direction of  $N$ .

### 3.2.2 Early methods

A method of slices was firstly used in 1916 for a stability analysis of the Stigberg Quay in Gothenburg, Sweden. In 1936 The Ordinary method was introduced by Fellenius, which was followed by the Janbu and Bishop methods in the mid 1950's. All of these methods are, as mentioned above, based on the discretization of a sliding mass into slices. What separates these methods from each other however, is the way in which they treat interslice forces and which static method they use, moment or force equilibrium, to derive either  $F_M$  or  $F_F$ .

The Ordinary or Swedish method neglects all the interslice shear forces, and is in fact the method used to obtain a starting value for  $N$  as described in the iterative solution in the previous section. The consequence of this is that the calculated factor of safety is rather unrealistic. On the other hand, this makes it possible to perform calculations by hand or in a spreadsheet, which of course can be useful sometimes also today but was very important before computers. The Ordinary method results in a moment factor of safety.

The 1950's methods, Janbu's Simplified and Bishop's Simplified methods were the first to incorporate interslice forces. These do however only include the interslice normal forces and not shear force. The difference between these methods is that Janbu solves the force equilibrium factor of safety and Bishop solves the moment factor of safety.

Along with the development of computers, more advanced methods became available and feasible to use with regard to the many iterative processes described previously.

### 3.2.3 Morgenstern-Price

One of those methods is the Morgenstern-Price method. It was also Morgenstern and Price that developed presented the interslice force function which is the key to be able to solve a limit equilibrium problem with regard to both interslice shear and normal forces. The Morgenstern-Price method, and other methods after that time, is called rigorous methods as they involve both shear and normal interslice forces. The factor of safety calculated by the Morgenstern-Price method also satisfies both the force and moment equilibrium equations. By iteratively changing  $\lambda$  in the interslice force function a convergence of the moment and force factor of safety can be obtained.

It is this method that is the default factor of safety value in Slope/W, and which has been used later in this master thesis when calculating slope stability.

## 3.3 Soil strength models

Another very important aspect of slope stability calculations is of course the actual soil parameters. The strength of a soil is not a unique value but depends on many factors such as the stress situation at breaking point, stress history, pore water and drainage conditions, loading/shearing rate, cementing and more.



“The quality of the output of a slope stability analysis in Slope/W is only as good as what you put in.”

-Victoria Svahn, 2010

So the most important task in any slope stability analysis is to assess all of these parameters and get them as close to reality as possible. This is done through geotechnical investigations, in this thesis study of old already existing investigations, and a study of the geological history. When the parameters are established, the modelling of the slope can begin.

Slope/W is based around a very graphical and user friendly interface where you start by drawing the geometry of the slope with drawing tools. The next step is to divide the soil mass into different regions depending on the soil properties for those individual regions. Each region is then assigned a specified material which contains unit weight and strength. Pore water pressure, as well as any surface water, external loads and structural reinforcements are added on later.

When it comes to specifying the material properties in Slope/W there are a number of base functions on how to define the properties. These functions differ in the way they distribute the soil strength to the region they are assigned. For example, and as is often the case, the soil strength increases with depth. To model such a state one chooses a material type for which you can specify that the strength shall increase X kPa every meter either from the top of the region layer or from a specified datum. In addition to choosing a material function that distributes the shear strength in a certain way, one also has to choose how the actual strength is modelled. It is this model that is used by the software to define  $s$  as described in the derivation of the factor of safety in Section 3.2.1 of this chapter.

### 3.3.1 Drained analysis

For a drained, effective stress, slope stability analysis, one has to assign the different regions Mohr-Coulomb models that simply define the strength according to the classic Mohr-Coulomb equation:

$$s = c' + \sigma' \tan \phi'$$

The factor of safety in a drained analysis is denoted  $F_\phi$ .

### 3.3.2 Undrained analysis

For an undrained analysis one can simply opt to set  $\phi = 0$  in the Mohr-Coulomb model or use a predefined material called “Undrained strength” where the material strength only is described by the  $c$  value and the pore pressure have no effect on the materials shear strength.

$$s = c_u = \tau_{fu}$$

The factor of safety in an undrained analysis is denoted  $F_c$ .

### 3.3.3 Combined analysis

As the name suggests, a combined analysis is a combination of the two above. This is a somewhat special feature that was originally put into the software in large part due to initiatives taken by Swedish users. It is a method to calculate a factor of safety which is unique to Scandinavia. It is used because of the special marine clay deposits which exist throughout this region. This factor of safety is a result of calculating the factor of safety of each slice for both drained and undrained conditions, and then choosing the lowest result. This calculation is something that is required as praxis in Swedish geotechnical engineering codes, see Table 1 (IVA Skredkommissionen, 1995).

Figure 5 Screen shot from Slope/W showing the inputs into the combined material model “Combined,  $S=f(\text{depth})$ ” where  $C_u$  changes with the depth from the top of the region this material will be assigned to and  $C$  is expressed through the ratio between  $C/C_u$ , for the undrained cases  $C$  is equal to  $C_u$ .

The values of  $c'$  and  $\varphi'$  differ from case to case, and as they are not fundamental soil properties they also change with the magnitude of the effective stress, but empirical knowledge has resulted in the following general rule for clays along Göta River (Sällfors, 1994):

$$c' = 0.1\tau_{fu} \rightarrow \frac{c'}{c_u} = 0.1 \quad \text{and} \quad \varphi' = 30^\circ$$

The combined factor of safety is denoted  $F_k$ .

### 3.4 Concluding remarks

Today there are many other advanced modelling tools, using finite element methods for example, which sometimes are used to complement the traditional methods for more complex soil and slope cases. The slopes that are analysed in this thesis however are very simple in the sense that they mainly consists of clay down to a depth far below any critical slip surface, and without any modelled reinforcement measures such as retaining walls, soil nails etc. In other words, these types of slope stability calculations are what the GLE methods initially was intended for, so the Morgenstern-Price method is regarded as well sufficient for the slope stability analysis in this thesis.

Another important note on the GLE method is that the normal stresses calculated at the base of each slice might not represent a fully realistic stress situation in the soil. This is because of the fact that the GLE method is based purely on statics without any constitutive strain-displacement equations. An example of the difference between the stresses calculated by a finite element-analysis and a limit equilibrium analysis are shown in Figure 6. The overall distribution is however similar, and even though the local slice forces might be slightly unrealistic the global factor of safety is still realistic (GEO-SLOPE International Ltd, 2008).

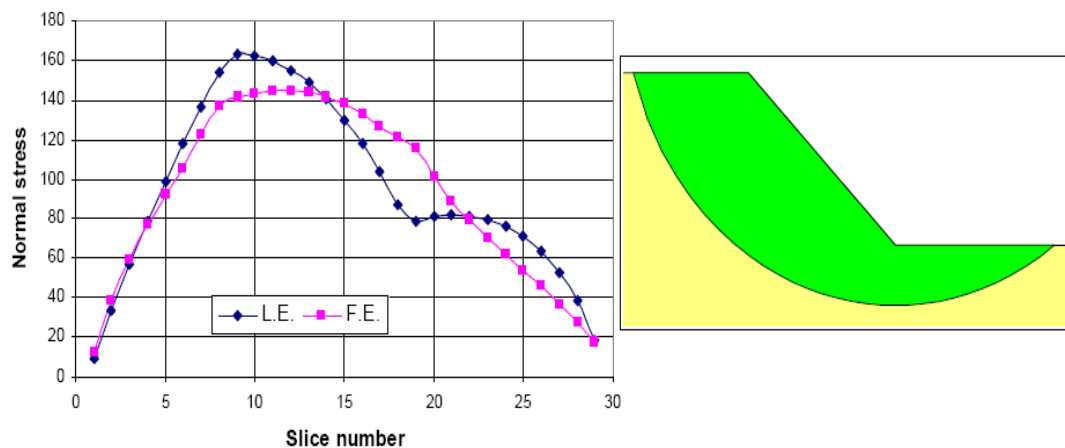


Figure 6 Difference in stress distribution between limit equilibrium (L.E.) and finite element (F.E) analysis along the base of each slice for the slip surface to the right in the picture (GEO-SLOPE International Ltd, 2008).

The uncertainties with regard to the calculated factors of safety that most effects the results in this thesis are however adjudged to be mostly related to the uncertainties in the soil strength parameters and the modelling of the slopes rather than the missing physics in the actual methods of analysis used by the software.

#### 3.4.1 The factor of safety

As mentioned in the previous section the factor of safety in the later parts of this thesis always refers to a Morgenstern –Price factor of safety as calculated by Slope/W 2007 and using a half sine interslice function if not mentioned otherwise.

To give some perspective on what a factor of safety means in the real world of construction and civil engineering a table is presented below with the required factor

of safety for different scenarios. According to the commission on slope stability, which wrote the Swedish recommendations for slope stability investigations, both the undrained and combined factor of safety should normally be evaluated for cohesive soils. And for both these factors of safety, the stability requirements should be met (IVA Skredkommissionen, 1995).

*Table 1 Recommended factor of safety for different scenarios (IVA Skredkommissionen, 1995).*

Investigation stage	Land use			
	New developments	Existing developments	Other land use	Natural areas
Geotechnical inspection/survey	At least a detailed investigation must be carried out	$F_c > 2$ $F_{c\phi} > 1.5$	$F_c > 2 +$ $F_{c\phi} > 1.5$	$F_c, F_{c\phi}$ and $F_\phi > 1$ (under the condition that the surrounding land is not affected)
Detailed investigation	$F_c \geq 1.7 - 1.5 +$ $F_k \geq 1.45 - 1.35$ $F_\phi \geq 1.3$ (sand)	$F_c \geq 1.7 - 1.5 +$ $F_k \geq 1.45 - 1.35$ $F_\phi \geq 1.3$ (sand)	$F_c \geq 1.6 - 1.4 +$ $F_k \geq 1.4 - 1.3$ $F_\phi \geq 1.3$ (sand)	$F_c, F_{c\phi}$ and $F_\phi > 1$ (under the condition that the surrounding land is not affected)
In-depth investigation (complementary investigations)	$F_c \geq 1.5 - 1.4 +$ $F_k \geq 1.35 - 1.30$ $F_\phi \geq 1.3$ (sand)	$F_c \geq 1.4 - 1.3 +$ $F_k \geq 1.45 - 1.35$ $F_\phi \geq 1.3$ (sand)	$F_c \geq 1.6 - 1.4 +$ $F_k \geq 1.4 - 1.3$ $F_\phi \geq 1.3$ (sand)	$F_c, F_{c\phi}$ and $F_\phi > 1$ (under the condition that the surrounding land is not affected)

## 4 Göta River

Göta River runs south from the city of Vänersborg at the southern shore of Vänern, the largest lake in Sweden, to the west coast where its outlet forms the island Hisingen, see Figure 7. The northern arm of this outlet is called Nordre River and the southern arm which divides the city of Göteborg retains the name of Göta River. The distance from Vänern to the outlet of Göta River is 93 km and the elevation between sea level and Vänern is about 44 m. Göta River is the largest river in Sweden with regard to flow and catchment area, with an average flow at the outlet of about 550 m<sup>3</sup>/s and a catchment area including that of Vänern of 50 299 km<sup>2</sup>.

The water level in Vänern and the flow in Göta River are regulated according to Swedish law. The level and flow are controlled through three hydropower dams along the river at Vargön, Trollhättan and Lilla Edet (the water level in Vänern is also regulated through dams upstream in rivers with an outlet in Vänern). The maximum allowed water discharge at the dam at Vargön is about 1000 m<sup>3</sup>/s and the maximum allowed water level in Vänern is 44.85 or 44.55 m above sea level depending on the time of the year. Due to these regulations the variation of water flow in the river has increased compared to the earlier natural flow, and between the years 1980 and 2005 the water flow in the river varied between approximately 125 and 1200 m<sup>3</sup>/s. During a 24 hour period the water flow can vary as much as 750 m<sup>3</sup>/s (Göta älvs Vattenvårdförbund, 2006).

The Göta River valley was created through erosion of a typical weak zone in the gneissic bedrock of the region. In parts of the valley the gneiss, with some elements of diabase and granite, reaches the surface but mostly it is covered with soil. This soil mostly consists of silt and clay deposits, sometimes very massive, that were formed both through glacial and postglacial processes. The glacial clay deposits which are the dominant type contain more elements of coarse soil particles compared with the postglacial deposits. The glacial deposits are often overlaid with postglacial deposits, and the glacial deposits are in some parts heavily eroded which have led to the surface being covered with more coarse material. The glacial clay deposits that have been eroded are possibly also overconsolidated (Klingberg, 2010).

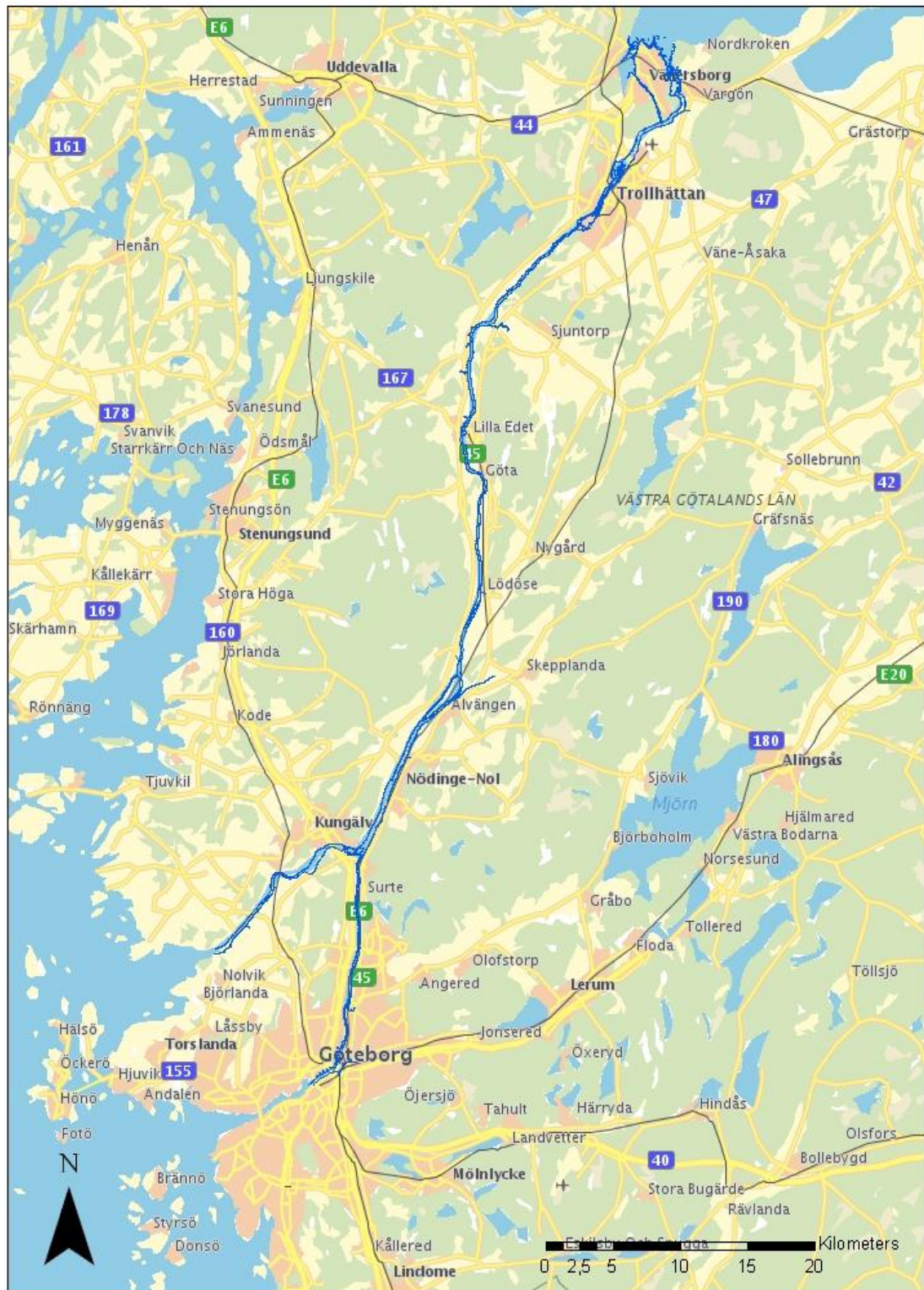


Figure 7 Göta River, highlighted with a dark blue colour, running from Vänersborg in the north towards Kungälv and Göteborg in the south (ArcGIS, 2011).



## 4.1 Geology

Göta River stretches along a regional weak zone in the bedrock. More specifically it is a fault zone which was subjected to vertical shear caused by tectonic activity 900-850 million years ago. However, the shape and geology of today's river and valley originates from the last ice age. Large deposits of fine grained sediments, or cohesive soils, were deposited in the valley both through glacial and postglacial processes. In the beginning the Göta River valley formed a sound connecting the open sea with what today is Lake Vänern. Because of the post glacial rebound the sound became smaller and smaller and the elevation between the sea and Vänern grew bigger and bigger. Following erosion of the uplifted soil sediments, the current stream bed was gradually formed, carving out the current river path, a process that in part still is active to date. This whole process started with the recession of the melting ice at about 12 000 years ago. About 2000 years ago the river had developed to a relatively similar appearance as of today (Klingberg et al, 2006).

Except for the large clay deposits there are elements of till, sand and gravel in the river bed but their influence on the overall geomorphologic processes of the rivers are negligible (Sundborg & Norrman, 1963). The processes that have shaped the stream and river bed of Göta River are very much a matter of erosion of cohesive soils.

There is normally a geologic and morphologic distinction between the southern and northern part of Göta River. Geographically the northern part usually is regarded as the river section between Trollhättan and Lilla Edet and the southern part is Göta River south of Lilla Edet. This is mainly because of a threshold in the elevation at Lilla Edet. This threshold was enhanced by the construction of a dam in conjunction to the water lock and subsequent hydro power plant at Lilla Edet in 1916 and 1918-1926 respectively (Göta älvs Vattenvårdförbund, 2006). The construction of the dam rose the water fall from about 4 m to 6.5 m. This water level change and its effects is one of the things differentiating the northern part from the southern part of the river. A second main factor that separates the two sections of the river are that the glacial rebound has progressed further above Lilla Edet with the consequence of the river having eroded deeper down into the sediments. This means that the river bank slopes are much steeper and higher in the north where the slope crests can reach as high as 20m above the water level. In the south the river banks in many places don't rise up more than one meter. The third main factor that separates north from south is that the southern part has more postglacial clay, whereas glacial clay dominates in the north.

The soil profile down to the bedrock is for the entire area dominated by a thick layer of glacial clay. This layer is at some parts underlain with glaciofluvial deposits, till or different mixes of friction soil. A comparatively thin layer of postglacial clay was deposited on top of the thick glacial clay. Due to the glacial rebound/ land heave described earlier the northern soil profile looks like the southern profile except that the top has been eroded down. That is why there is less postglacial clay in the north, as well as why the bedrock is closer to the river bottom. In some parts where there are subsurface peaks in the bedrock they penetrate all the way up to the river bottom. In the southern part of the river the bedrock lays at a depth of as much as 220 m, a depth that consequently decreases gradually going north (Klingberg et al, 2006; Sundborg & Norrman, 1963).

Because of the earlier conditions of the valley where much of the clay was deposited in a marine environment there is a significant existence of so called quick clay in the area. The quick clay exists as layers or planes in clay sediments with normal sensitivity, but in many places the entire clay stratum consists of quick clay (Lindskog, 1983). This is of course a very important feature of the area's geology as quick clay is a highly sensitive and unpredictable soil and as such has a major impact on slope stability. The reason behind the high sensitivity of quick clay is that it has developed through post glacial land heave and subsequent leaching of saline pore fluids, causing an unstable mineral structure. Subjected to external forces and/or heavy saturation quick clay can rapidly transform from a relatively stiff state into a liquid and sliding mass.

## 4.2 Morphology

The most extensive paper on the hydrology and morphologic processes in Göta River was perhaps written by Sundborg and Norrman at the Swedish geological Survey in 1963: *Göta Älv hydrologi och morfologi- med särskild hänsyn till erosionsprocesserna*. This paper was the result of archive and literature studies and field investigations carried out between the years 1958-1961. These investigations were initiated as a response to the large and devastating landslides in Surte 1950 and in Göta 1957. The aim of those studies and investigations was primarily to establish the morphologic processes occurring at the time, especially fluvial and wave erosion which was thought to be the main causes of landslides along the river. Although these investigations were carried out more than 50 years ago and limited to the technology and knowledge of that time it was indeed a very comprehensive research program combining the areas of geology, hydrology and geotechnical engineering (most of the geotechnical investigations, such as slope stability calculations, were however presented in a separate paper). They include a large amount of soil sampling, echo soundings and seismic sampling, hydrological and wave measurements and even direct visual observations from scuba diving. The study also includes an attempt to compare the new bottom topography measurements with measurements from the late 1800s up to the 1950s. The aim of those comparisons were the same as the aim in this thesis when comparing data from 2003 with data from 2009, thus Sundborg's and Norrman's conclusions with regard to this is therefore of great relevance.



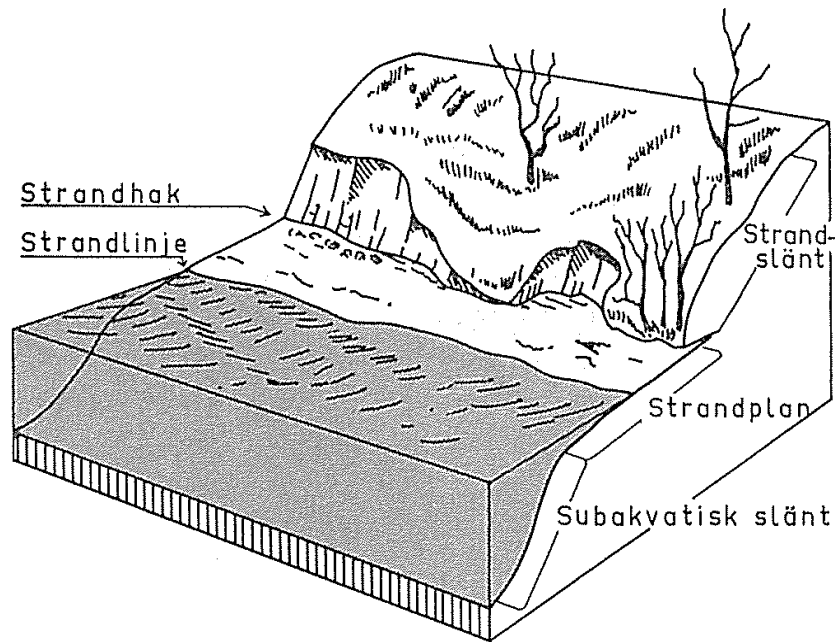


Figure 8 Illustration of a typical river bank and its morphologic features. Strandslänt = bank slope, strandplan = bank terrace, subakvatisk slänt = subaquatic slope, strandhak = shore scarp, strand linje = shore line at mean water level (Sundborg & Norrman, 1963).

#### 4.2.1 Wave induced erosion and river banks

The longest free water surface on the river is about 3000 m and maximum wind gusts in the region can reach up to about 30 m/s with average wind speeds around 5 m/s (Drobic, 2011). This is well sufficient for the generation of wind waves, but partially because the actual wind speeds at the river surface normally is much lower than those measured at weather stations the wind generated waves are smaller than those figures and classical wave theory would suggest. According to Sundborg and Norrman (1963) the environmental and natural conditions along Göta River means that wind generated waves only reach a significant wave height of ca 30 cm about 90 hours per year, and this only at the end of long straight sections of the river. More important are ship induced waves. As Göta River is a prominent shipping lane there is a daily traffic of large ships capable of producing waves with a maximum height of well over 30 cm. These ship induced waves usually lasts for periods of 10-30 seconds for each ship passage, but more significantly they occur all along the river as opposed to wind induced waves (Althage, 2010). Sundborg and Norrman (1963) also acknowledged this in their report and since that time the ship traffic has only increased due in part to dredging and deepening of the channel and the opening up to ship traffic during wintertime in 1974 (Göta Älvs Vattenvårdförbund, 2006).

In Figure 8 the main morphological features for a typical river bank in Göta River can be seen. The wave induced erosion creates what is called an abrasion platform, a shallow plane with varying width and a low to very low slope gradient (the bank terrace in Figure 8). Abrasion platforms are typically covered with a layer of loose material such as sand, gravel or coarser fragments that has been accumulated by wave currents or are sorted residual material resulting from the waters inability to transport them. For cohesive sediments in general and Göta River in particular, the abrasion planes lack these covers of coarser materials due to the lack of coarser soil sediments

in the local geology. Only temporary are the abrasion platforms covered with material eroded from the bank slope. The abrasion platforms may however be covered with underwater vegetation which protects it from erosion and even causes sedimentation of small grained soils. These depositions are then washed away during the fall and winter seasons.

Sundborg and Norrman (1963) estimated wave induced currents close to the bottom of the abrasion platforms to 70 – 80 cm/s. Because of cohesive soils high resistance to erosion the erosive processes of the abrasion platforms occurs through flaking and breaking up of fragments along weak zones in the clays as well as through corrosion, see Chapter 2. This often leaves the bank terraces with a hard, flat surface with rifles caused by erosion along weak zones and fractures. If the abrasion platform has been formed in old landslide masses the detailed relief and overall patterns are more irregular.

Another result of the properties of clays and cohesive soils are that the bank slopes can become very steep. For friction soils the erosion at the base of the bank slopes creates a parallel displacement of the bank slope in accordance with the soil's friction angle. In cohesive soils steep bank slopes are developed from where soil material loosens and falls down on the plane mainly because of spalling caused by drying-rewetting and freezing-thawing. These steep bank slopes might of course also become so unstable that landslides occur, and the bank slopes particularly in the northern part of the river are characterized by numerous old landslide scars. Especially vulnerable for wave abrasion are bank slopes at the sides of small estuaries caused by streams and creeks running into the river. In general the erosion of bank slopes and continuous widening and development of abrasion platforms are also something that differentiates the northern part of the river from the southern. Today many of the most vulnerable stretches of the river have been provided with erosion protection. This protection is usually in the form of larger rocks and stones which form a protective layer at the base of the bank slope, which waves are unable to erode (Sundborg and Norrman, 1963).

Another feature that is specific for the northern part of the river is the rise in water level caused by the dams and locks at Lilla Edet. This water level rise in some places resulted in “double” bank terraces. This happened when a new bank terrace was developed according to the new water level and shore line while the old bank terrace still retained its form below the new terrace. The rise in water level also created very large and wide bank terraces at places where large, flat and graded areas used for industrial purposes near the river became inundated. This means that some of the bank terraces visible today were not originally formed by natural wave abrasion (Sundborg and Norrman, 1963).

South of Lilla Edet the erosion of the bank slopes is very insignificant compared to the north of Lilla Edet. One sign of this is the vegetation on bank terraces and bank slopes that with a few exceptions is prevalent throughout the southern part of the river (Lindskog, 1983). As mentioned earlier the bank slopes south of Lilla Edet are generally very low compared to their northern counterparts, so the erosion of the bank slopes, even if it would have been more substantial, is of relatively low significance with regard to the global slope stability.

### 4.3 Erosion of river bottom

The two main processes that cause bottom erosion in Göta River are fluvial erosion and corassion. The current flow velocity of the water in Göta River however is relatively low, and clay is not easily eroded directly by water because of its cohesive properties. A typical value of shear force along the river bed caused by the flow in Göta River is 4 Pa, and a typical shear strength value of weak clay is around 5000 Pa (Rankka, 2010). Hence the process which most affects the river bed of Göta River is corassion. This happens when particles that are more easily transported by water than the clay, such as sand and gravel, is transported along the bottom, grinding on the clay surface. Sundborg and Norrman (1963) mention examples of narrow canyon-like formations several meters deep with near vertical walls that have been carved out by corassion.

Where the first process mentioned above occurs it mainly occurs along weak zones in the clay and along layer boundaries in the clay deposits. Because of the nature of corassion, grinding by larger particles, the erosion occurs in trenches or gutters where coarser material accumulates. Many indicators of this being the dominating and most active erosion process can be seen when studying geophysical images and data of the river bottom, see Chapters 5, 6 and 8.

#### 4.3.1 Summary of Göta River geology and morphology

- Göta River runs along a rift valley from lake Vänern to the sea and it started to develop about 12 000 years ago after the latest glaciation.
- Göta River is the largest river in Sweden with regard to flow.
- Typical layering is; thick clay deposits up to a depth of about 100 m (smaller depths in the north), friction soils and gneissic bedrock.
- Some of the clay is highly sensitive quick clay, formed partially by artesian water pressure and subsequent leaching.
- Göta River Valley is the most landslide prone area in Sweden, and the place of many devastating landslides in recent history.
- Due to a threshold in water level at Lilla Edet Göta River is often divided into a northern and southern part (upstream and downstream, respectively, of Lilla Edet). In the northern part: bedrock closer to surface, more firm clay, large water depth (20+ meters in some places), steep and high river banks, water regulated through dams in Lilla Edet and Trollhättan (hydro power and locks). In the southern part: deeper clay deposits (mainly post glacial), river banks often not more than a meter high, shallow river (down to about 6 m in some places), softer clay, more dense population and industrial activity along river.
- Göta River is an important and relatively heavy shipping lane and ship induced waves are an important source of erosion.
- The flow of the water is relatively low, causing too little shear stress to erode cohesive soils directly. Therefore most of the erosion is believed to be caused by corassion and/or waves.
- Erosion in the northern part mainly occurs on the river banks. In the southern part mainly in the deep causeway, bottom erosion, or in some literature referred to as deep erosion.

## **5 Topographic, geophysical and hydraulic data used in study**

A basis for much of the analysis work in this thesis was a rather large amount of topographic, geophysical and hydraulic geographical data from Göta River Valley. This work includes involvement in the production of some of the data, as well as extensive use of basic spatial and 3D analyst tools in ArcGIS. A large number of shapefiles, primarily slope profiles, have also been produced and stored during this process.

The first aim of using these datasets has been to create and extract slope profiles for the analysis of slope profiles themselves, as well as extraction of slope profiles to be used in slope stability calculations. The second aim was to try and quantify and determine the geometric characteristics of fluvial erosion in the river with regard to the slope profiles.

### **5.1 Topographic and bathymetric data**

The data used in this study to create the slope profiles was an existing dataset of topographic and bathymetric data. This dataset was compiled by Vattenfall Power Consultant AB in 2008 by merging several previously existing echo sounding measurements and digitized maps with an airborne laser scan (LIDAR) of the terrain surrounding the river, see Figure 9 for overview of dataset. The original primary purpose of this DEM was for Vattenfall AB Hydropower, Swedish National Grid and the Swedish Maritime Administration to use it for hydraulic modelling and analysis for preparedness plans in the case of a dam failure in Göta River.

The LIDAR scan was performed by COWI AB in 2006. This was done from a height of 1000 m and resulted in a resolution of 1-2 measuring points per square meter, totalling 255 million points for the whole area. This data is regarded as very detailed. Most of the river bathymetry in the original DEM originated from two different echo soundings; one performed by The Swedish Maritime Association in 2003 and the other carried out by Marin Mätteknik AB on behalf of SGI in 2004. Of these two echo soundings most measuring points used in the DEM are from 2003 with 36 million points between Hjällbo just south of Agnsesberg and Trollhättan to the north. About 1 million points from the 2004 echo sounding as used to fill in blank spots left by the 2003 echo soundings at various stretches along the river. There were other sources of bathymetric data in the original DEM, but areas of the river containing that data was not analysed in this case study. The DEM was also produced and quality checked according to the Swedish Standard SIS/TS 21144:2004, Engineering survey for construction works - Specifications for producing of digital terrain models (Hedvall, 2008; Marin Mätteknik AB, 2004). Further information regarding the SIS standards can be found at [www.sis.se](http://www.sis.se).

One important factor for the original DEM is that there are no measured bathymetric values between 0 and 2 m water depth due to the practical setup of boat and measurement equipment. This means that there are blank spots in the source data, in particular close to the shores. In the original DEM however these blank spots was covered with interpolated values through an inverse distance weighted interpolation. This interpolation was also done for areas outside the river such as areas occupied by

large buildings. In addition to this a mean value filtration of the original data was carried out with a filter size of 5x5 pixels to smoothen the data. The completed DEM has a grid size of 1x1 m (Hedvall, 2008).

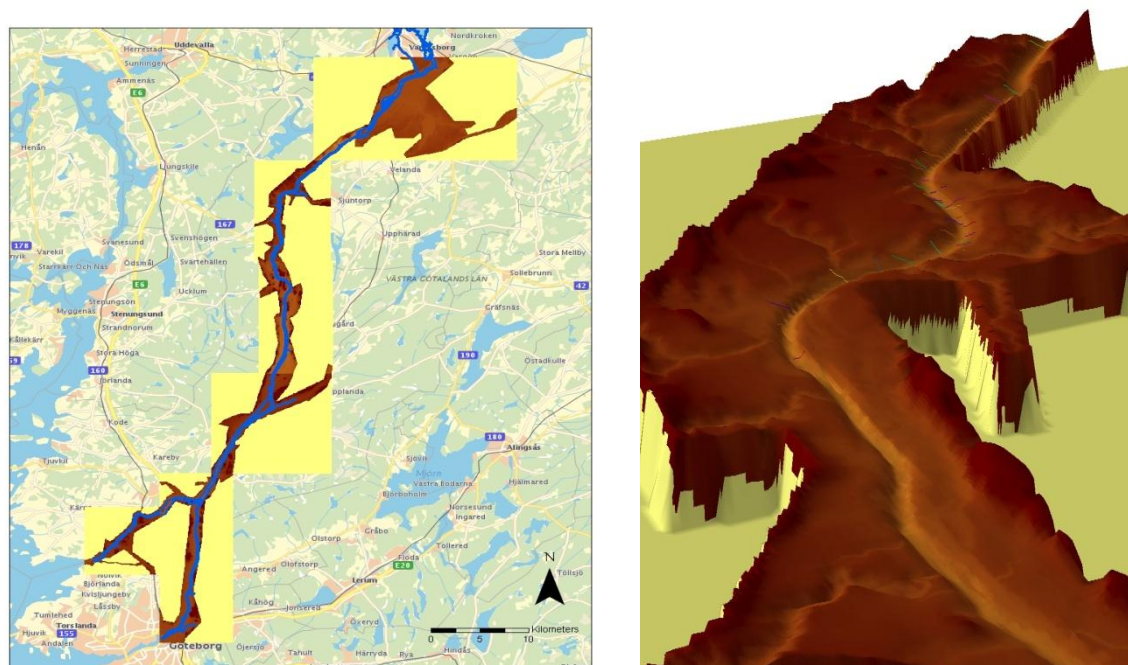


*Figure 9 To the left: Extent of the DEM which is formed by five tiles covering all of Göta Älv including some its tributaries. The elevation is represented in a brown scale while the distinct yellow parts represent no value pixels. To the right: 3D rendering of a section of the DEM with slope profiles visible as colored lines along the riverbank (ArcGIS, 2011).*

In 2009 another multibeam echo sounding was carried out on behalf of SGI by Marin Miljöanalys AB (MMA). This was the most comprehensive to date and it covered the entire length of both Göta River and Nordre River, it also had a much greater lateral coverage of the river sections (Marin Miljöanalys AB, 2009). Because of this, this newer data was merged with the original DEM and subsequently replaced most of the old bathymetric data in the DEM from 2003 and 2004. It is this enhanced DEM that has been used in this thesis work, and which is seen in Figure 9.

The DEM is clearly detailed and accurate enough for the purpose of studying and extracting realistic slope profiles from the Göta Älv valley, which also was the main purpose of the 2004 and 2009 echo soundings. The interpolation of the bathymetric values in the DEM was not considered to be a problem because the main, and most interesting, parts of the slopes under the water surface are at depths larger than 2 m. And even though the purpose of the total DEM originally was not to analyse slope profiles and slope stability, the echo soundings ordered by SGI in 2004 was in fact to study sub aquatic slopes, which naturally means that the bathymetric data from this source is well sufficient for the purpose of this case study.

### 5.1.1 The 2003-2009 bathymetric dataset

This dataset, which in this report sometimes is referred to simply as the *2003-2009 dataset*, is the result of subtracting the bathymetric values of the 2003 echo sounding from the values of the 2009 echo soundings. While subtracting one raster dataset from another might sound like a simple GIS operation, it had its difficulties in this case caused by the fact that SGI didn't have access to the actual 2003 dataset and that the different original datasets was in different coordinate systems. Part of the work carried out in this thesis was to discuss and analyze these issues with the erosion expert group at SGI and the Swedish Maritime Administration which was in possession of the original 2003 data. Eventually this resulted in the creation of the 2003-2009 dataset carried out by the Swedish Maritime Administration on behalf of SGI.

To evaluate the accuracy of and calibrate the dataset comparisons were made between the different datasets of measurements on surfaces on the river bottom where the change in elevation between 2003 and 2006 is expected to be zero. The surfaces used in this case were concrete structures in several of the water locks in the river. This analysis showed that the 2009 MMA data possibly should be adjusted with -0.07 m. Subsequent visual observations of the dataset at different places showed that this adjustment indeed gives a general pattern of erosion and sedimentation that looks closer to what would be expected based on existing knowledge of the erosion processes in the river (Persson & Tengbert, 2010).

The resulting dataset covers the entire river to the extent of the 2003 echo sounding, and though the accuracy of the data was much discussed and constitutes a large uncertainty in this study, the producer of the data was confident that the dataset should be accurate even for small changes, <10 cm, in the bathymetry between 2003 and 2009 (Persson & Tengbert, 2010).

In Chapter 6, a number of examples and observations made using this dataset are presented. It should also be pointed out that in the following chapters where images of this dataset is presented yellow and red indicates a lowering of the bottom surface, where red is the lowest value. At the other end of the colour spectrum is blue, which indicate a raised bottom topography.

## 5.2 Additional sonar data

In addition to the bathymetry measurements carried out in the 2009 echo sounding, both side scan and backscatter data was collected.

### 5.2.1 Backscatter

Bathymetric data is assessed from the speed of sound in the water and the time it takes for a sound beam to be reflected against a surface. Combining these factors then gives the distance the sound beams have travelled, which in the end results in a 3D surface such as the DEM above.

Backscatter data is what you get when you instead analyze the strength of the reflected sound, i.e. the amplitude of the reflected sound waves. Another term for backscatter data is amplitude data. Simply explained; when a sound wave hits a surface a certain amount of its energy is absorbed, resulting in a reflection containing less energy than the incoming wave. The amount of energy that is reflected depends on the properties of the reflection surface. A hard surface gives a stronger reflection and a soft surface gives a weaker reflection.

The idea of this data is to provide a picture of what the bottom surface material consists of. Soft clay sediments give a very different amplitude reflection than for example gravel which is much harder. The challenge involved in the creation of such datasets is to determine what the different type of reflection profiles actually represents on the bottom, and this usually requires some amount of soil sampling to verify and calibrate the data. This verification was carried out by MMA by looking at already existing samples from the river taken by SGI and SGU over the years, as well as new samples that was taken by MMA for the explicit purpose to be used in the backscatter analysis.

The resulting classification of this dataset looks as follows (Marin Miljöanalys AB, 2010):

*Table 2 Classification of backscatter data.*

Class	Soil/bottom type
1	Clayey mud, muddy clay- very loose sediments. Probable sedimentation bottom.
2	Clay, mud, silt, plant material- loose sediment. Probable sedimentation bottom.
3	Fine sand, silt, hard clay, plant material. Probably a mixture of sedimentation and erosion/transport bottom.
4	Sand – coarse sand. Probable erosion/transport bottom.
5	Sand with gravel, gravel, rocks. Probable erosion/transport bottom.



In total a little more than 100 samples were available for verification, although many of these were deemed unusable due to the poor accuracy in the positioning of the samples. As an example there are many areas in the river where the surface sediments differ with 3-4 classes within  $\pm 10$  m from a sample location. Another issue is that backscatter data from a high frequency echo sounding, as in this case, only penetrate 0-2 cm into harder material such as sand and gravel which is something one needs to be aware of when analysing this data: the classification is only refers to the very top layer, particularly for class 3-5. MMA has however concluded that overall the dataset is of good quality, even though a larger and more purposely planned sampling would enable the possibility for a more proper statistical analysis and verification of the backscatter data.

### **5.2.2 Side scan**

This data is used to create a visual image of features and objects on the bottom which is reminiscent of a photograph. It is however not based on electromagnetic waves as photography, but on sound waves and echo sounding techniques. The fundamental difference between side scan data and the echo sounding measurements described above is that side scan is beamed out horizontally, or sideways, which is what the name refers to. This creates a “shadow effect” behind each object or feature that is hit by the echoes, and these shadows can later be interpreted to create very graphical images where the resolution is dependent on the frequency of the echo sounding.

This technique is very commonly used to detect wreckages and other manmade objects. But they can also be used to view natural bottom features, such as in Figure 10 where the slide mass from the Ballabo landslide (see Chapter 8, Section 8.2), clearly can be seen protruding out into the river.

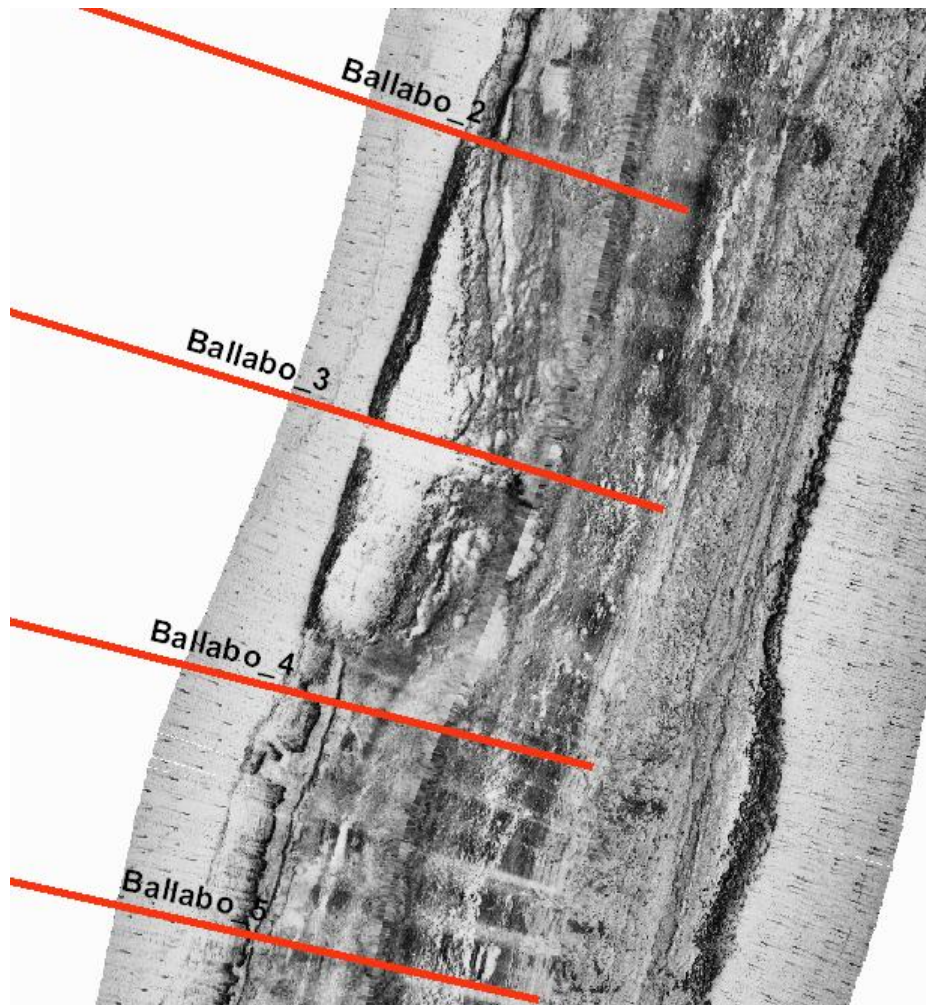


*Figure 10 Side scan image of the old Ballabo landslide. The line Ballabo\_3 crosses through the centre of the landslide soil mass (ArcGIS, 2011).*

### 5.3 Hydraulic shear stress data

The final piece of data that was used and analysed in ArcView is a dataset created by SMHI by the use of a hydraulic model that calculates shear stress between the water and the river bed. This data has been provided to SGI by SMHI as a part of the Göta River commission and the erosion expert group (Persson, 2011). The data shows the hydraulic shear stress along the entire river based on the three river flows of 1030 m<sup>3</sup>/s, 1250 m<sup>3</sup>/s and 1500 m<sup>3</sup>/s. These flow rates are very high, much higher than the normal flows of today. The purpose of studying those higher flows is to model potential effects of a possible larger amount of precipitation that might occur in region in the future due to climate change.

## 5.4 Comments

In Table 2, the classification of the backscatter data, there is in addition to the soil type for each class a description of the bottom type- if it is subjected to sedimentation, erosion or a combination of both. As a result of the work carried out in this thesis, it has to be pointed out that determining if an area is subjected to erosion or sedimentation cannot be done simply by looking at soil type or backscatter class. It might hold true for certain areas where there is a specific morphology, but it should not be applied as a general rule for the whole river.

In general there are clearly many uncertainties with regard to all of these datasets, and one single master thesis is not enough to address them all too any real depth. In Chapter 8 however, an approach on how to deal with this data and related uncertainties for assessing erosion is presented in the case studies. One might say that anyone of these datasets is not sufficient on its own for establishing the nature of and in particular the rate of erosion and sedimentation processes. But by combining all of the datasets, and using geological and geomorphologic knowledge and observations it is possible to make certain probable assumptions with regard to erosion and sedimentation.

The topographic data in the form of the DEM is in itself relatively accurate and the DEM is very useful for analyzing slope profiles and their overall geometries, see Chapter 7.

## 6 Observations of erosion and sediment transport processes and patterns

Presented in the following sections are some samples from the geophysical and topographic data described in the previous chapter. These samples show different features of erosion and sediment transport that can be observed in the GIS data on the Göta River bottom. These samples clearly show that the data is accurate enough to be able to observe certain geomorphologic processes, such as moving sand ripples and dunes. Another very interesting observation is what appears to be a relatively small sub aquatic landslide that would have occurred in the area of Ekbacken sometime between 2003 and 2009.

### 6.1 Sand dunes and ripples along the bottom

One of the most characteristic features of sand sediment transport, both under water and on land, is the creation of sand dunes which propagate forward like ripples in the direction of the wind or water. This phenomenon occurs almost everywhere in Göta River where the bottom consists of sand or sandy soils. Figure 11 shows a clear example of this outside the village of Nol.

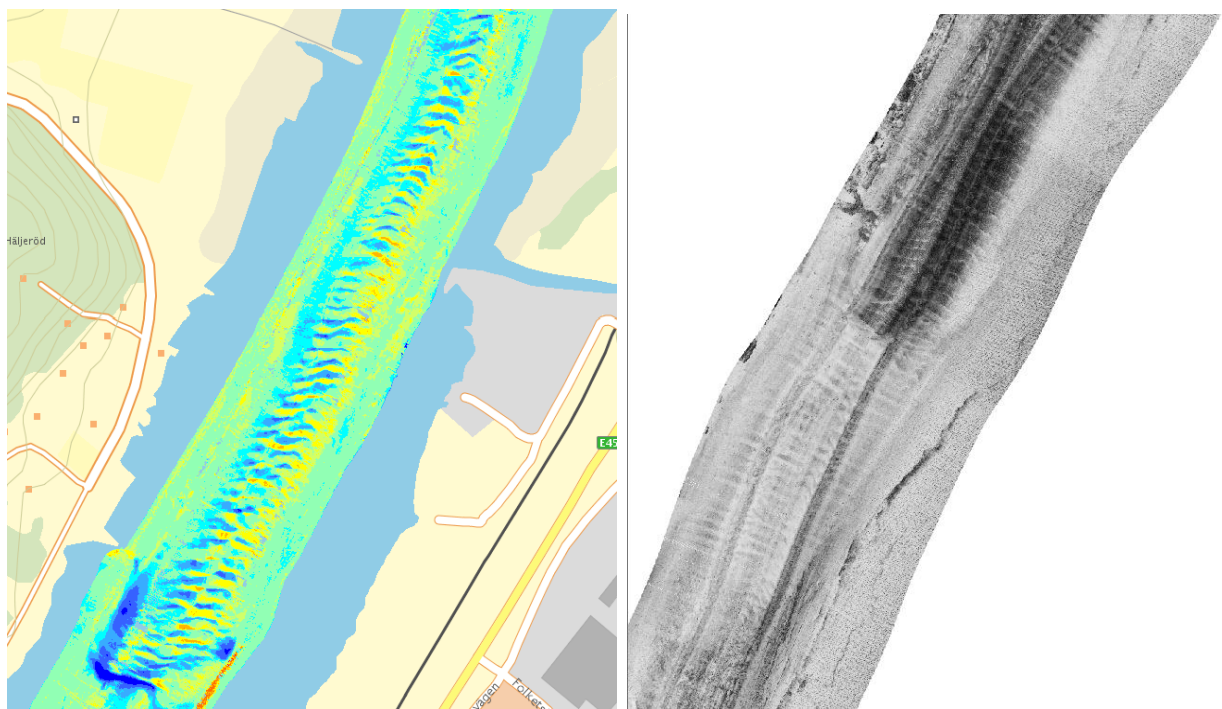


*Figure 11 Sand dunes outside of Nol. To the left: 2003-2009 dataset, where the blue stripes represent the moving crests of the sand ripples in 2009, and the corresponding yellow stripes represent the troughs. To the right: backscatter image of the same area (ArcGIS, 2011).*

Looking at the backscatter image in Figure 11 above, and comparing it to the backscatter image in Figure 12 (Ship dock at Lödöse) there is a clear difference in bottom texture and pattern. This is an example of the difference in the erosion and

sediment transport processes between a clay and sand bottom. This also confirms the general theory about the bottom erosion of clay sediments in Göta River occurring along trenches and being caused by corassion.

## 6.2 Propeller induced bottom erosion

Figure 12 below shows images of backscatter and the 2003-2009 dataset showing the river bottom of a small ship dock close to Lödöse. In the backscatter image, contours of the erosion trenches are visible both along the deep channel of the river, as well as along the bottom in the ship dock. The 2003-2009 dataset image shows a red patch, a deepening of the bathymetry, at the mouth of the dock, a possible result of propeller induced erosion. Figure 13 shows the ship lock, up-stream, at Lilla Edet. In the 2003-2009 dataset there are clear patterns of yellow and red color at the entrance/exit to the lock, suggesting propeller induced erosion caused by ships as they accelerate when they leave the lock.

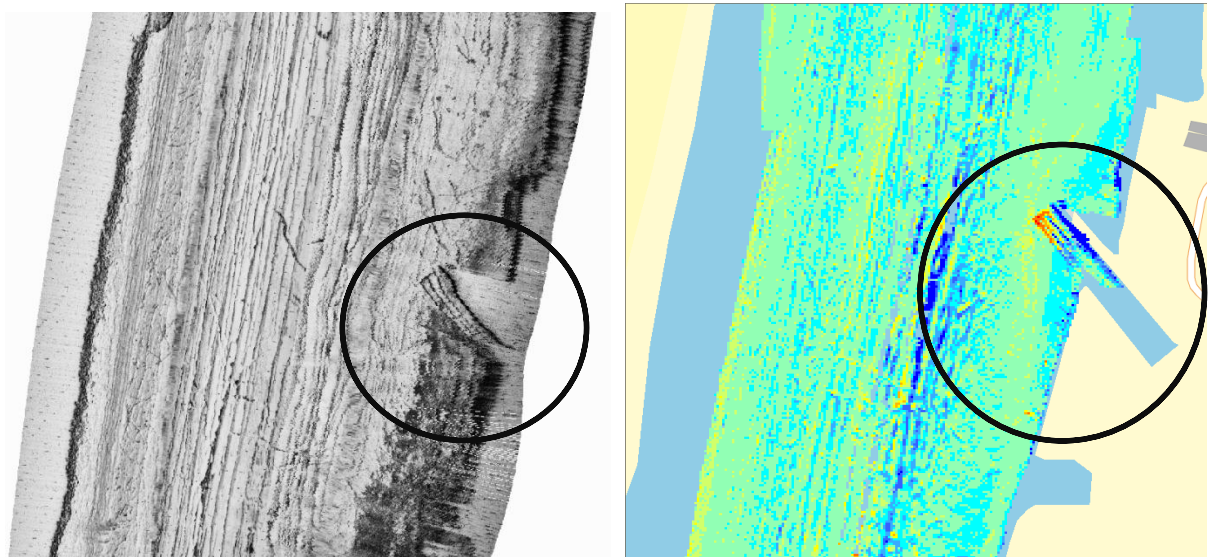


*Figure 12 Ship dock at Lödöse and possible propeller induced erosion. To the left: backscatter data. To the right: 2003-2009 dataset, same area (ArcGIS, 2011).*

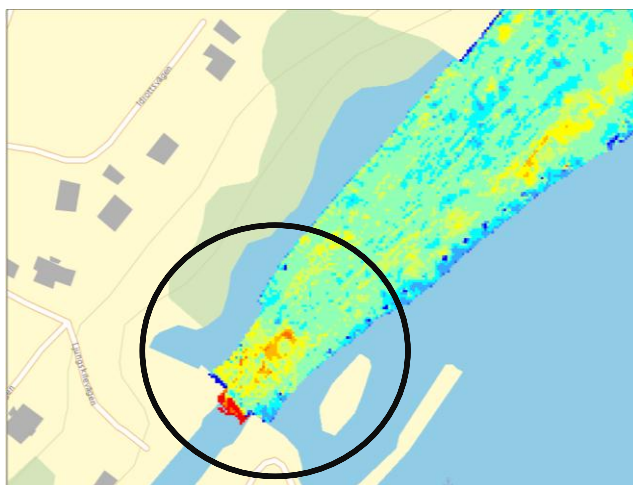


*Figure 13 Ship lock, up-stream, Lilla Edet. Entry/exit to the lock marked by the black circle (ArcGIS, 2011).*



### 6.3 Possible subaquatic landslide at Ekbacken

Figure 14 below shows the 2003-2009 dataset from a section of Göta River close to Ekbacken. There is an abrupt discontinuity in the overall patterns visible on the right slope of the deep river channel. The coloring pattern indicates that soil has been removed and possibly deposited directly below further down the slope, which would be expected for a typical landslide.

The bottom image in Figure 14 shows a close up of the area, as well as profiles that were drawn through the possible landslide. Profiles 1 and 3-6 are presented on the next page.

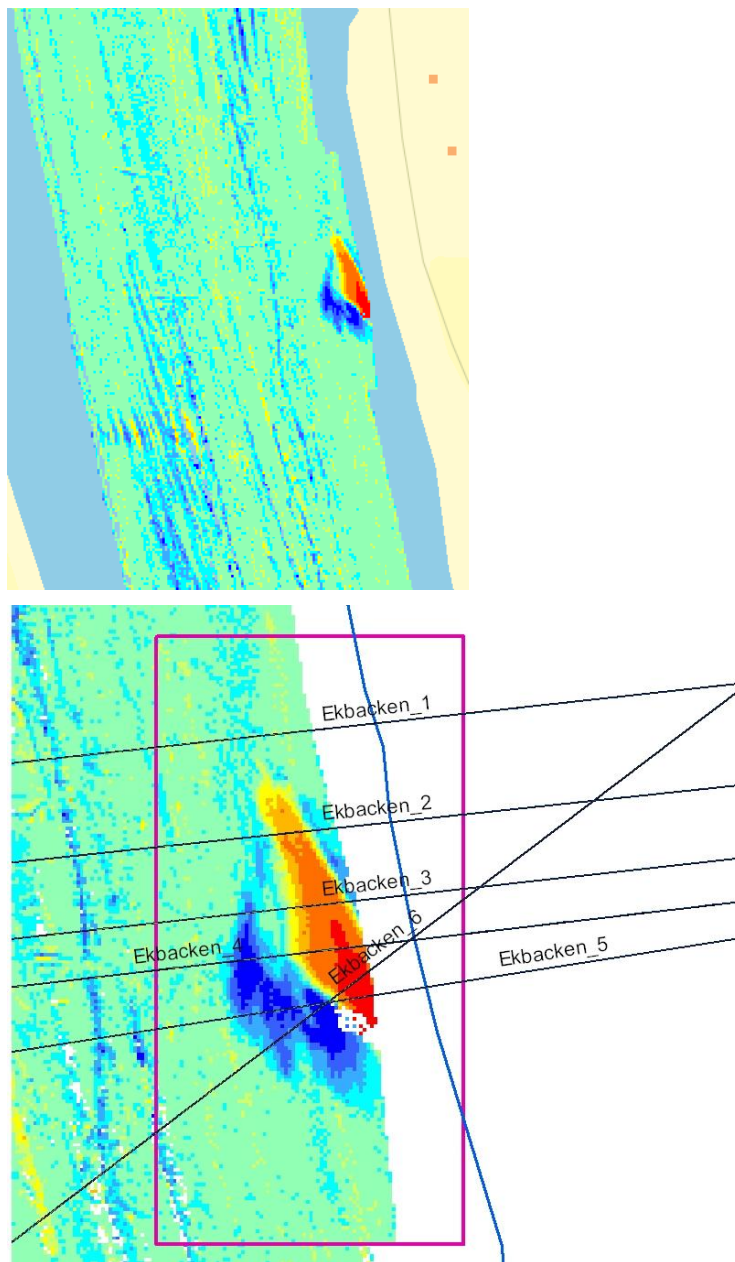


*Figure 14 2003-2009 dataset at Ekbacken, showing possible subaquatic landslide (ArcGIS, 2011).*

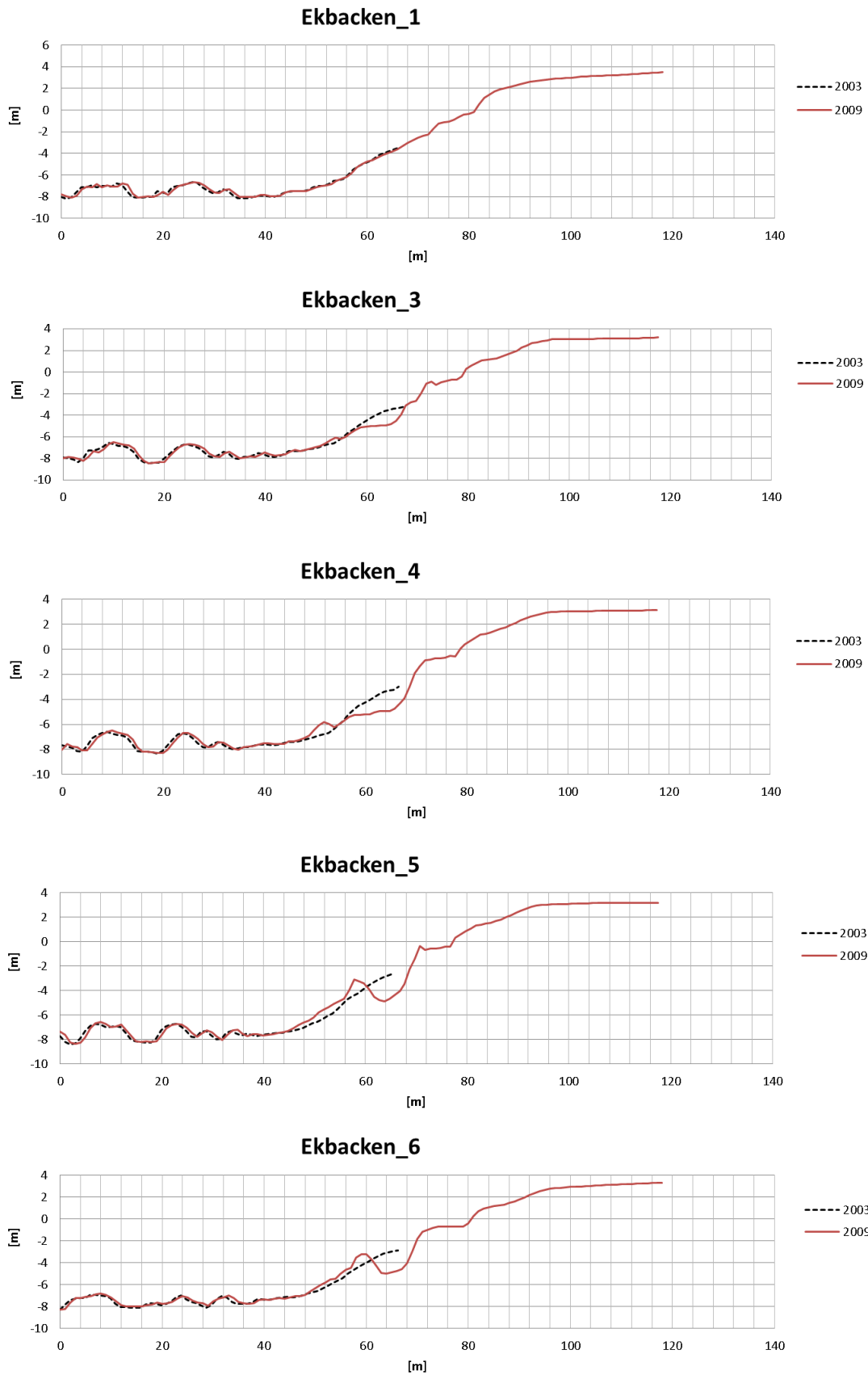


Figure 15 Slope profiles drawn through the possible subaquatic landslide at Ekbacken, showing bathymetric values from 2003 and 2009.

In the profiles in Figure 15 the underlying bathymetry changes that have given rise to the color pattern in the previous figures are clearly visible. In particular the profiles in *Ekbacken\_3* and *Ekbacken\_4* show characteristics of a typical landslide slip surface and signs that deposits of the land slide soil mass is lying below the slip surface. *Ekbacken\_1* is a slope profile just to the north of the possible landslide, and it can be assumed to represent a typical pre-landslide slope of that area. It also shows very little signs of any type of significant erosion between 2003 and 2009. The profiles in Figure 15 also show what appears to be distinct erosion trenches along the deep section of the river,  $0\text{ m} < x < 40\text{ m}$ , in particular the larger trench at  $12\text{ m} < x < 24\text{ m}$ .



## 7 Study of slopes

The purpose of this case study was to extract and classify different subaquatic slope profiles along the Göta River valley. Using ArcView and the DEM of the Göta River valley (see Chapter 5) a number of slope profiles were created along sections of the river. These profiles were then classified mainly with regard to their subaquatic part, that is, the geometry of the slopes beneath the water line. The different classifications were then used to obtain a generalized slope profile representing each class. The slope profiles were also analysed further to see if the different classes, or the generalized slope profiles, could be correlated to parameters such as: river curvature or other geometric, hydrological or geological properties of the river and river banks.

### 7.1 Sampling and extraction of slope profiles

The topographic dataset described in Chapter 5 was analysed in ArcMap. Using geological, physical and thematic maps as well as satellite photos, suitable areas of Göta River were identified for the extraction of slope profiles. These slope profiles were obtained by creating a polyline shapefile and then drawing a single 2D line in the area of interest. This line was then converted into a 3D feature by 3D Analyst using the DEM as the source for z-values. From the resulting 3D polyline a profile was created by using the tool “Create Profile Graph”. This creates a 2D-profile with the z-values on the y-axis and the corresponding length coordinate of the line as x-values, resulting in a profile of the topography along the drawn line. This data, or profile, was then directly exported as a table in Excel-format where they were re-plotted with the sub aquatic portion of the profile plotted in a different style.

The technical part in ArcMap of creating and exporting the slope profiles into Excel data format is rather straight forward. The more interesting part of the whole process was to determine where in the river to draw the lines and profiles. That is, what defines a suitable and interesting area for a slope profile?

The following were the criteria used for identification of such areas:

- **Geology**- the objective of the thesis was to study slope stability and the slopes of most interest were therefore those containing clay or silty soils. An area with exposed bedrock or any other surface geology was therefore not of interest. All the obtained slope profiles represent slopes in clay or silt deposits.
- **River geometry**- i.e. the planar curvature of the river was of interest because of the intention to analyse any correlation between the river geometry and slope profile types. Slope profiles were sampled to include slopes from all types of river geometry.
- **Topography**- the topographic features of the local landscape was also a factor in the sampling of slope profiles as the topographic isolines were used to identify areas that appeared more critical from a slope stability point of view. As well as trying to sample as many different types of slope geometries as possible.

The slope profiles were drawn from near the bottom of the respective sub aquatic slope 250 m outwards. The directions of most slope profiles are such that they were drawn perpendicular toward the most apparent direction of a potential land slide. This process of drawing slope profiles to be studied may be seen as a form of stratified sampling or purposive sampling.

## 7.2 Analysis and classification of slope profiles

As described in Chapter 4 there is a general geologic and morphologic distinction between the upper and lower part of Göta River. Because of that distinction the study of slopes was divided into two sections which have been studied separately. These two sections are: *Trollhättan – Lilla Edet* and *Lilla Edet – Kungälv*, referred to as the northern part and southern part respectively. The part of the river south of Kungälv hasn't been studied to the same extent as the upper and lower sections. This is mainly due to the lack of bathymetric data from 2003 for this section. However, some slopes from this area are presented and studied in connections to the case study of the old Agnesberg landslide area in Chapter 8.

### 7.2.1 Trollhättan – Lilla Edet

In this section a total of 55 profiles was analysed and a first visual analysis of the slope profiles resulted in an identification of eight different typical geometries, or classes. These typical profile geometries are presented below (note that the drawn shapes below are not drawn according to real proportions as the slopes have been exaggerated to better visualize the differences in shape):

#### 1. High terrace- steep slope

Distinct subaquatic terrace with a rather steep slope, approximately more than  $25^\circ$ . The steepest slope measured among the samples in the case study was about  $45^\circ$ . The height of the terrace is approximately more than 5 m. For most samples in the case study the heights were around 10 m. The water depth above the actual terrace is small, in general a maximum of about 1-3 m decreasing towards the shore line. Notice the concave shape of the steep slope



#### 2. High terrace- gentle slope

This profile has the same attributes as the *high terrace - steep slope* except the shape of the slope is a little different (less concave) and not as steep, with a gradient less than  $25^\circ$ .



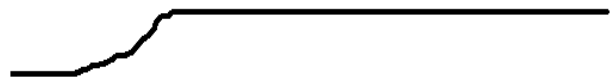
### 3. Low terrace

Same overall shape as the *high terrace-steep slope* profile with the difference that the height of the terrace is smaller than 5 m.



### 4. Long terrace

This class can refer to any of the terrace type profiles described above (1-3) with the addition that it has a very long terrace, approximately more than 50 m long.



### 5. Double terrace

This double terrace profile simply refers to two distinct terraces placed on top of each other. The combination of terraces can be any of the above (1-6), i.e. two low terraces, one high and one small etc.



### 6. Deep terrace

This type of profile also refers to any of the terrace profiles 1-6 but with the difference that the actual terrace lies very deep beneath the water surface compared to the usual rather shallow terraces.



## 7. Straight even profile

This type is a rather even and smooth profile that more or less has a continuous slope angle from the bottom of the river up to the shore line. This slope often continues at the same angle above the water.



## 8. Straight un-even profile

Similar to the *straight even profile* in the regard that it doesn't have any distinct terrace structure. As the name suggests it is however more uneven and rough. It becomes smoother above the water.



This classification of the slope profiles obtained from the DEM does not take the geometry of the profiles above water into account. The reasons for this is that the focus of this thesis is on the stability of subaquatic slopes and that the profile above the water differ from slope to slope, i.e. the geometry above water does not appear to be directly related to the underwater geometry.

It is important to realise that in reality no profile is identical to any other, there are always small variations. The classification in this case study is only an approximation of the existing profiles. The results of the classification of the slope profiles are presented below in the form of a frequency table:

Table 3 Slope class frequency table from slopes between Trollhättan and Lilla Edet.

Class	Absolute frequency	Relative frequency
1	13	24%
2	12	22%
3	1	2%
4	5	9%
5	4	7%
6	1	2%
7	13	24%
8	6	11%

It is clear that the dominant slope profile type among the sampled slope profiles is a slope with a high terrace. Together these two classes which both represent high under water terraces account for close to 50 % of the total slopes obtained in the case study. It is also clear that of the remaining 50 % class 7 and 8 which also share some basic similarities, class 7 is basically a smoother version of class 8, dominates with 35 % of the total.

The most significant observation in this classification is that even though the classification has to be regarded as a sometimes rough approximation it is possible to make a classification. Profiles show clear, distinctive features that they share with profiles at other locations of the river. Another significant observation is that regardless of the true relative frequency of class 1, it does exist. This is significant because this is the slope type which in theory should be the most critical with regard to slope stability failure due to the steepness and height of the slope. Several of these class 1 slopes indeed have a slope gradient of up to 45°.

It is not easy to make any initial quantitative statistical inferences from this data as the sample of slope profiles cannot be regarded as a fully random sample. It is however adjudged that this data gives a good indication of the different slope profiles that exist in the river, as well as that the main slope types are class 1-2 and class 7-8.

### **7.2.2 Lilla Edet - Kungälv**

An additional 16 slopes was drawn south of Lilla Edet and north of Alvhem. This second round of sampling showed that the classes attained from the first sampling also can be used to classify slope profiles south of Lilla Edet, despite some general differences in the geology and geometry of the river between these sections. There are however some differences with regard to the distribution of the classes in the second sampling, see Table 4 below. A general observation for the second sampling is that the slopes show a smaller height. The typical terraces of class 1 and 2 are much smaller and the slopes rarely show a difference in height of 10 m which was quite common in the first sample. This is also what is to be expected with regard to the geology of the river, see Chapter 4 about Göta River

As seen in the Table 4 there is a slight different from the first sampling, with a much higher frequency of class 5 which in this sampling has the same frequency (31%) as both class 7 and 8. Similarly to the sampling of the profiles north of Lilla Edet however class 1 and 2 dominates with about the same relative frequency.

There are a few cases in this second sample where the profiles classed as 5 were not easily distinguished from class 2 and class 8. As this second sample is relatively small, if two or three of these profiles would instead be classified as a 2 or 8 the distribution in this second sample would be very similar to the first sample.

*Table 4 Slope class frequency table from slopes between Lilla Edet and Kungälv.*

<b>Class 1</b>	<b>Absolute frequency</b>	<b>Relative frequency</b>
1	2	13%
2	4	25%
3	0	0%
4	0	0%
5	5	31%
6	0	0%
7	1	6%
8	4	25%

### **7.3 Connection between classes and river geometry**

The natural question after classifying the slopes is to ask if these classes have anything in common except their specific shapes. Are there any obvious connection between the different slopes and other parameters? One of these parameters is the planar geometry or curvature of the river. This is a parameter that is easily observable and it was recorded in the slope databases along with each slope profile. This parameter also becomes easy to analyse because the slope profiles either lie in a straight section of the river or an outer or inner curve, so there are only three different “values” this parameter can take.

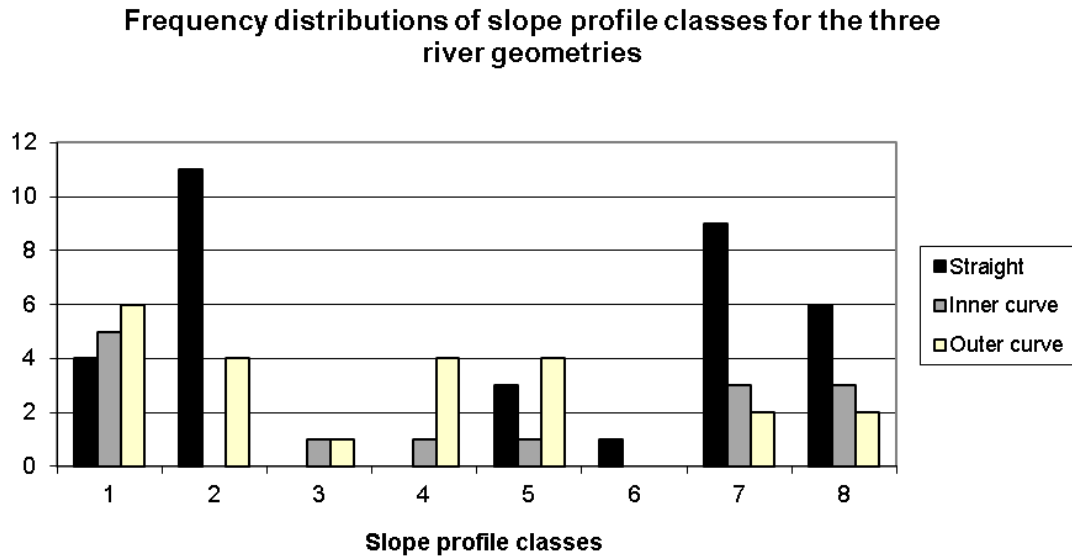


*Figure 16 Frequency distribution of slope profile classes for the river geometry.*

In Figure 16 above the number of slopes for each class that is situated in each type of river geometry (straight, inner curve and outer curve) is shown. Overall the distributions for straight sections and inner curves are quite similar to the class distribution for the whole population of profiles. The most interesting difference is that for profiles in inner curves there are none classified as 2. There are none classified as 6 either, but that is of very small significance as there are only one profile classed as 6 for the entire population whereas there are 15 profiles classified as 2 for the entire population.

Regarding the profiles situated in outer curves, the distribution over the classes is a little different. Perhaps the most significant observation between river geometry and profile classes is that class 4, profiles with very broad terraces, only seem to exist in or very close to outer curves. With regard to class 5 having a relatively large number in outer curves also have to do with the same factor described in the previous section for the profiles south of Lilla Edet; that is an uncertainty in the classification. If only a few of those would have been classified as an 8 then the distribution of profiles in an outer curve would also be similar to the distribution for the whole population with exception for class 4.

## 8 Case study of slopes and erosion at old landslides

The purpose of the work in this chapter is to attain a number of case slopes, including geometry, geotechnical properties and erosion, to use for subsequent slope stability analysis. The two largest landslides in Göta River the last 20 years are the landslides in Agnesberg 14th of April 1993 and in Ballabo 16th of April 1996, both of these locations lie south of Lilla Edet. As these landslides occurred in modern time, they have been thoroughly investigated with modern methods and techniques. This includes geotechnical soil investigations and soundings of the areas close to the land slides in an attempt to backtrack and reconstruct the slopes as they looked before they failed. This information is very useful for the subject of this thesis as these are slopes that most likely have failed because of eroding effects on their respective sub aquatic bank terraces (Sandebring & Ottosson, 1994; Andersson et al, 1999). They provide an indication of the different slope geometries and geotechnical parameters that evidently has given cause for landslides, and they make it possible to test and possibly verify different erosion models on real cases. Another importance of studying old known landslide areas is that they provide a form of reference for slope profiles from other parts of the river. If a random slope profile from a northern section of the river show a similar geometry as the slope profile right through the old land slide at Agnesberg it would be reasonable to assume that area also has been subjected to a landslide of the same magnitude.

This chapter include the same type of analysis methods based on the same data that has been used in Chapters 5- 7, but applied specifically to the areas of the old landslides. These analyses have then been complemented with information from the official investigations of these landslides carried out by SGI. Those reports are from the Agnesberg landslide Larsson et al (1994) and Sandebring & Ottosson (1994), and for the Ballabo landslide Andersson et al (1999).

### 8.1 Agnesberg

Agnesberg is located about 5 km north of Gothenburg city and 5 km south of Kungälv on the eastern side of the river where Göta River splits into its two outlets, see Figure 7 in Chapter 4. The area where the landslide occurred is an industrial area, with a ground surface that has been graded and filled with different material over time to accommodate different industrial activities and facilities. Below the ground surface the geological conditions are for this area of Göta River; a large postglacial clay deposit down to a depth of about 40 m.

#### 8.1.1 Slope profiles

In the aftermath of the landslide many measures were taken to reinforce, stabilize and prevent any further landslides from occurring in the area. These measures included dredging and placement of blasted rock rubble and small rock on the river bottom, excavation of soil on land to minimize the load on the slope, as well as lime cement columns and geosynthetics (geonets), see Figure 17. These measures obviously affect the geometries of the slopes in the area, and therefore slope profiles have been extracted both from within the area where measures has been taken and outside of it, see Figure 17.

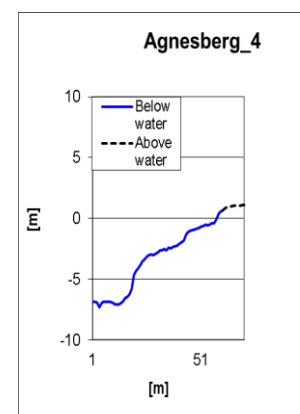
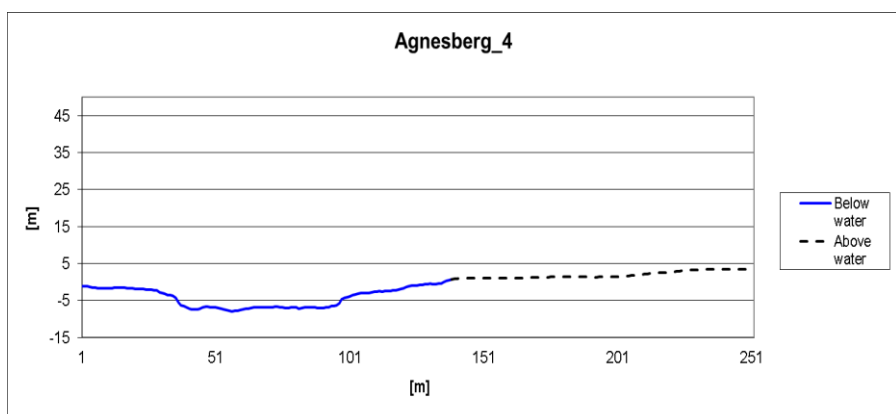
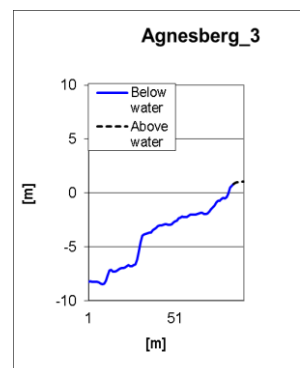
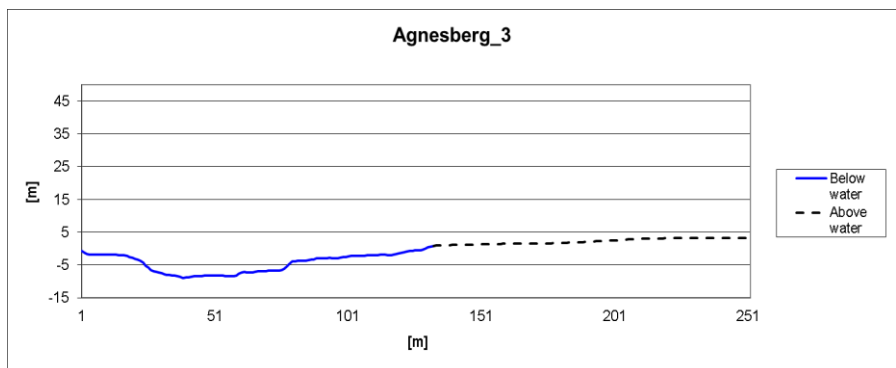
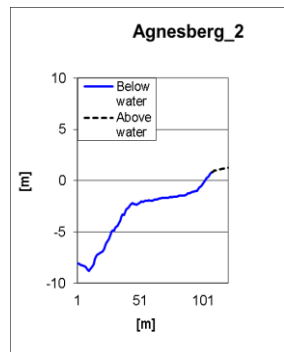
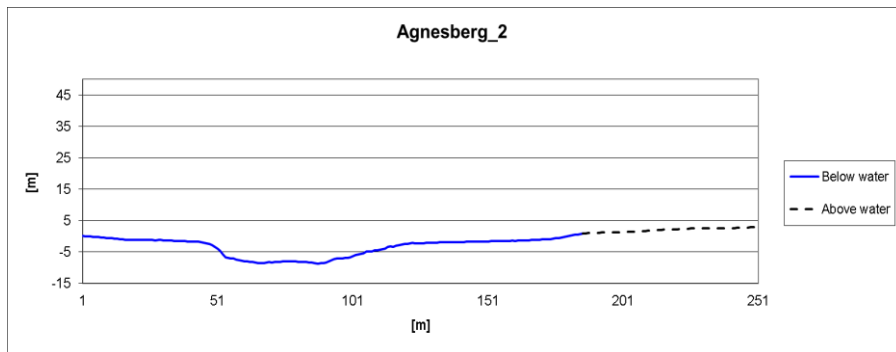
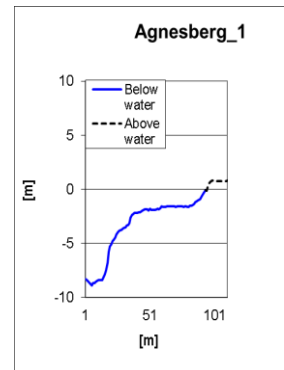
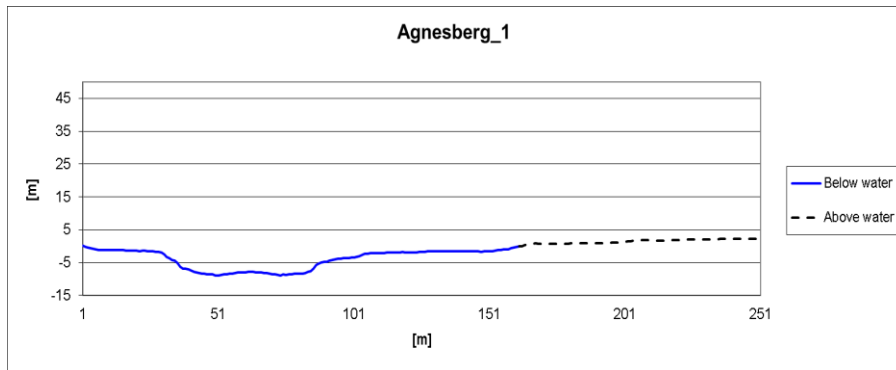


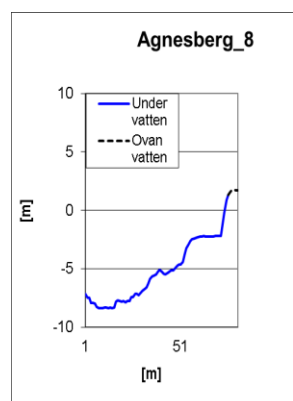
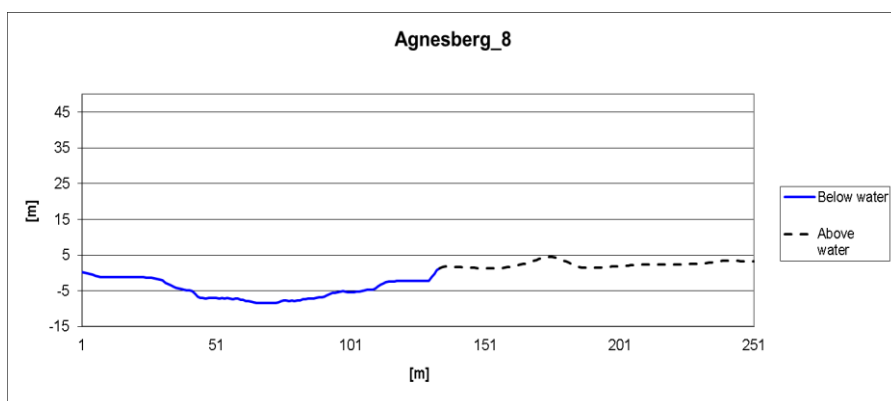
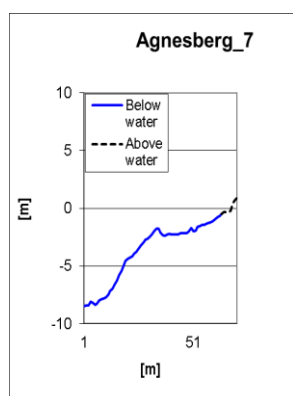
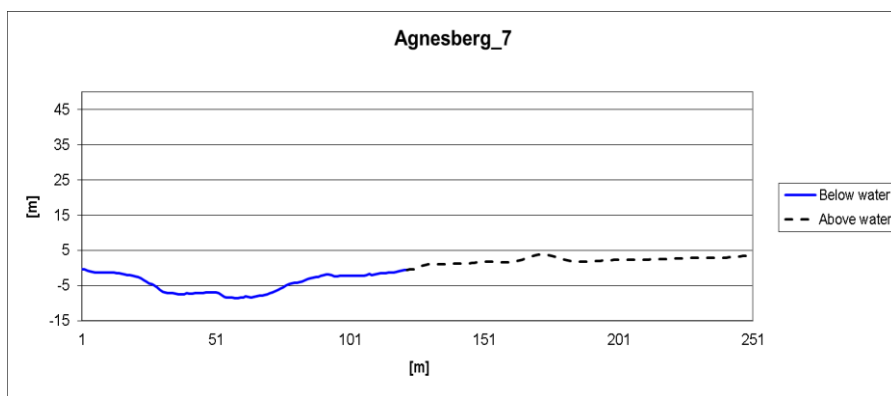
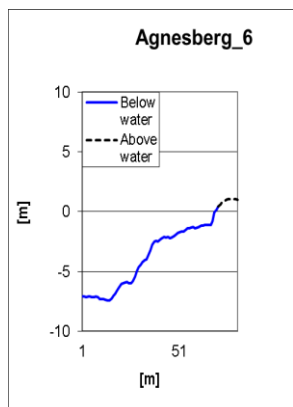
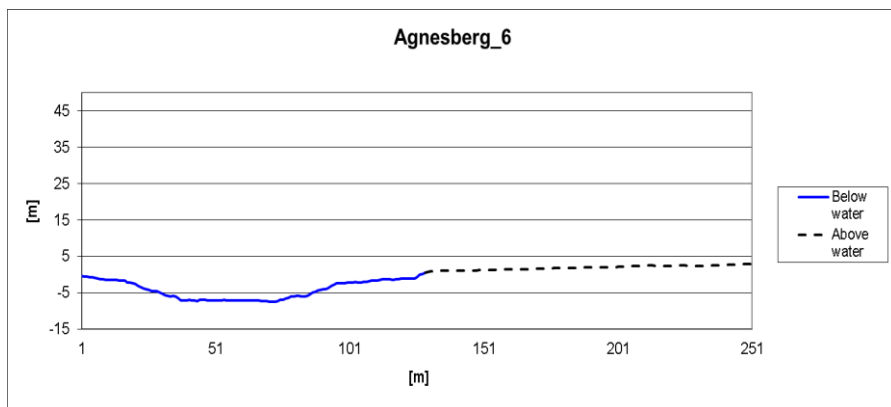
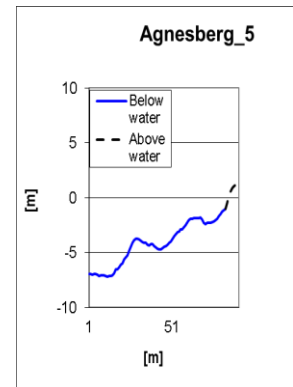
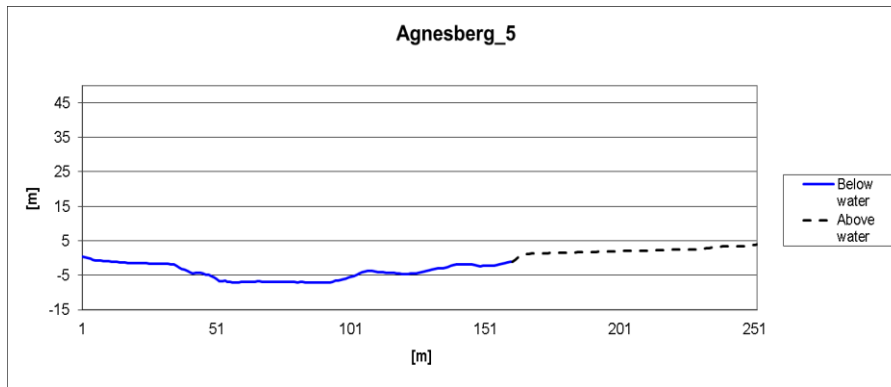


Figure 17 To the left: map of the measures taken in the aftermath of the Agnesberg landslide to reinforce and stabilize the river bottom (Sandebring, 1994). To the right: map of the same area showing profile lines (ArcGIS, 2011).

Table 5 Summary of the measures taken in the aftermath of the landslide to reinforce and stabilize the river bottom at each of the eight extracted slope profiles.

Slope name	Bottom conditions
Agnesberg_1	No measures
Agnesberg_2	No measures
Agnesberg_3	Rockfill towards subaquatic slope
Agnesberg_4	Lime cement pillars, blast rocks, rockfill
Agnesberg_5	Old mud slide
Agnesberg_6	Lime cement pillars, blast rocks, rockfill
Agnesberg_7	Rockfill towards subaquatic slope
Agnesberg_8	No measures





The profiles cover the entire length of the lines as they are drawn in Figure 17 and the smaller boxes to right show the eastern bank of the profile in a much different scale where the topographic variations are more easily observed. The features that would be expected to be seen in the profiles because of the landslide itself and the stabilizing measures taken afterwards are visible in the profiles in the figures. For example Agnesberg\_1 and Agnesberg\_2 don't show any signs of a berm at the foot of the steepest slope leading down to the deep shipping lane. Whereas Agnesberg\_3 and Agnesberg\_6 have a clear showing of what resembles such a thing, also to some extent Agnesberg\_7. This would be because of the rock fill that has been placed in accordance to Figure 17. The profile Agnesberg\_4 doesn't show this so clearly, but that profile is very close to the land slide and that area has been subjected to additional measures which might have given it a different appearance. The fact that the sub aquatic slope of Agnesberg\_4 has the lowest height of them all could be an indication that the blast rock that was put in that section has filled up the entire width of the bottom thus not leaving a berm.

Agnesberg\_5 which is the section that cuts right through the landslide shows the very distinct geometry of a bank terrace that has collapsed. Agnesberg\_8 however which would be expected to look similar to Agnesberg\_1, Agnesberg\_2 or Agnesberg\_7 looks very different. Studying a satellite photo of the area it however becomes very clear that the reason for this is most likely the pier where large ships or barges seem to dock for on and off loading of scrap goods, see Figure 18.

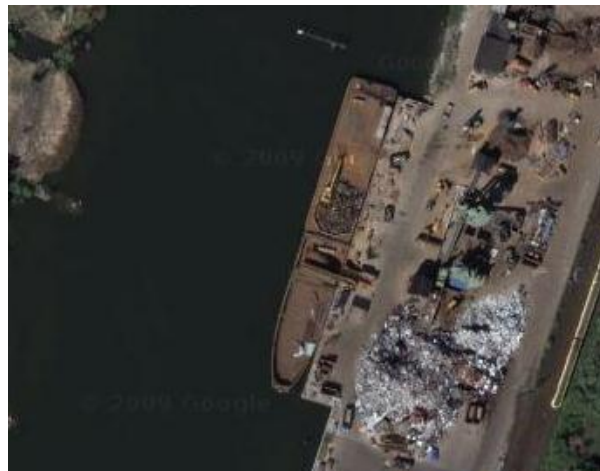


*Figure 18 Pier and barge/ship for transport of goods, in the area for Agnesberg\_8 (Agnesberg, Sweden, 2011).*

The two profiles Agnesberg\_5 and Agnesberg\_8 will be disregarded for further analyses because they are considered not to represent natural slopes in the area. In Agnesberg\_2 and Agnesberg\_6 the sub aquatic slopes towards the river bottom have a rather constant angle, as has the bank terrace. The profiles Agnesberg\_1, Agnesberg\_3, Agnesberg\_4 and Agnesberg\_6 instead have a geometry that consists of an intermediate plane between the sub aquatic slope and bank terrace, see Figure 19. These two geometries, from now on simply referred to as profile Type 1 and 2 respectively, form the base of further erosion analyses in this chapter and slope stability calculations in Chapter 8.

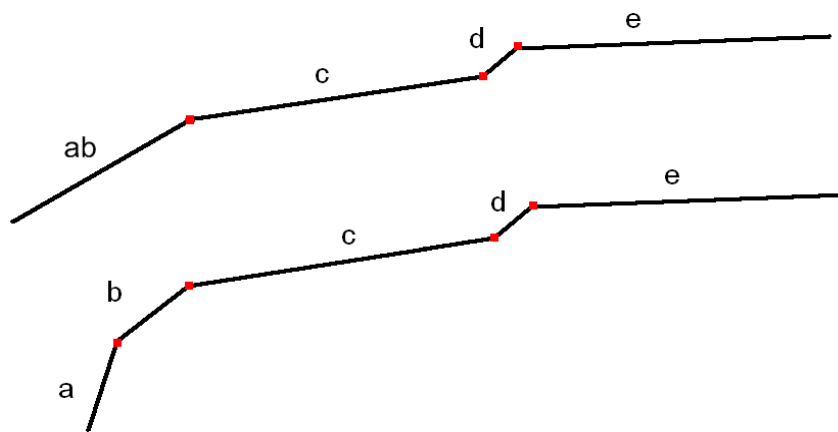


Figure 19 Conceptual drawing of the two basic geometries attained from the slope profiles in Agnesberg. Type 1 at the top and Type 2 at the bottom.

In Table 6 the slope in degrees and vertical height of the sub aquatic slopes are presented. The sub aquatic slope of Type 1 is represented by one single line called *ab*. The sub aquatic slopes that belong to Type 2 has been divided into *a* and *b*, see Figure 19 above. The height column show the heights for each of these two slopes, *a* and *b*. The adjusted height column shows the heights adjusted for any rock fill birms and other measures at the foot of the slopes, i.e. the height adjusted to conditions more similar to what they are assumed to have been before the landslide at Agnesberg.

Table 6 Slope and height of Agnesberg profiles.

Profile	Slope [ ° ]	Height [m]	Adjusted height [m]
Agnesberg_1_a	30,6	2,4	
Agnesberg_1_b	13,8	2,0	
Agnesberg_2_ab	10,2	6,3	
Agnesberg_3_a	29,1	2,8	4,5
Agnesberg_3_b	4,6	0,9	0,9
Agnesberg_4_a	28,2	2,1	3,0
Agnesberg_4_b	12,4	1,1	1,1
Agnesberg_6_ab	15,6	3,4	4,8
Agnesberg_7_a	18,9	3,1	4,1
Agnesberg_7_b	11,0	1,7	1,7

The values for the parts *ab*, *a* and *b* has then simply been averaged, the average values are presented in Table 7. The slope and width of the upper planes of the bank terraces vary between all of the different slopes. It has been approximated to resemble the geometries of Agnesberg\_2 and Agnesberg\_6. The major part of the profile that is on land, section *e* in Figure 19, has been calculated as an average of all the Agnesberg profiles. The values for *c*, *d* and *e* in Figure 19 are presented in Table 7 and the final geometries of the slopes are presented in Figure 20.

*Table 7 Values for the two type slopes.*

Profile	Slope [ ° ]	Height [m]
ab	12.9	5.6
a	26.7	3.5
b	10.4	1.4
c	3	1.6
d	12	2.0
e	1.3	2.1

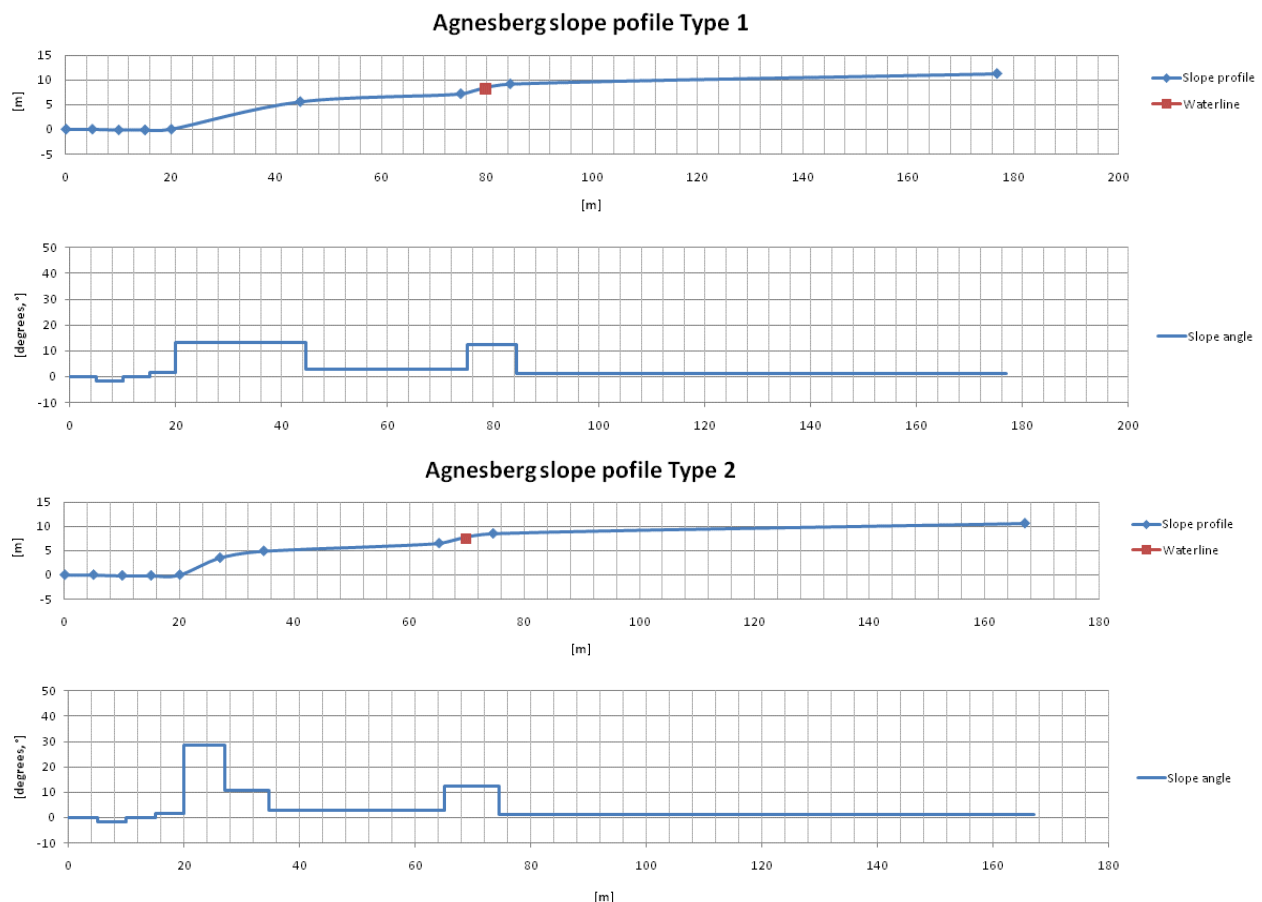


*Figure 20 Final geometries of the Agnesberg type slopes.*

### 8.1.2 Geotechnical conditions and parameters

Geological and geotechnical conditions in the area have some local variations and the parameters and conditions presented must be regarded as a generalization of the overall conditions. These conditions and properties were investigated and determined by Larsson et al in 1994.

The geology in Agnesberg does not differ from the overall description of the southern part of Göta River as described in chapter 3. This means there is a layer of clay about 35m down from the ground surface. Beneath the clay there is another thick deposit of soil, but this deposit consists of unspecified friction material. This sequence of clay and friction material creates a closed aquifer in the friction soil with an artesian water pressure that corresponds to a free water level of about 6-8 m above the ground surface, which means ground water is seeping upwards through the clay, although very slowly because of the clays low permeability.

The postglacial clay was deposited in a marine environment and there are traces of shells and other organic matter particularly in the top layer. The top layer is defined as grey highly plastic clay about 13 m thick, whereas the lower clay layer is grey and plastic with less organic matter. Because of the artesian ground water pressure significant leaching of the clay has occurred and the clay is very sensitive. The ground surface consists of about 1 m of compacted fill material. The clay beneath dry land is adjudged to be normally consolidated, and the clay beneath the river is overconsolidated due to the simple fact that the space currently occupied by the river used to be clay.

The pore water pressure profile from the ground water level down to the friction soil is regarded as having a constant gradient. The same goes for the pore water pressure profile from the bottom of the river down the friction soil. The gradient between these two pore water pressure profiles differ however, with the gradient increasing with thicker clay layers which means it is greater below the river. Along the border between the clay and the friction soil deposits the water head is 7-8 m higher than the ground level.

According to evaluations of the shear strength 45-75 m inland from the river the undrained shear strength is almost constant, about 12 kPa, down to 10 m below the ground surface. Thereafter it increases with about 0,8 kPa/m down to 18 m and after which it increases with 1,5 kPa/m. Closer to the river the distribution looks the same but the undrained shear strength is over all about 1 kPa less. Under the river the shear strength varies with the depth of the river, and Larsson et al (1994) has estimated the empirical shear strength according to Figure 21. These values were also confirmed to be close to the real values down to a depth of 14 m below the water surface. Beneath 14 m the real values were approximately 20% higher than the empirical values.

Other geotechnical parameters and properties are:

$$c' = 0.1\tau_{fu} \quad (\text{not less than } 1.5 \text{ kPa in the upper layers})$$

$$\gamma_{clay} = 18 \frac{kN}{m^3}, \gamma_{crust} = 20 \frac{kN}{m^3}, \gamma_{friction\_soil} = 20 \frac{kN}{m^3}$$

$$\varphi'_{clay} = 30^\circ, \varphi'_{crust} = 36.5^\circ, \varphi'_{friction\_soil} = 39^\circ$$

GWL (ground water level): 1m below the ground surface.

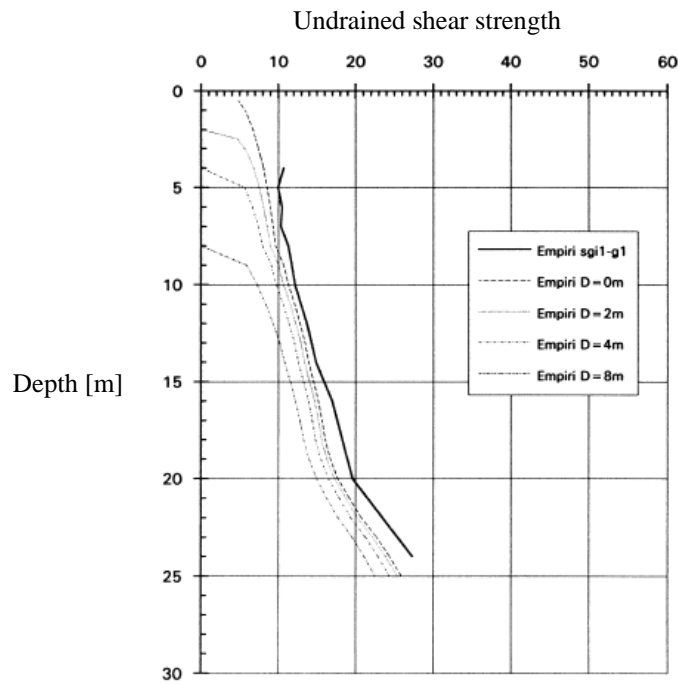


Figure 21 Empirical undrained shear strength beneath the river at various depth (Larsson et al, 1994).

### 8.1.3 Erosion

To model erosion in the river in the area of the Agnesberg landslide the two bathymetric datasets from 2003 and 2009 as well as the full DEM model have been studied carefully both directly south and directly north of the area where most of the stabilizing and reinforcing measures were taken.

An overview of the dataset containing the difference between 2003 and 2009 reveals patterns of negative values forming elongated patterns in the river, an example of this can be seen in Figure 22 with very distinct yellow bands in a north-south direction. For these datasets negative values (yellow and red) means that there has been an increase in depth from 2003 to 2009. Because of the clear patterns and values that seem to exceed the error margins it would be easy to make the assumption that these bands indeed represent areas of the river bed where significant erosion has taken place. These patterns also coincides well with the theory that corassion along narrow trenches and gutters along the bottom is the dominating form of erosion.



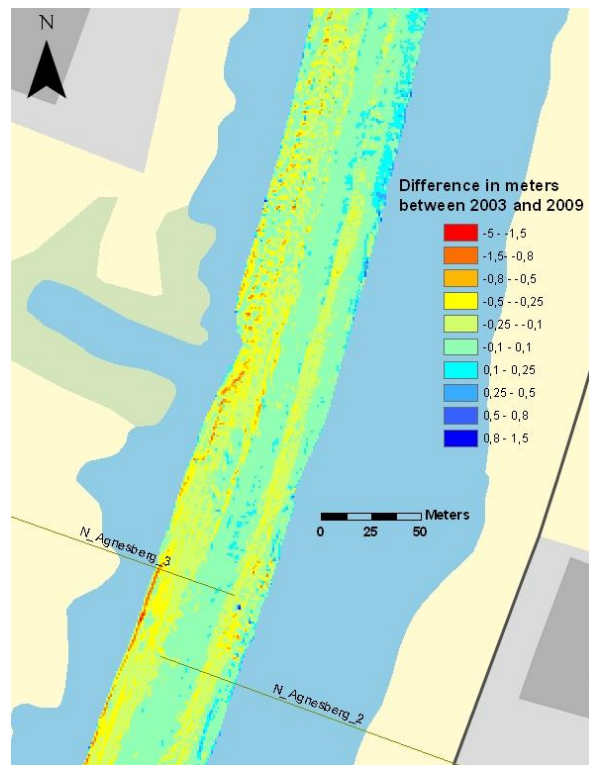
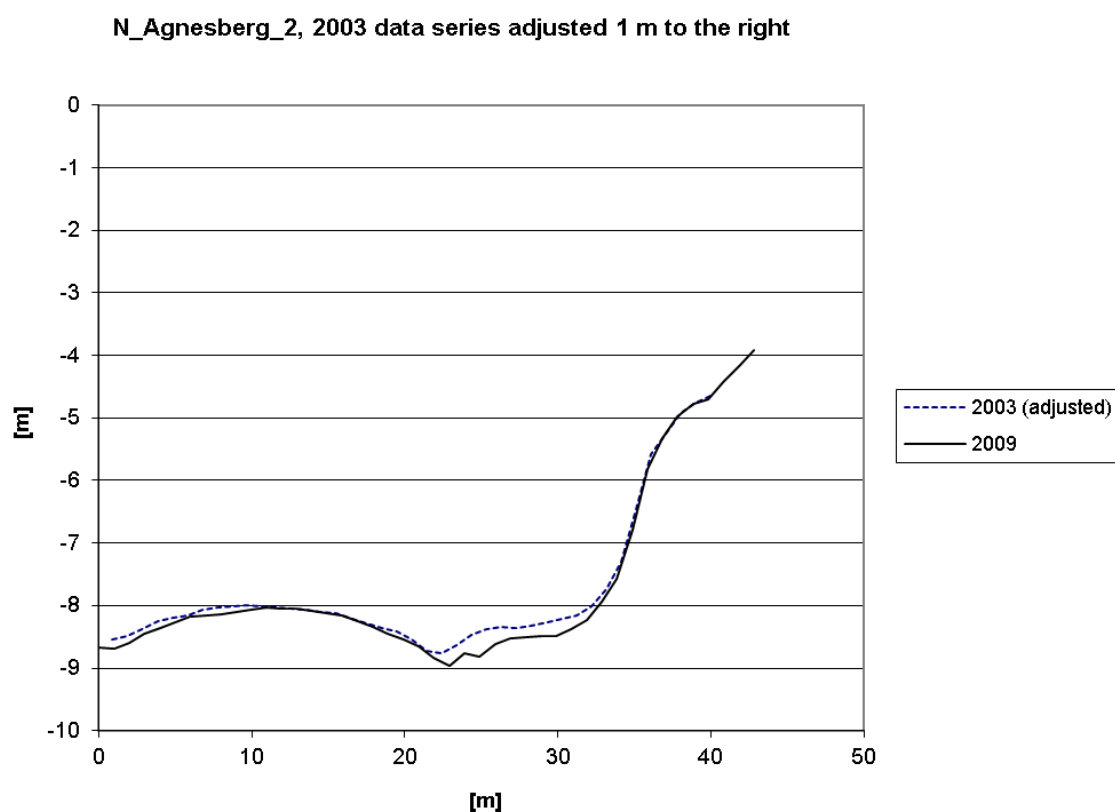
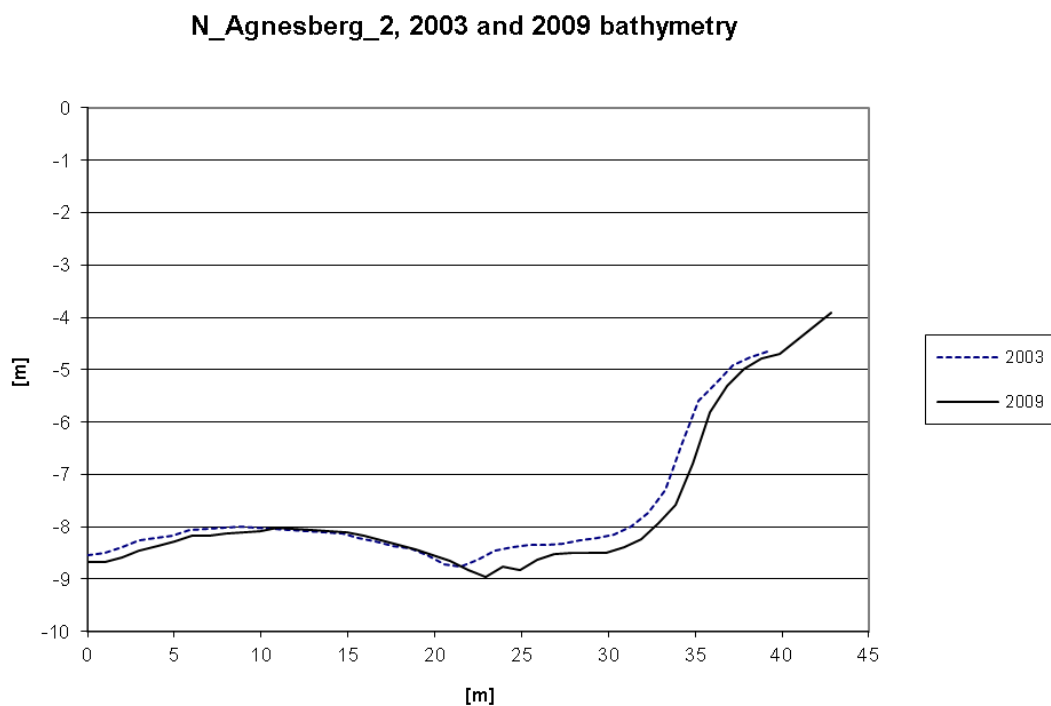


Figure 22 A typical pattern of bathymetry difference between 2003 and 2009 just north of Agnesberg Landslide. Negative values, represented in yellow and red colours, form two distinct bands in north-south direction. Also visible at the bottom of the picture are the two cross sections N\_Agnesberg\_3 and N\_Agnesberg\_2 (ArcGIS, 2011).

A closer look at these patterns and corresponding data however reveals that this first interpretation might not be entirely accurate. It is well known that the positioning of the measuring equipment and the eco soundings are not exact. It is difficult to exactly match the two different datasets and create a dataset where a measuring point in the 2003 dataset corresponds to the same actual coordinate in 2009. The subsequent data processing and transformations between coordinate systems etc. can also give rise to further uncertainty. In the case of uncertainties with regard to the actual eco soundings, it is hard to pin point specific errors as it could vary very much along the river.

Studying this data from another view, such as part of the cross section N\_Agnesberg\_2 shown in Figure 23, the part that is represented as yellow in the dataset in Figure 22 is very clear. Almost the entire cross section from about 20 to 40 m in x direction shows that the 2009 values are consistently lower than the 2003 values. From 0 to 20 m in x direction the datasets also appears to be mismatched.

As most of the general theories regarding erosion in Göta River do not support that the river bed would erode in this manner, it is assumed that one of the datasets or both of them are out of position. The 2003 values are assumed to be too far to the left, or east, relative to the 2009 data in his area. In the bottom graph in Figure 23 the 2003 data was adjusted 1 m to the right. The adjustment gave a very good fit of the two profiles, and gave an appearance more similar to what one would expect taking the Göta River morphology and erosion theories into consideration; that is, very little or no direct fluvial erosion of clay surfaces, but erosion caused by corassion.



*Figure 23 Plots of cross section N\_Agnesberg\_2 north of Agnesberg for 2003 and 2009 bathymetry. Top: the original plot of the datasets. Bottom: the 2003 data values has been adjusted and moved 1 m to the right relative to the 2009 data series.*

The dataset containing the difference between 2003 and 2009 is not accurate in this area, resulting in the exaggerated impression of erosion as seen in Figure 22. This phenomenon was also observed in other areas along the river, which also at first glance gave clear impressions of significant erosion and similar patterns to the one in Figure 22. There are however as many areas where this problem does not exist, which might indicate that this is an issue that is related to the positioning of the measuring equipment during the actual eco soundings, as otherwise the whole dataset would have shown the same displacement.

One such area could be found south of the Agnesberg landslide, see Figures 24-25. About 700-1200 m south of the Agnesberg landslide site, cross sections without the same type of supposed error as described above was identified. This area was therefore chosen for further analysis, to see if it would be possible to describe and parameterize characteristic erosion for subsequent stability analysis of the *type a* and *type b* Agnesberg profiles.

The river bottom in this area shows a special characteristic where the middle of the deep causeway has a slightly higher elevation than closer to the edges. This means that the bottom becomes deeper as you move out from the middle in both directions, forming something that could be described as two shallow trenches running along both sides of a centre ridge. This characteristic is also very clear in Figure 23, meaning the area north of Agnesberg is morphologically similar. This is of course also a good indication that the area at the old landslide also shared this feature before the landslide.

This is clearly seen in the DEM 2009 model of the area in Figure 24, where the yellow-green-blue band in the middle represents the elevated centre ridge and the orange-red colours besides it represent these trenches. Further out the colours rapidly become dark blue as the sub aquatic slopes rises up from the trenches.

The theory is that the primary erosion taking place in this area would be through corassion, where courser soil particles accumulate in these trenches and “grind” down the clay as they are transported along the bottom by the water. To test this, two lines were drawn, one along the bottom of the eastern trench and one along the top of the ridge in the DEM 2009 model. In Figure 25 the 2003-2009 dataset for the same area is presented with these lines, and it directly becomes obvious that there tend to be more yellow colour along the trench line than the ridge line. It is also clear that the 2003-2009 dataset does not show the same strong yellow band as in the Figure 22 north of Agnesberg caused by the possible positioning error.

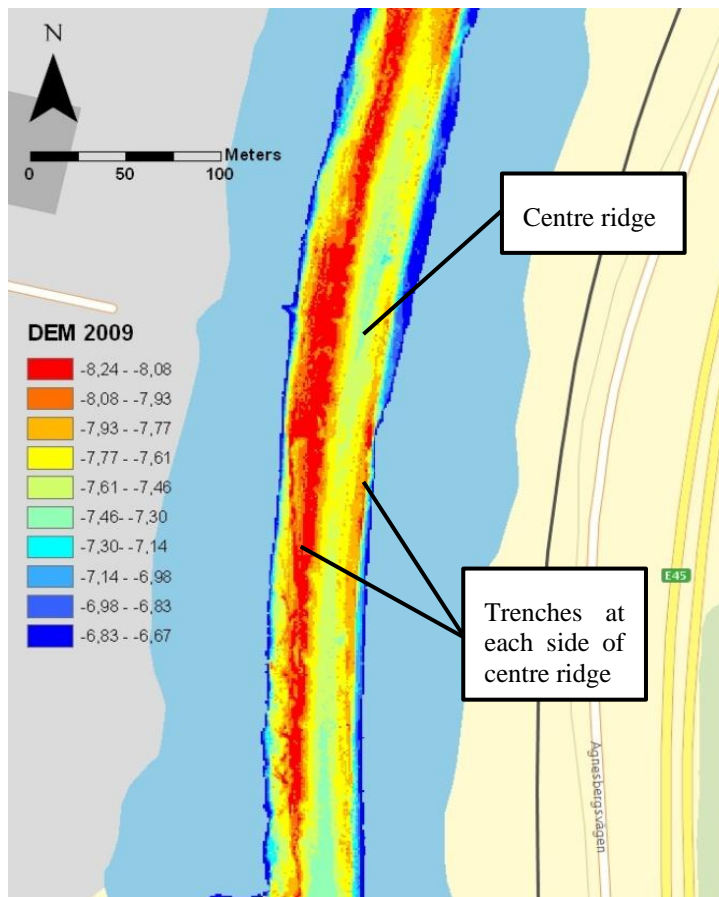
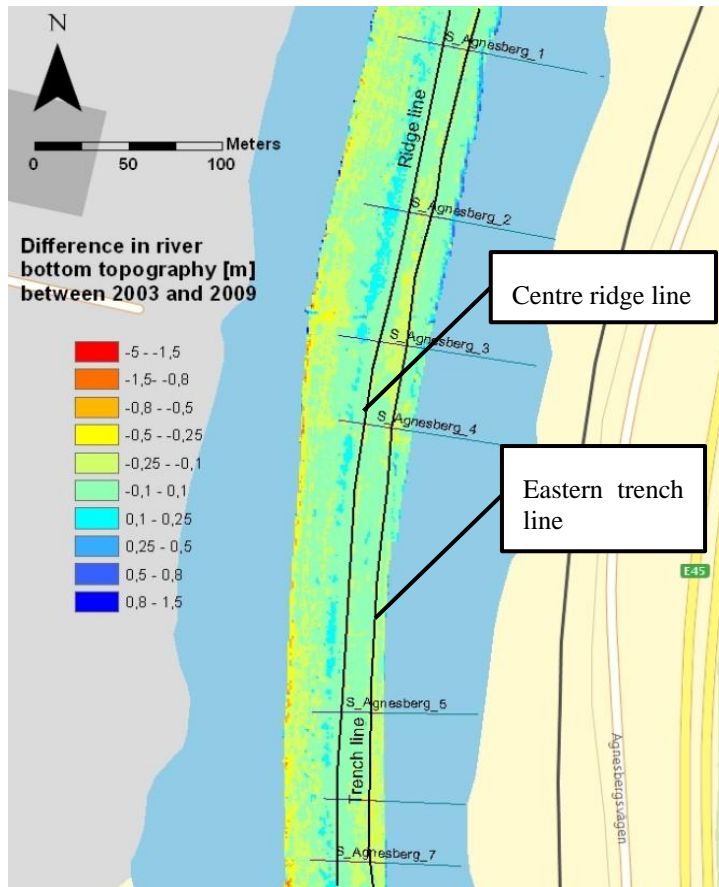


Figure 24 South of Agnesberg. DEM 2009 model, bathymetric data from 2009, showing a centre ridge and two trenches along the side of the ridge. The trench to the left, west, being wider (ArcGIS, 2011).



Figur 25 The same area as in the previous figure, but instead showing the dataset 2003-2009. Also visible are the ridge line, the eastern trench line and some of the cross sections extracted from this area (ArcGIS, 2011).

To analyse and verify the erosion theory further, as well as quantifying and parameterize the possible erosion, values from both the DEM and the 2003-2009 datasets were extracted along the lines using 3D-Analyst in ArcGIS. These values are presented in Figures 26-27.

The ridge and trench lines were drawn from north to south, meaning that in the diagrams  $x = 0$  refers to the northern point of each line. The trench line and ridge line naturally doesn't follow the same coordinates, or are perfectly parallel to each other, but they are close enough for them to be plotted together and for those plots to be relevant. Figure 26 simply shows the elevation along each line. The average elevation for the ridge and trench respectively is -7.71 m and -7.56 m, meaning that overall it is in fact a rather shallow trench relative to the ridge. Figure 27 shows the values of the 2003-2009 dataset, i.e. the changes in elevation between those years along each line. In Table 8 the statistics of these values are summarized.

*Table 8 Summary of statistics from the values along trench and ridge line.*

	Trench line	Ridge line	Trench line where the 2009 data adjusted with -0.07 m	Ridge line where the 2009 data adjusted with -0.07 m
Max:	0.05	0.07	-0.02	0.00
Min:	-0.29	-0.18	-0.36	-0.25
Average:	-0.12	-0.03	-0.19	-0.10

These numbers show, and verify, that the change in elevation is indeed much larger along the trench than on the ridge. The average decrease of elevation in the trench is -12 cm. Along the central ridge the values oscillate closer to 0 cm with -10 cm being the average. Regardless of the uncertainty in the echo soundings themselves, there is an association or correlation of elevation change between the trench and the ridge in the sense that there is a larger possibility that any given point along the trench has been subjected to a larger elevation decrease than any given point on the ridge line than vice versa.

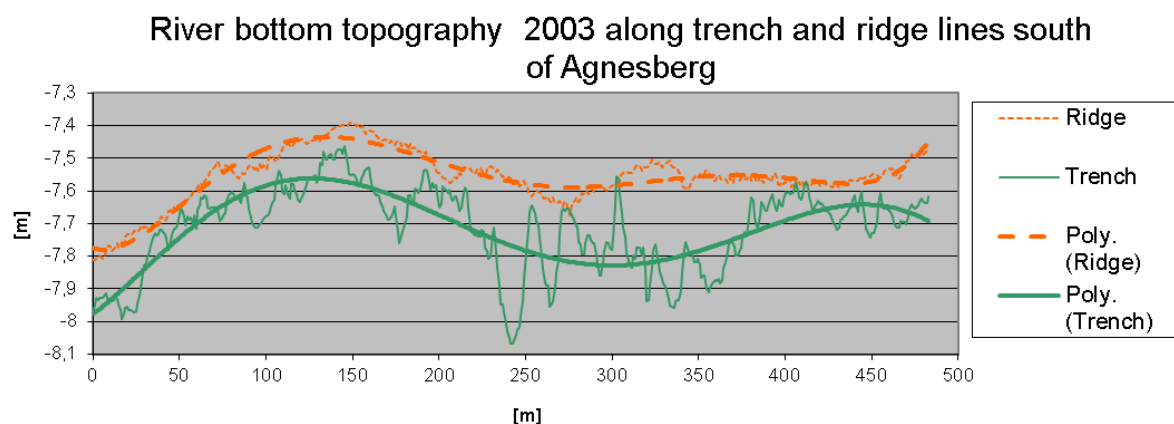


*Figure 26 Bathymetry values along ridge and trench lines.*

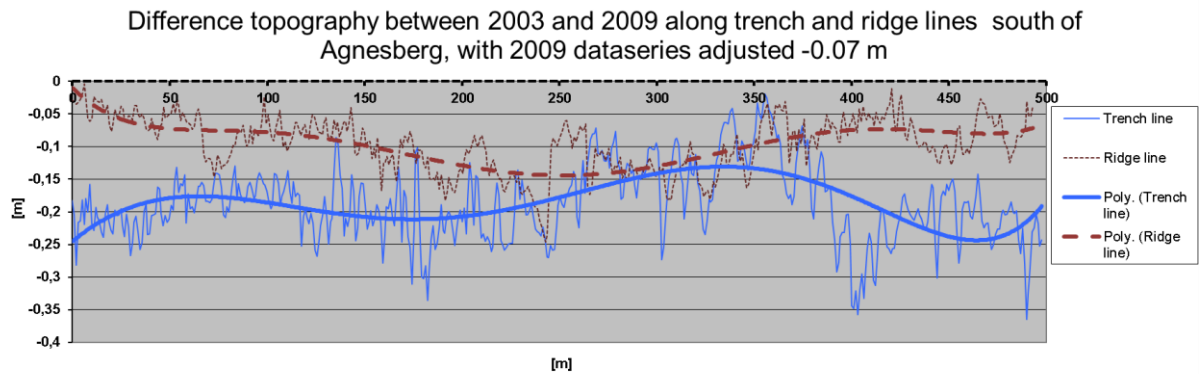


Figure 27 Values of the 2003-2009 dataset along ridge and trench line, i.e. the change in bathymetry between 2003 and 2009.

All of these things indicate that the active and dominating erosion is a corassion process in the trench line. Figure 28 which show backscatter data (see Chapter 5, Section 5.2.1) for the area also indicates that sand and coarser material has accumulated along the trench line. The patterns might not be that easy to distinct, but along the trench line there is more purple and red, indicating fine to very coarse sand and possibly hard clay and organic material. Along the ridge there is however more clearly a band of green and black- indicating very soft clay and mud sediments. The trench and ridge lines are shown in white, not to be confused as representing class number 5 in the backscatter classification which is also represented by white colour.

As an estimate of the rate of the erosion, to be used for slope stability calculations, an average of the values in the 0.07 m adjusted data series was calculated. This yielded a value of -19 cm, see Table 8. Spread over 6.5 years this gives an annual average erosion rate in the trench of about 3 cm. By adding appropriate geometries of the trench to the *Type a* and *Type b* slopes described in Section 8.1.1 the result is erosion modelled as corassion along a trench at the base of the subaquatic slope, see Figure 29.

This erosion can be parameterized either as time or depth. Having time as a parameter is not without risk, as this would assume hydraulic and other conditions which affect the corassion to stay the same as during the time period between 2003 and 2009. Climate change could for example affect hydrological conditions, and geotechnical factors such as a change of consolidation, which is a very important factor when it comes to erosion of cohesive soils, might also change the erosion rate as the erosion reaches deeper and deeper clay. Anthropogenic factors such as ship traffic, as well as marine constructions and regulations of water flow in the river will also play a role.

It should also be noted that the erosion value used is the average value for the whole data series. The average value for the top 10 % of the biggest negative changes in elevation between 2003 and 2009 is -0.29 m, or 4.5 cm/year, which is an erosion rate 50 % higher than the average.



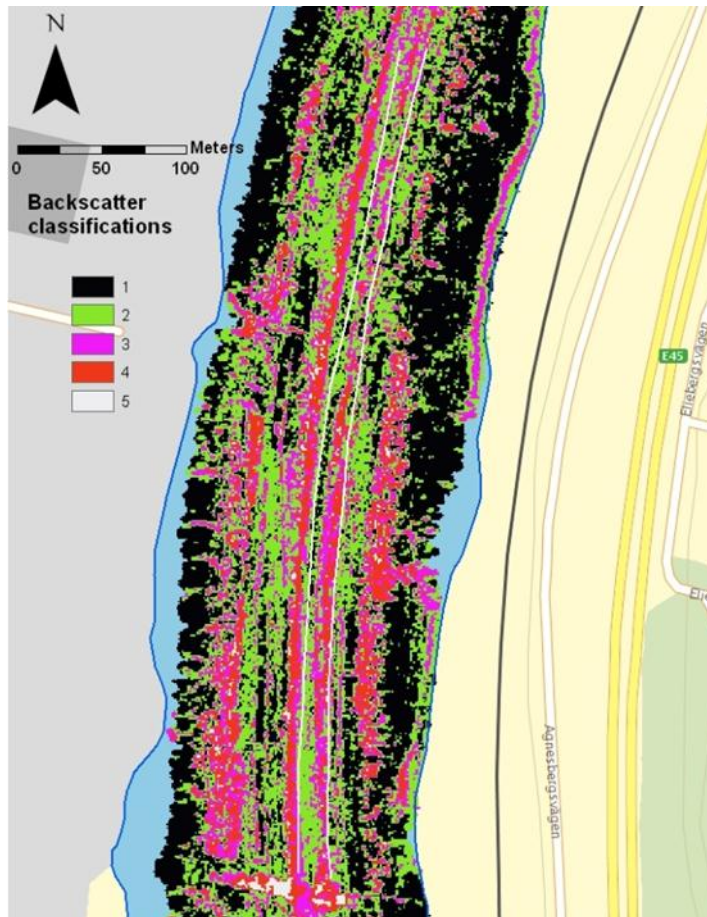


Figure 28 Backscatter data for the studied area. The ridge and trench lines are seen as white lines. See Chapter 5, Section 5.2.1 for details with regard to the classification (ArcGIS, 2011).

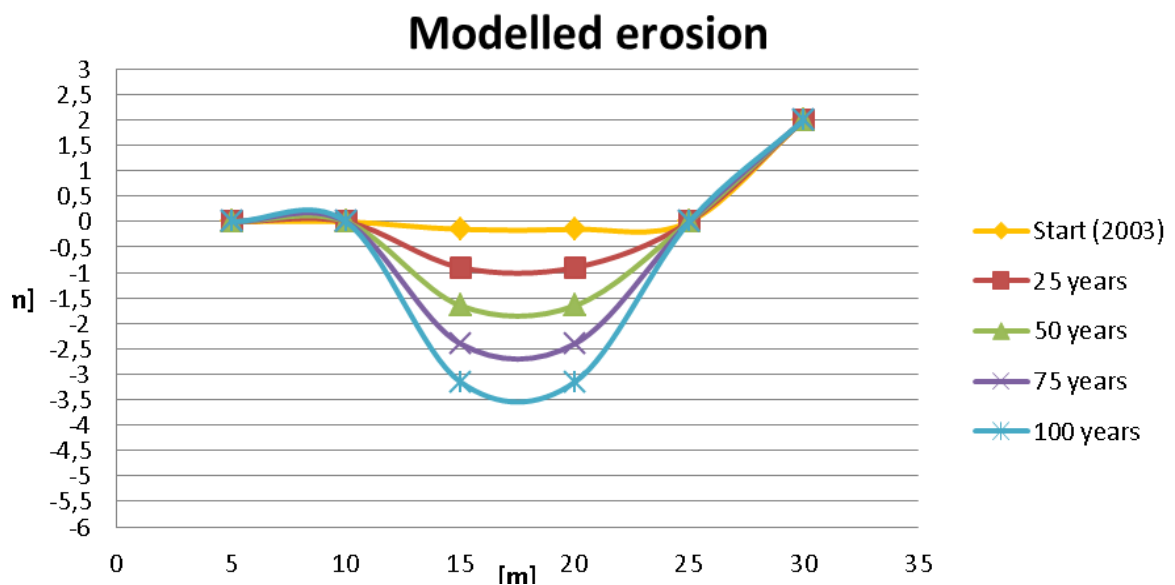


Figure 29 Erosion modelled as corassion in trench at base of sub aquatic slope.

## 8.2 Ballabo

Ballabo is located about 5 km south of Lilla Edet on the western bank of Göta River and the local area has been prone to large landslides earlier in history, the oldest documented land slide dating as far back as the year 1733. In 1957 the well-known landslide Götaskredet took place about 1.8 km north of Ballabo, a landslide which covered an area of 15 ha. The Ballabo landslide which occurred 16th of april 1996 affected a stretch of about 110 m along the river, and reached about 50-70 m inwards. The site of the Ballabo land slide is surrounded by farmland, sloping gently upwards from the river at a slope of 1:50 (Andersson et al, 1999).

### 8.2.1 Slope profiles

Five slope profiles have been extracted from the area as shown in Figure 30-31. As there were no subsequent reinforcement and stabilization measures taken in the river in the same way as was the case for the landslide in Agnesberg, the geometric profiles of the slopes and river bank right next to the landslide area is considered to be very similar to the slope that failed. By looking at the extracted profiles in Figure 32 the characteristic shape of the subaquatic slope and bank terrace quickly becomes quite clear, as does the effects of the landslide on the profile geometry by comparing profiles 1 and 2 north of the landslide with profile 3 (Ballabo\_1, Ballabo\_2 and Ballabo\_3). Profile 4 (Ballabo\_4), to the immediate south of the landslide, shows a partial reverse in the geometry towards that of slope 1 and 2. However by looking at profile 5 and also by studying the height contour lines in Figure 31 it seems as though the area to the south might also have been subjected to a landslide at some point in time. The river bottom of profile 5 shows the typical uneven characteristics of a landslide, as well as an apparent subsidence of the land above the water line similar to that seen in profile 3. The height contours in Figure 31 also show a distinct bulge toward the deep part of the river centred on profile 5. Because of this the profiles 1 and 2 were considered to be most representative of the characteristic slope profile geometry of slopes not subjected to previous landslides of the area,. As profile 2 is smoother than profile 1 the type profile representing the Ballabo area was firstly chosen to simply be slope profile Ballabo\_2. However, as subsequent slope stability calculations showed that this slope had a safety factor close to 1, depending on varying parameters, it was decided to also include an additional slope profile in the analysis to be able to study long term effects of erosion on the slope stability.



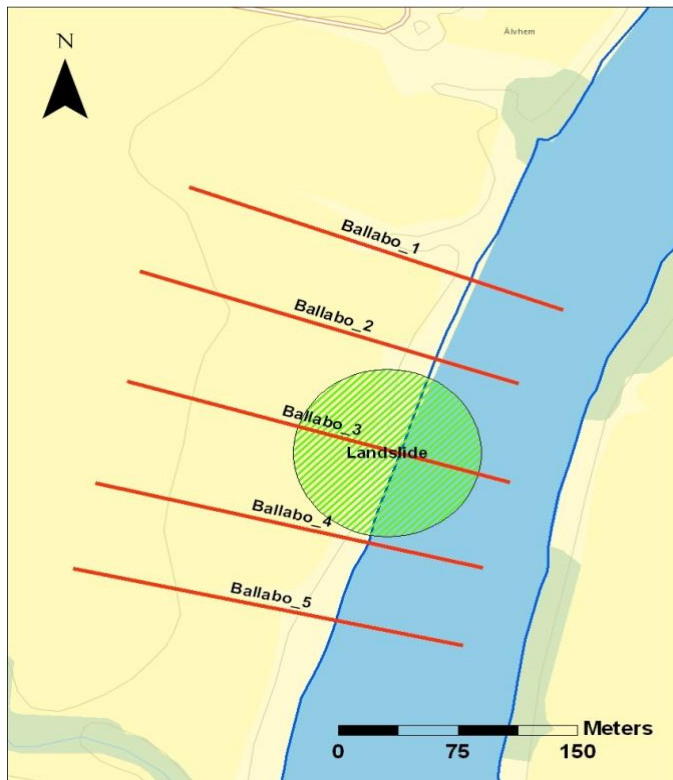


Figure 30 Area of the old Ballabo landslide, with marked landslide and drawn profiles (ArcGIS, 2011).

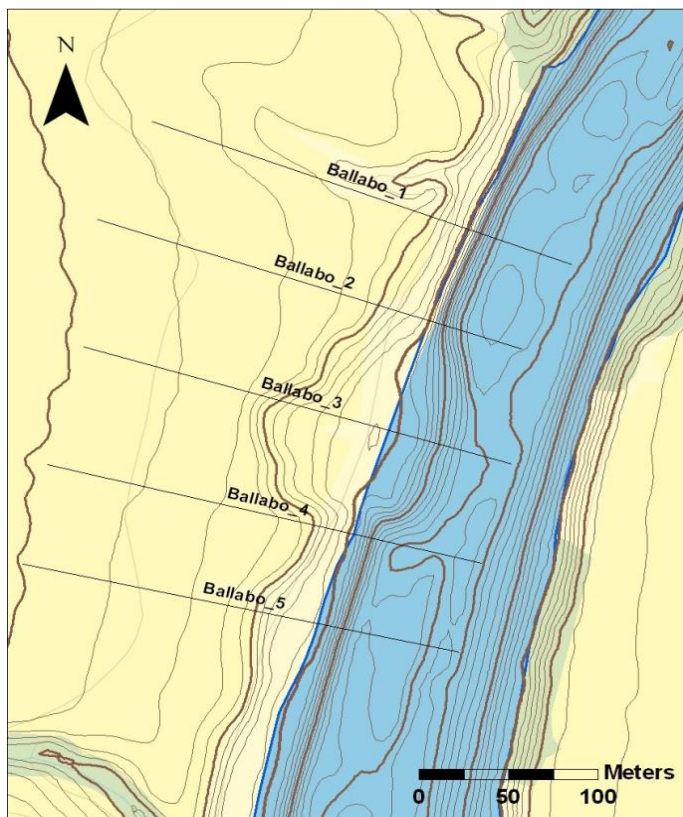


Figure 31 Area of the old Ballabo landslide, with marked profiles and topographic isolines (height contour lines) (ArcGIS, 2011).

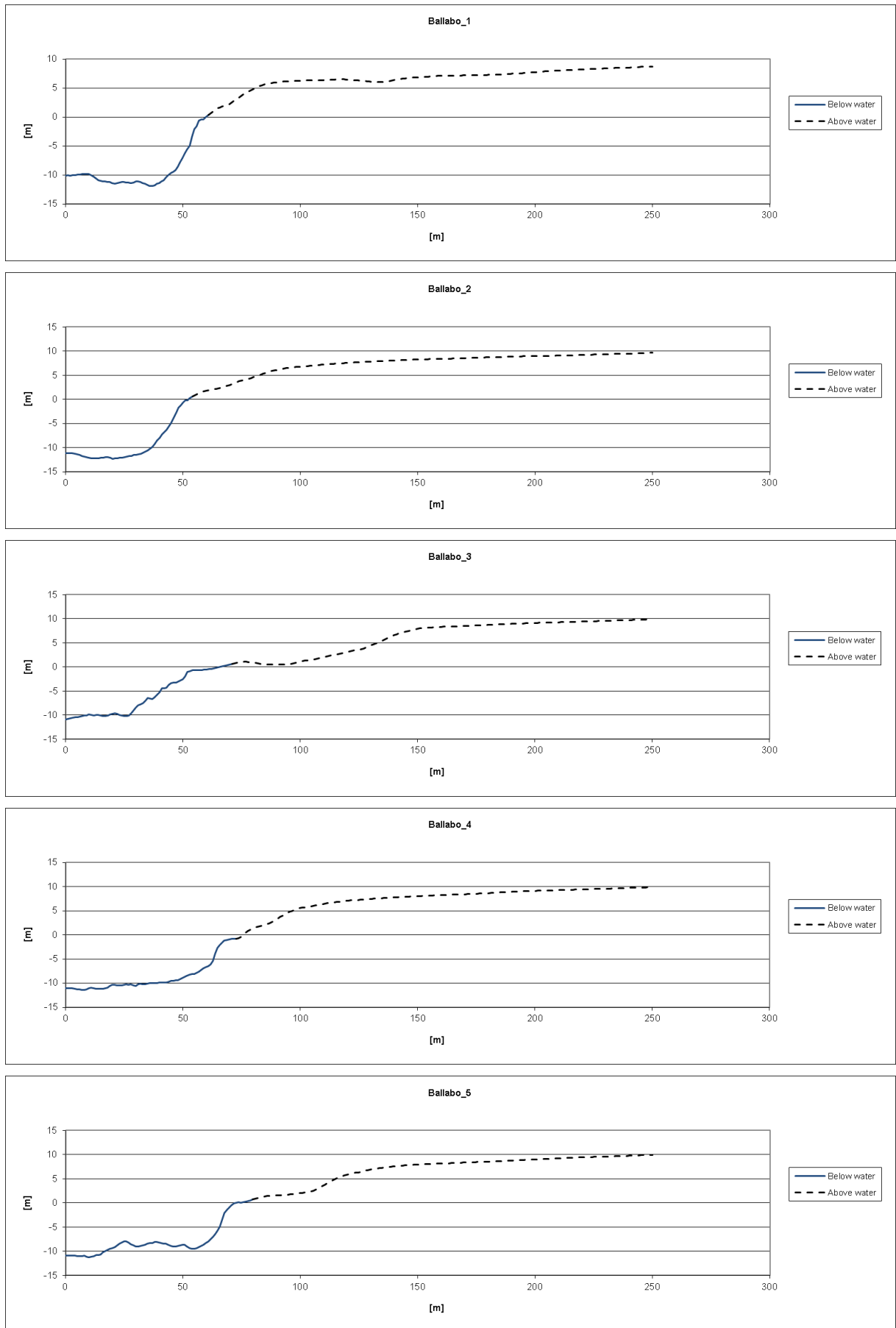


Figure 32 Ballabo profiles seen in the figures on the previous page.

The final geometry, including the slope angles, for the Ballabo type profiles can be seen below:

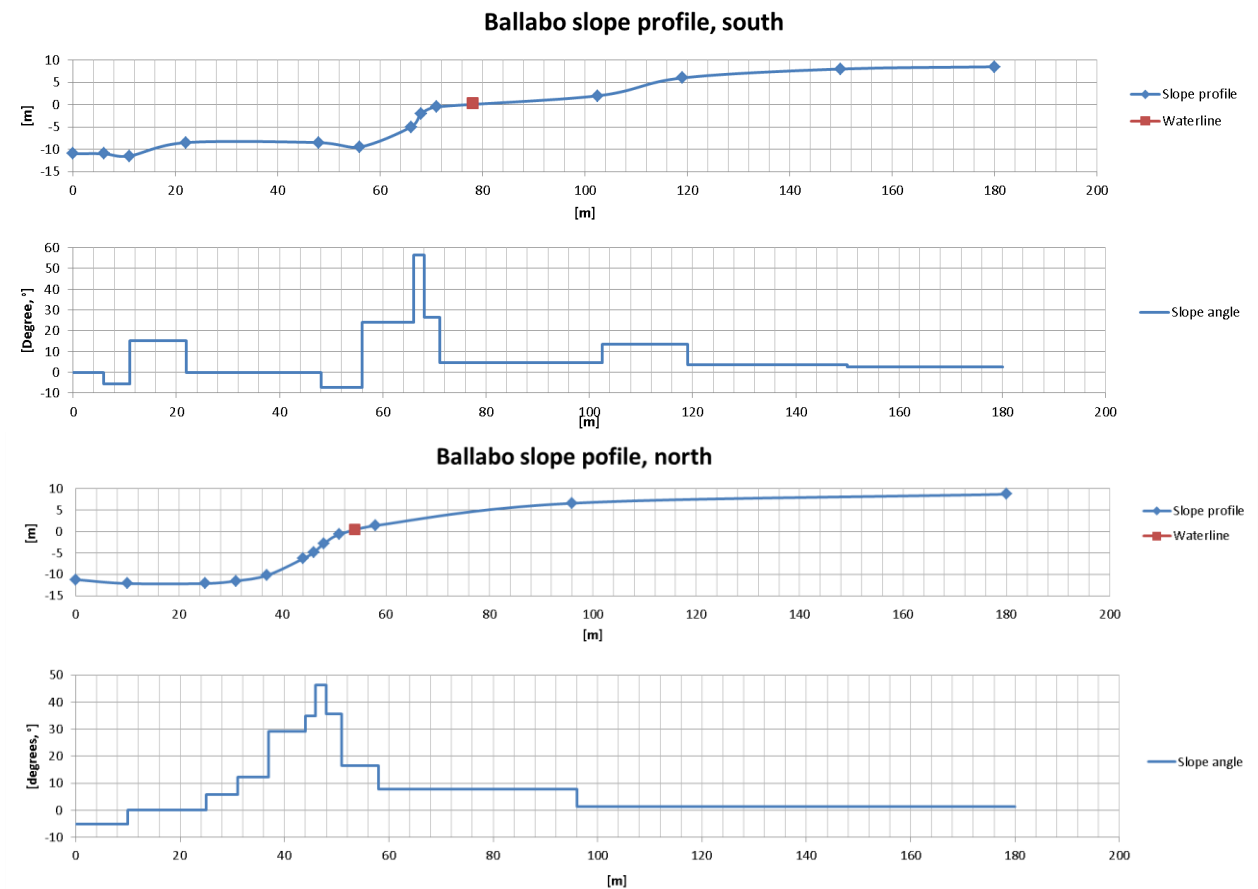


Figure 33 Geometry of the slopes to the north and south of Ballabo.

## 8.2.2 Geotechnical conditions and parameters

The soil in the area mainly consists of postglacial silt and clay and various mixtures of the two, and the total depths of the soil sediments are about 50 m. The clay is probably underconsolidated with cohesionless soil, modelled as a typical layer of 15 m friction soil (Mohr-Coulomb;  $\gamma = 20 \text{ kN/m}^3$ ,  $\phi' = 39^\circ$ ) in the slope stability analysis.

The top layer on land consists of high-plastic muddy clay and silty clay. Beneath this the clay is high to very high-plastic to a depth of 25m, and below this level the soil consists of silty clay and clayey silt with shells. Down to 25 m the sensitivity of the clay is low to medium, below this it is high. The clay is slightly over consolidated with an overconsolidation corresponding to about  $1.25 \cdot \sigma'_{v0}$ , which is normal for the region.

On land behind the slope crest, at about coordinates 96:6 m in the north Ballabo slope profile in Figure 33, the undrained shear strength is constant down to a depth of about 7.5 m at 15 kPa. Between this depth and down to a depth of 16.5 m the shear strength increases with on average 0.83 kPa/m. Below this depth the rate of increase rises to 1.17 kPa/m.

In the slope closer to the river the undrained shear strength is constant at about 20 kPa down to the level of -4 m (with the 0-level referenced as in Figure 33). Below this level it increases on an average with 0.58 kPa/m down to level -10 m. After that the increase rises to 1.13 kPa/m.

Where the river has a depth of about 2 m, the shear strength can be described as increasing from 12 kPa at level -2 with on average 1.31 kPa/m to the level -10 and there under with 1.08 kPa/m. Where the water depth is 8 m, the undrained shear strength can be described as increasing from about 14.5 kPa at the level -8 with on average 1.57 kPa/m down to the level -20 from which it increase with 1.08 kPa/m

The groundwater level was at the time of the investigations rather stable throughout the year at a depth of about 0.5 m below the ground surface. The pore water pressure showed a profile with an increase with depth slightly higher than hydrostatic pressure, and in the friction soil layer at about 50 m depth the ground water flows freely and gives rise to artesian water pressure.

Other geotechnical parameters and properties are:

$$c' = 0.1\tau_{fu}$$

$$\gamma_{clay} = 16 \frac{kN}{m^3}, \gamma_{crust} = 20 \frac{kN}{m^3}$$

$$\varphi'_{clay} = 30^\circ, \varphi'_{crust} = 36.5^\circ$$

These geotechnical parameters form the base for both of the Ballabo slopes. For the south Ballabo slope however, there is an additional region added to represent the soil mass on the river bottom. The strength of this mass is uncertain, both as it is assumed to be formed through an old landslide the strength is assumed to be less than the soil on the same level in the slope. Measurements from the slide mass in the Ballabo landslide shows shear strength of 8 kPa, however as the Ballabo landslide is much younger than the possible landslide to the south would be the shear strength in that slide mass would likely be higher due to. A subsequent sensitivity analysis with regard to this parameter shows that the combined factor of safety changes from 1.092 to 1.093 when changing the undrained shear strength from 8 kPa to 16 kPa, meaning the effect of a variation within this range has a very limited effect on the global slope stability. In the following calculations of the slope stability the value of this parameter was set to 12 kPa.

### 8.2.3 Erosion

Using the same approach as for Agnesberg in Section 8.1, firstly overviewing the bathymetric dataset as well as the 2003-2009 dataset, Figures 34-35, it quickly becomes apparent that the bottom topography looks different from Agnesberg. The river bottom is much more hilly and varying with elevation differences up to about 5 meters between the deepest holes and hills in the centre of the river.

Looking at the 2003-2009 dataset the old landslide mass is the feature standing out the most. This slide mass is clearly indicated as the area which has been most subjected to erosion between 2003 and 2009, something that would be consistent with the fact that this soil is more soft and loose than the surrounding soil and therefore would be less resistant to erosion. Another fact that would make it more erodible is that because of the way the soil mass bulges out from the river bank it causes a hydraulic shear stress exerted on the river bottom by the flow of the water that is about 2-3 times higher on the slide mass than shortly upstream according to the hydraulic model by SMHI, Figure 36. All in all, this suggests that the 2003-2009 dataset is accurate enough in this section to indeed give an indication of possible erosion between these years.

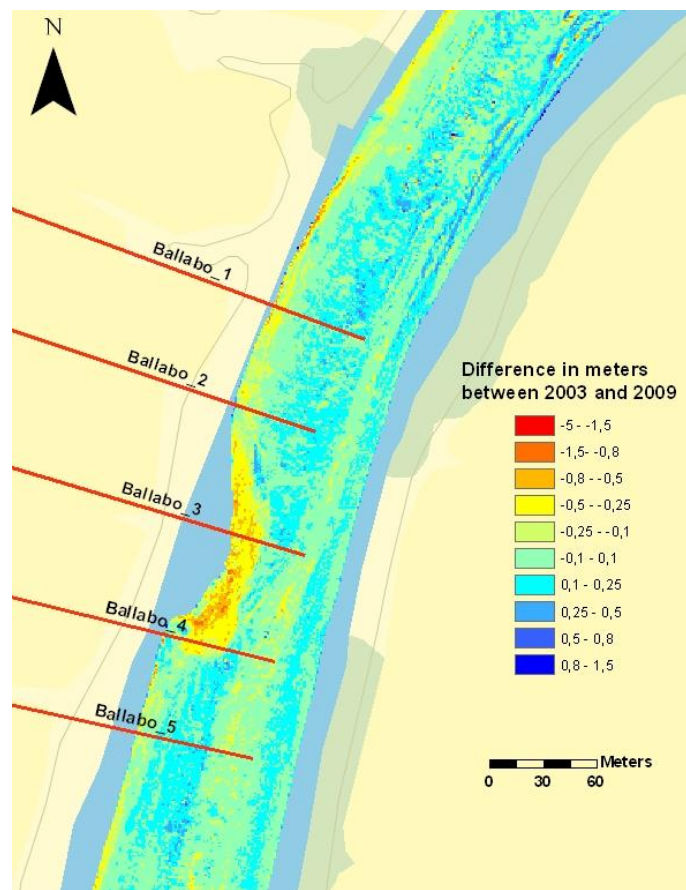


Figure 34 The 2003-2009 dataset for the Ballabo area. The old Ballabo landslide is clearly visible under the Ballabo\_3 profile as a yellow and red bulge toward the middle of the river, indicating the erosion of the old landslide mass (ArcGIS, 2011).

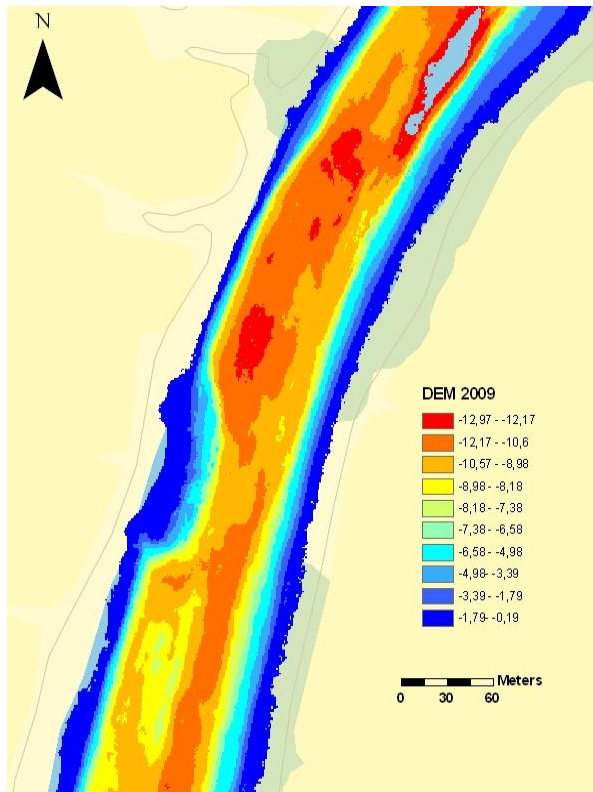


Figure 35 River bathymetry of the Ballabo land slide area. In this figure the old land slide mass is clearly visible as a blue bulge, meaning that the soil mass covered the river bottom with several meters of clay of which most is still left (ArcGIS, 2011).

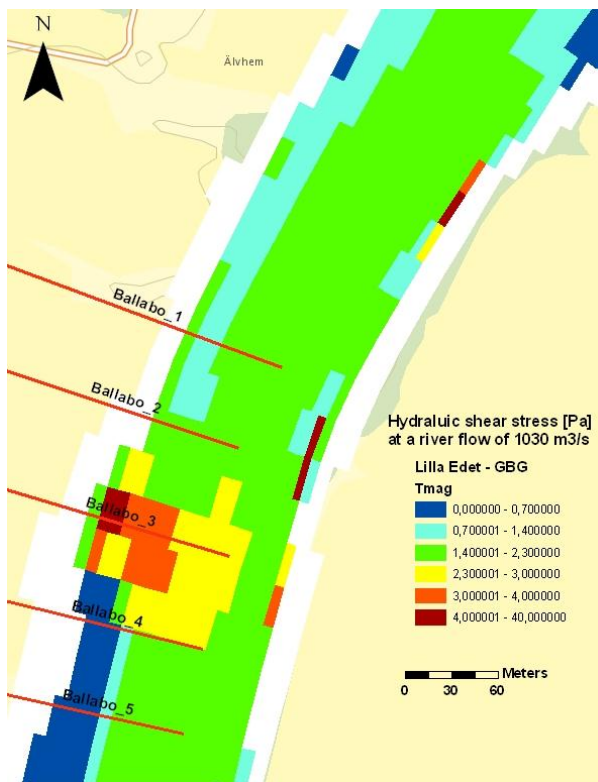


Figure 36 Hydraulic shear stress along the river bed clearly heightened over the old land slide mass (ArcGIS, 2011).

As was the case with the 2003-2009 dataset at Agnesberg, there are also signs of the 2009 bathymetry being set too far to the left (east) relative to the 2003 bathymetry data. The possible effects of this can clearly be viewed north of the old landslide as the yellow-red band that follows the edge of the 2003-2009 dataset, and on the opposite side as a turquoise-blue band.

#### **8.2.3.1 North of Ballabo**

North of Ballabo where the river bank show rather smooth and typical profiles of large sub aquatic slopes that descend straight down to deepest part of the river section. About 50 m north of the old landslide mass there is a distinct depression or deep hole in the river bottom, visible as a distinct red patch in Figure 35. Previous erosion has thus been concentrated to that side of the river and at the foot of the sub aquatic slope, similarly to the modelled erosion in Agnesberg but with a much wider “erosion trench”. In this case however, there are no clear indications of any active erosion from studying the 2003-2009 dataset. One reason for this could be that there simply is no active erosion taking place due to inability of the water flow to erode anymore soil by neither direct fluvial erosion nor abrasion. Compared to Agnesberg the river at Ballabo is much deeper and the river geomorphology is older, meaning that the river might have reached a form of equilibrium when it comes to the bottom erosion. There is a limit of how deep Göta River can erode relative to land heave, the difference in elevation between the sea floor and the river. Another possibility could be that the Ballabo landslide cut of the abrasion flow along the river bottom. It is obvious when looking at the hydraulic shear stress in Figure 36 that the shear stress is lower both to the north and particularly to the south of the old landslide mass. This would mean that the Ballabo landslide mass effectively could have stopped any previously active erosion that was taking place to the north and south.

As the first slope stability calculations for the Ballabo North slope resulted in a factor of safety below 1 at 0.973, it would be of little interest to study how any further erosion might affect that slope. Instead the approach in this case has been the reversed, backtracking to determine how much soil would have to be added to make the slope stable. The model used to add this soil is based on the assumption that the erosion has happened along the bottom as described above. To get a picture of how the geomorphology could have developed into its current state a profile through the middle of the deep red patch was compared to a profile just north of the this deep patch, see Figure 37. In this figure it is visible that the profile through the deep patch is very similar to the profile to the north, with the exception that the river bottom is lower. The adding of soil, or backtracking of erosion, will therefore be modelled by simply raising the points in the bottom region of the Ballabo North slope in Y direction, see Figure 38. This is done in Slope/W simply by raising the first five points in the slope profile by 0.4 m increments. It should be pointed out while the geometric changes might look similar to what a sedimentation process would look like the effects are not the same as the soil properties of a sedimentation soil would be very different. The properties of the soil added in this modelling have the same properties as the underlying soil, with a continuous increase in undrained shear strength from the same datum as the current underlying soil.



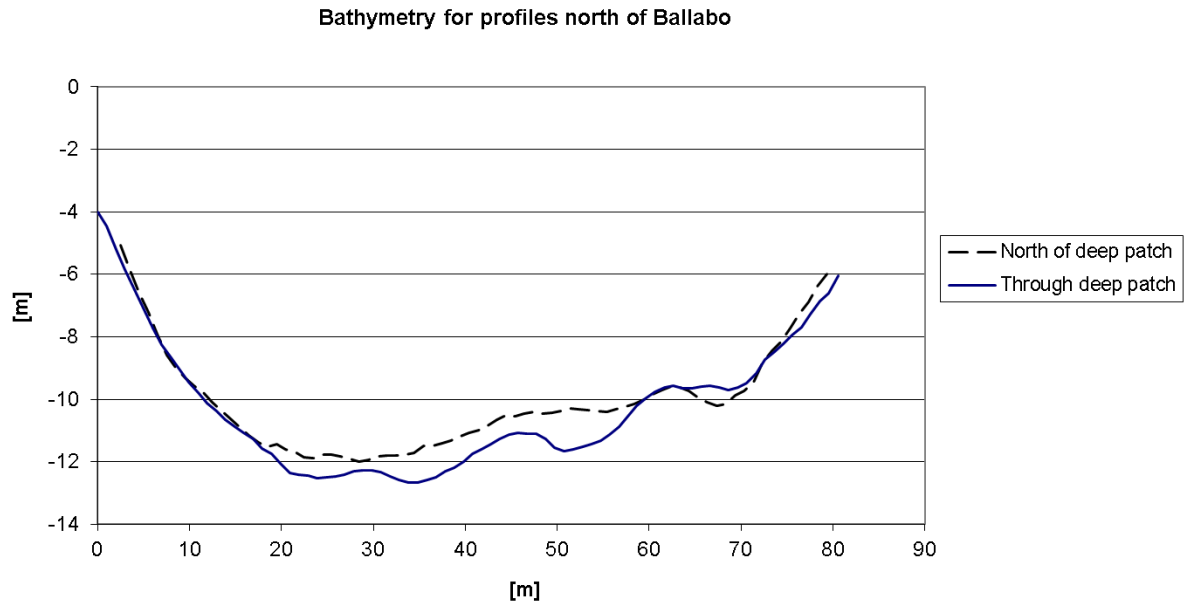


Figure 37 Comparison between profiles directly through and north of the deep patch. Not be confused with a comparison of one single profile between 2003 and 2009.

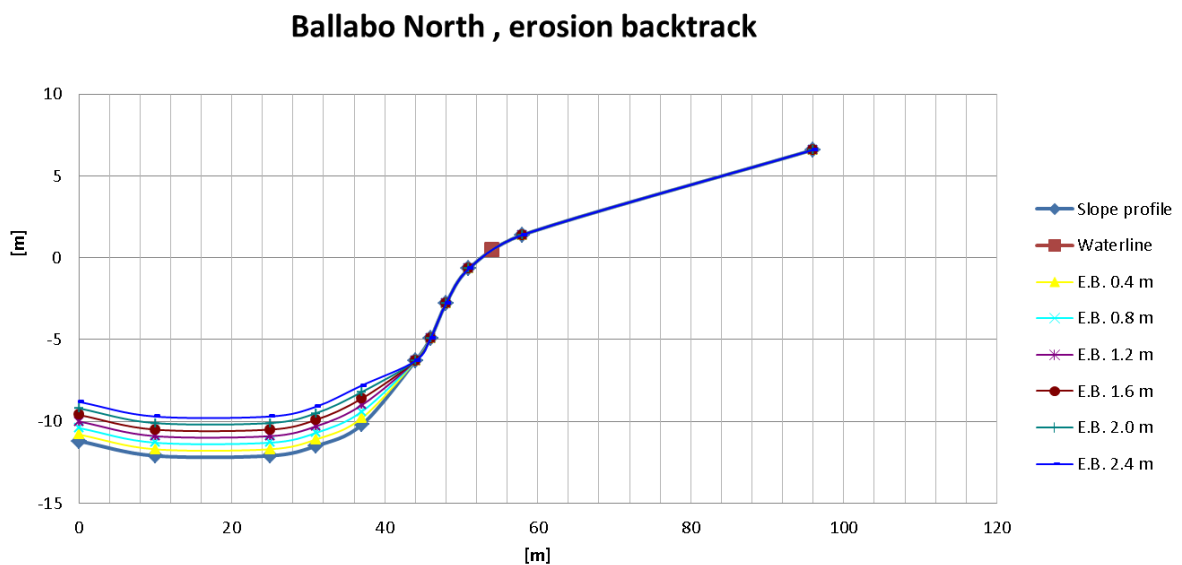
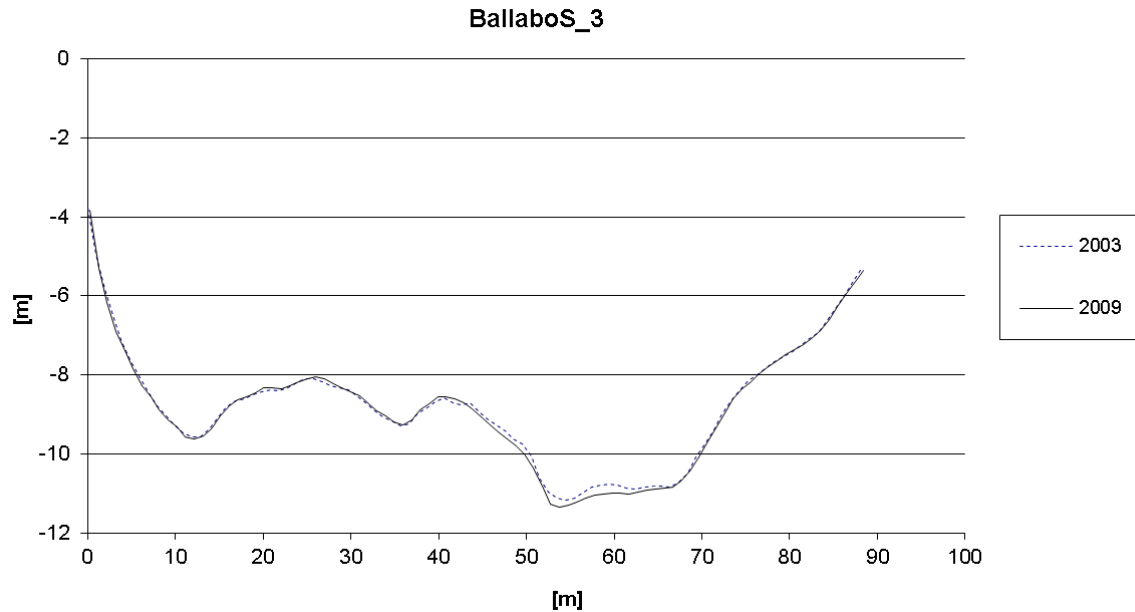


Figure 38 Modelling of the possible erosion history for the Ballabo North slope.

### 8.2.3.2 South of Ballabo

Similarly to the erosion situation north of the Ballabo landslide, the erosion processes that was taking place previously to the old landslide was most likely also disrupted due to changes in the hydraulic flow caused by the landslide soil mass. Shown in the figures below is a close up of a profile of the entire length of the river bottom in this area.





*Figure 39 Profile of the river bottom in the area directly south of the Ballabo landslide. Both the 2003 and 2009 bathymetry values are shown.*

The Ballabo South slope is to the left, and the soil mass from the possible old land slide is visible below the slope and up to about 50 meters. At the 10 and 50 m mark there are two visible valleys, and one theory is that these constituted two for the river characteristic erosion trenches. As is visible by studying the profile above, there are no indications of changes in bathymetry up to about 50 m. This would be consistent with the theory that the erosion processes in this part of the profile have ended due to the Ballabo landslide.

Between 50 and 65 m, the deepest part of the river in this river section, there is however an indication of on-going erosion. This would also be consistent with the same theory described above as this part does not lie directly downstream from the old Ballabo landslide mass. In fact the flow of water over this part of the river might instead have increased due to the geometric changes caused the Ballabo landslide. This pattern was the same for several profiles taken in this area, and is also visible by looking at the lowest part of the profiles in Figure 39.

The erosion for the Ballabo South slope has because of this been modelled in two ways. The first one is according to the pre Ballabo landslide erosion, where the soil mass between  $10 \text{ m} < x < 50 \text{ m}$  in Figure 39 was where most of the erosion was taking place, eventually eroding the entire soil mass. The second erosion model is the current situation, where erosion only is taking place in the deepest part  $50 \text{ m} < x < 70 \text{ m}$ .

For the first erosion case points 4,5 and 6 for the South Ballabo profile in Figure 33 are lowered with the same distance  $x$  which is the erosion parameter. In the second case, points 1 and 2 are instead lowered with the distance  $x$ . The difference in the second case is about 20-30 cm, indicating a possible erosion rate of about 3 - 5 cm/year in the deepest trench today.

## 9 Results from slope stability calculations

The slope profiles, related geotechnical properties and the erosion described in the case studies in the previous chapter, where subsequently modelled in Slope/W 2007. The results from these slope stability calculations are presented in this chapter as the factors of safety plotted against their respective erosion parameters defined in the previous chapter. The factors of safety are all Morgenstern-Price factors of safety, calculated with a half sine interslice force function for slip surfaces deeper than 30 cm. The differences between the two factors of safety presented in this chapter are due to the modelling of the soil strength, i.e. combined or undrained analysis. The factor of safety for both the subaquatic slope and the full slope are presented in each case, where the subaquatic slope factor of safety refers to a slip surface which is entirely below water, and the full slope factor of safety refers to slip surfaces that reach above the water level onto land.

### 9.1 Agnesberg slopes

This section presents the results from slope stability calculations on the slopes from the case study of Agnesberg, see Chapter 8, Section 8.1.

*Table 9 Results from slope stability calculations for the Agnesberg Type 1 slope.*

Erosion parameter		Subaquatic slope		Full slope	
Depth of erosion [m]	Estimated time [year]	$F_k$	$F_c$	$F_k$	$F_c$
0	2003	1.229	1.326	1.299	1.318
0.75	2028	1.229	1.297	1.291	1.302
1.50	2053	1.218	1.263	1.278	1.283
2.25	2078	1.177	1.215	1.256	1.261
3.00	2103	1.123	1.158	1.233	1.237

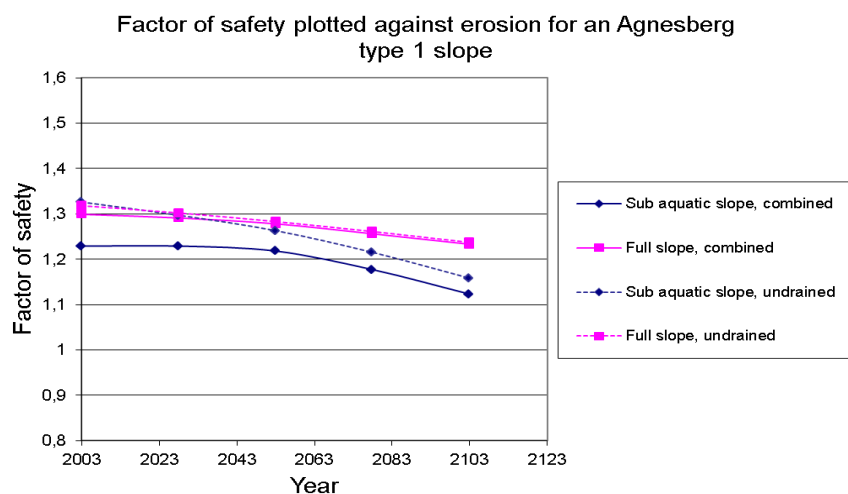


*Figure 40 Plot of the factor of safety against erosion parameter for the Agnesberg Type 1 slope.*

Table 10 Results from slope stability calculations for the Agnesberg Type 2 slope.

Erosion parameter		Sub aquatic slope		Full slope	
Depth of erosion [m]	Estimated time [year]	$F_k$	$F_c$	$F_k$	$F_c$
0	2003	1.124	1.242	1.376	1.389
0.75	2028	1.047	1.175	1.343	1.355
1.50	2053	0.977	1.087	1.31	1.325
2.25	2078	0.914	1.011	1.28	1.291
3.00	2103	0.874	0.968	1.249	1.258

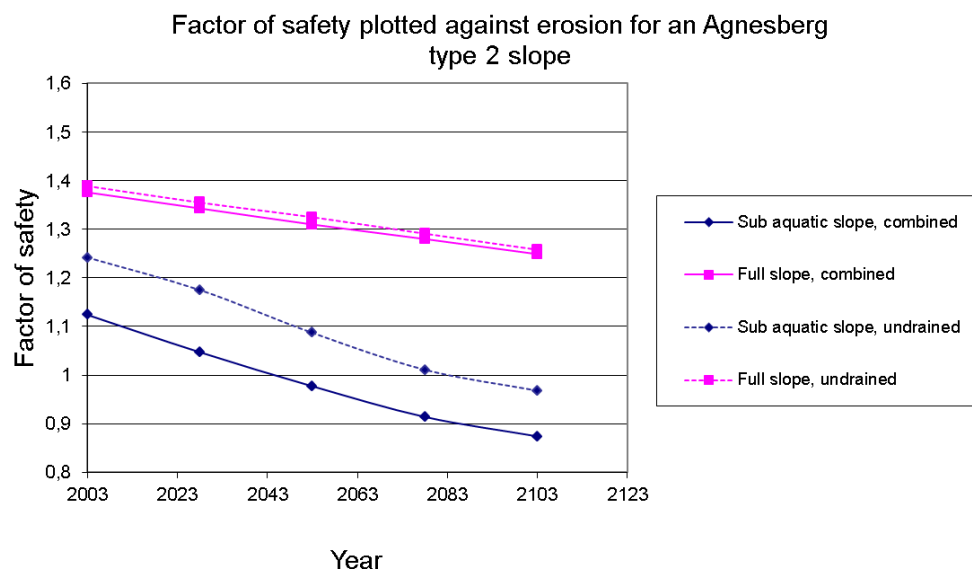


Figure 41 Plot of the factor of safety against erosion parameter for the Agnesberg type 2 slope.

### 9.1.1 Comments

Overall it is obvious that the undrained analysis gives a higher factor of safety than the combined analysis, which is to be expected. This difference is much greater for the sub aquatic slope than for the full slope, where the undrained and combined analyses are quite close to each other.

The slopes from Agnesberg are very similar, near identical, both when it comes to the geometry and the geological conditions. There is however an important difference which is the inclination of the sub aquatic slope. The Type 1 slope for most parts has a much lower inclination of its sub aquatic slope, see Chapter 8, which causes a higher factor of safety for the sub aquatic slope. On the other hand the full slope, reaching all

the way back on land, actually shows a lower factor of safety for the Type 1 slope than for the Type 2 slope. This is likely to be because of the larger mass of the Type 2 slope in the sub aquatic part of the profile, a consequence of the geometry, which causes a greater passive pressure to resist the active pressure from the land masses.

However, the rate of change for the factor of safety for the full slope with the erosion is higher for the Type 2 slope. This is also the case for the sub aquatic slope, where the Type 1 sub aquatic slope barely seems affected at all for the first 50 years while the Type 2 factor of safety rapidly drops below 1.

The resulting factors of safety in these calculations compare rather well with the official investigation of the Agnesberg landslide, which indicates that the slopes in this thesis have been accurately modelled in Slope/W. The slip surfaces for the sub aquatic and full slope also compare well. The official investigation resulted in  $F_c$  and  $F_k$  equal to 1.24 and 1.22 respectively for the most critical sub aquatic slip surface using Bishops method. Using Janbus method the corresponding factors of safety was 1.25 and 1.02. For the full slope the official investigation results showed a lowest critical slip surface with  $F_k = 1.36$ , with a number of critical slip surfaces reaching about 10 m in land from the shore with  $F_k$  below 1.4 (Larsson et al, 1994). In the official investigation they also varied the geometry for the sub aquatic slope stability calculations by altering the slope angle between 30° and 60° and came to the conclusion that this geometry variation had a modest effect on the factor of safety. Furthermore it is obvious that it is the drained conditions that dominate the combined analysis.

## 9.2 Ballabo slopes

This section presents the results from slope stability calculations on the slopes from the case study of Ballabo, see Chapter 8, Section 8.2.

### 9.2.1 Ballabo South: erosion of assumed old landslide mass

The results below are from the Ballabo South slope where the erosion has been modelled as an erosion of the assumed old land slide mass on the river bottom at the slope toe. This erosion action would presumably have been very active before the old Ballabo landslide, but as a result of that landslide changing the flow of water it is assumed to be more or less inactive today. The undrained analysis of the sub aquatic slope has been left because of the very high factor of safety (well above 3), as it was not near any critical values.

*Table 11 Results from slope stability calculations for the Ballabo South slope with erosion of assumed old landslide mass.*

	Sub aquatic slope		Full slope	
Erosion [m]	$F_k$	$F_c$	$F_k$	$F_c$
0.00	1.148	-	1.093	1.132
0.25	1.139		1.089	1.126
0.50	1.130		1.085	1.124
0.75	1.123		1.080	1.120
1.00	1.117		1.075	1.117
1.25	1.111		1.071	1.114
1.50	1.104		1.067	1.113
1.75	1.063		1.063	1.112
2.00	1.056		1.059	1.106

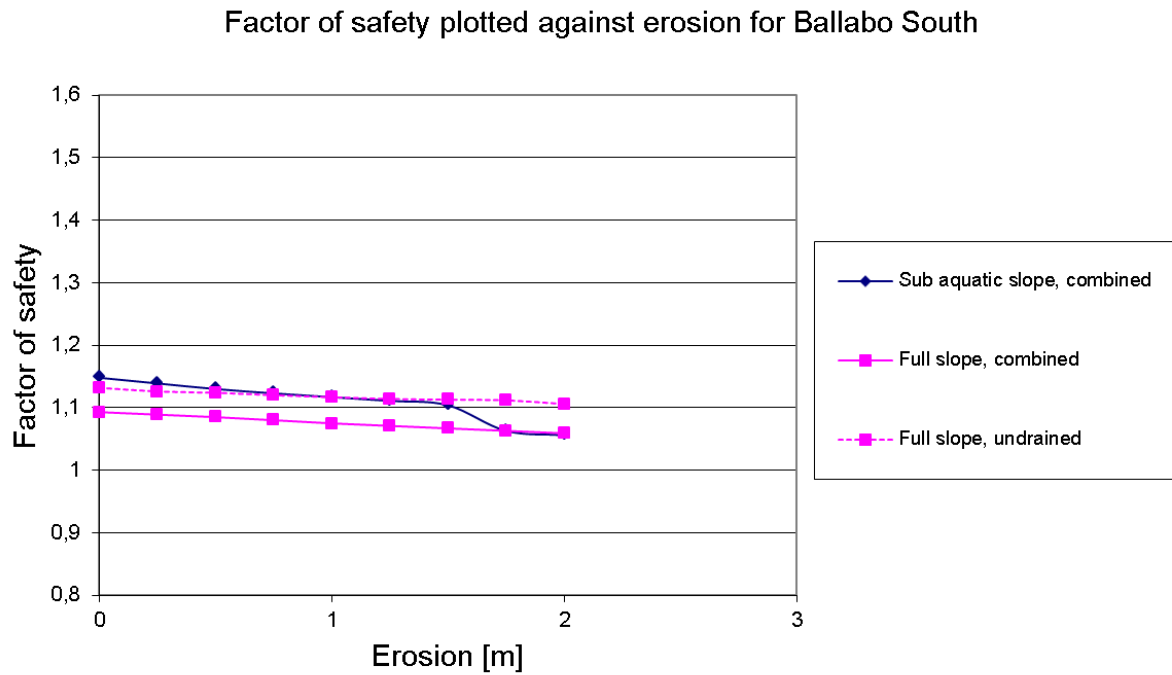


*Figure 42 Plot of the factor of safety against erosion parameter for the Ballabo South slope with erosion of assumed old slide mass.*

#### 9.2.1.1 Alternative modelling of the slope

As is visible in Figure 42 there is a rather big jump on the curve for the subaquatic factor of safety between the erosion values of 1.50 and 1.75 m. A closer analysis of the two slip surfaces for these values of factor of safety showed that the reason could be due to the shape of the slip surface and the fact that these slip surfaces crosses two regions in the Slope/W model with different soil strength, see Figures 43-44.

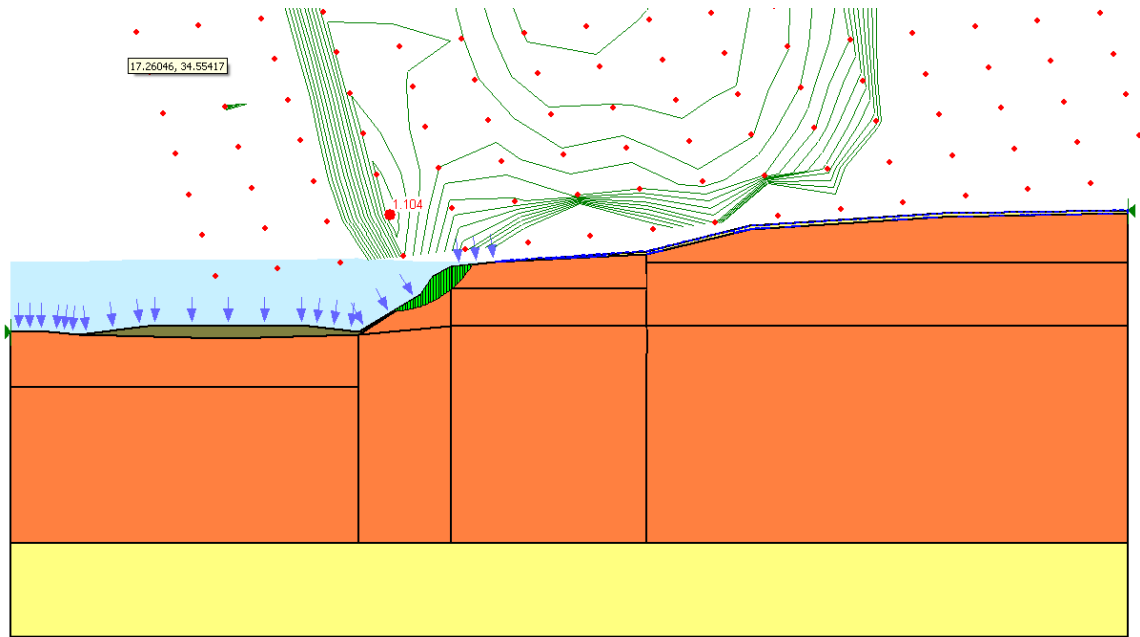


Figure 43 The most critical sub aquatic slip surface at an  $Fk = 1.104$  and erosion of 1.50 m of the presumed old landslide mass seen as the brown region in the image (Slope/W, 2011).

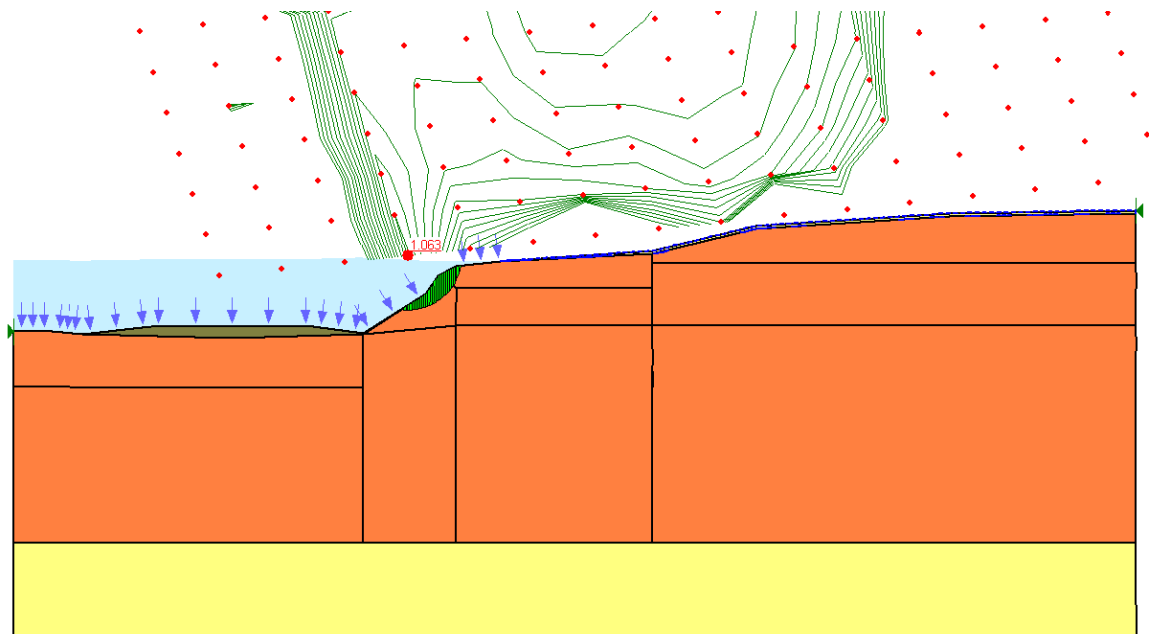


Figure 44 The most critical sub aquatic slip surface at an  $Fk = 1.063$  and erosion of 1.75 m of the presumed old landslide mass seen as the brown region in the image (Slope/W, 2011).

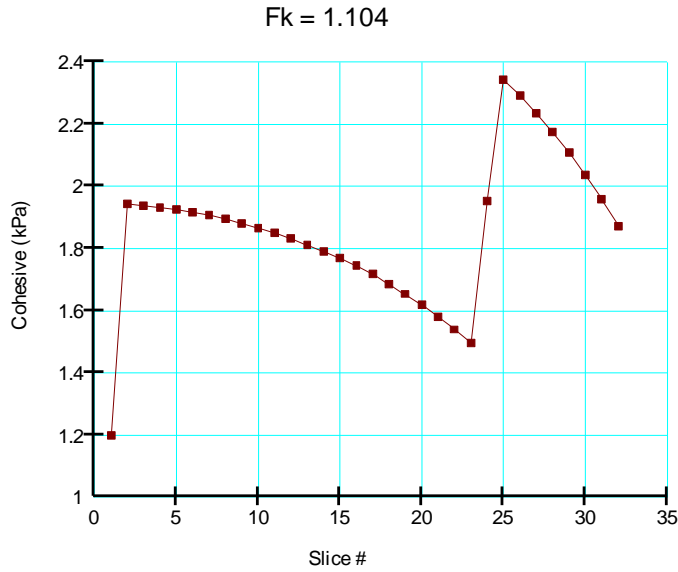


Figure 45 Plot of the cohesive strength for each slice in the slip surface seen in Figure 43 (Slope/W, 2011).

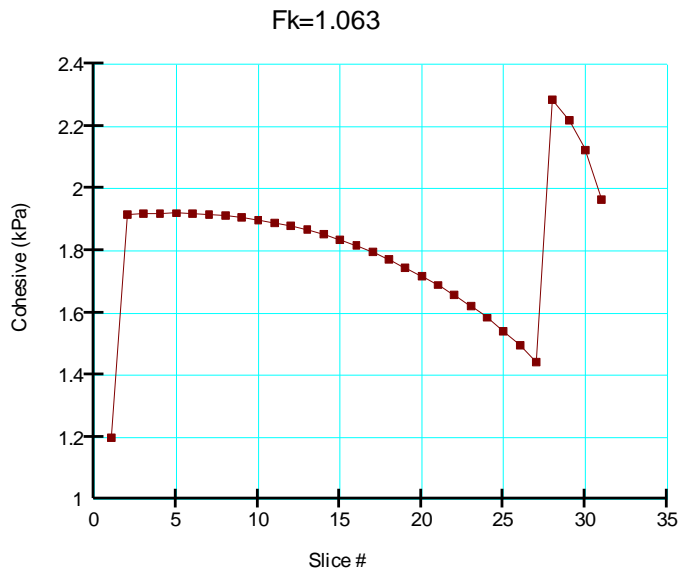


Figure 46 Plot of the cohesive strength for each slice in the slip surface seen in Figure 44 (Slope/W, 2011).

As seen in the figures above where the cohesive strength at each slice base is plotted for each slice there is a large jump around slice 25. This is where the slip surface crosses into another region in the Slope/W model with a higher strength. As the slip surface with the higher factor of safety passes through a comparatively larger part of the region with higher strength the effect is a comparatively much larger factor of safety. As this difference between the regions probably is an unrealistic model of the



soil in the slope, the region with the lower strength was remodelled and adjusted. This was done by raising the datum level from which the soil strength increases with depth from -2 m to +2 m. This resulted in the cohesive strength plot for the critical slip surface at an erosion of 1.75 m shown in Figure 47 below.

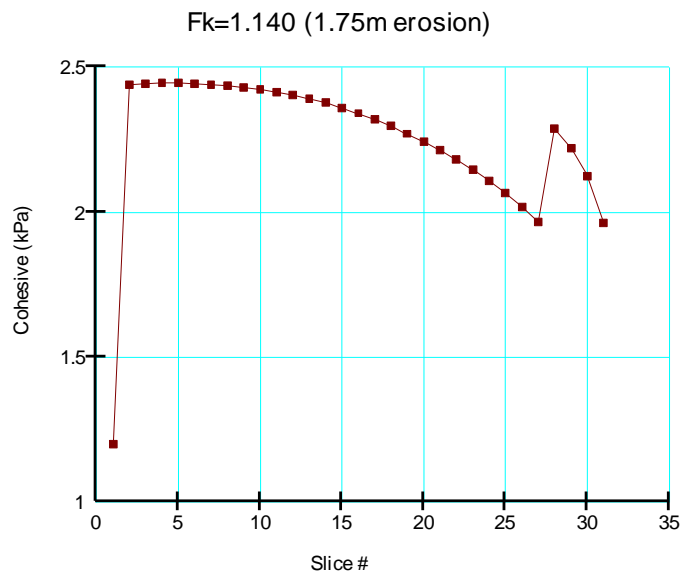


Figure 47 The cohesive strength for each slice in the slip surface in the alternative model at an erosion of 1.75 m (Slope/W, 2011).

The result of this new model is probably more realistic for the sub aquatic slope, with a smoother transition between the two regions. The very large jump visible in all three plots in Figures 45-47 between slice number one and slice number two is explained by the fact that the first slice lies in the assumed old landslide mass which is presumed to have much lower strength, meaning a sharp jump as this would be expected and realistic. The results of the factor of safety calculations for this alternative model are shown Table 12 and Figure 48.

As is visible in Figure 48 the alternative model has virtually no effect on the slope stability of the critical slip surfaces for the full slope, indicating that this might be a better model for slope stability calculations of this slope. However it raises the factor of safety for the sub aquatic slope, but as might have been expected does not change the sharp drop between an erosion of 1.50 and 1.75 m. In fact the drop becomes even larger and quite significant.

*Table 12 Results from slope stability calculations for the Ballabo South slope with erosion of assumed old landslide mass, alternative model.*

	Sub aquatic slope	Full slope
Erosion [m]	$F_k$	$F_k$
0.00	1.200	1.093
0.25	1.197	1.090
0.50	1.185	1.085
0.75	1.175	1.080
1.00	1.165	1.075
1.25	1.156	1.071
1.50	1.148	1.067
1.75	1.140	1.063
2.00	1.056	1.059
2.5	1.034	1.051
3.0	1.014	1.039
3.5	0.997	1.029

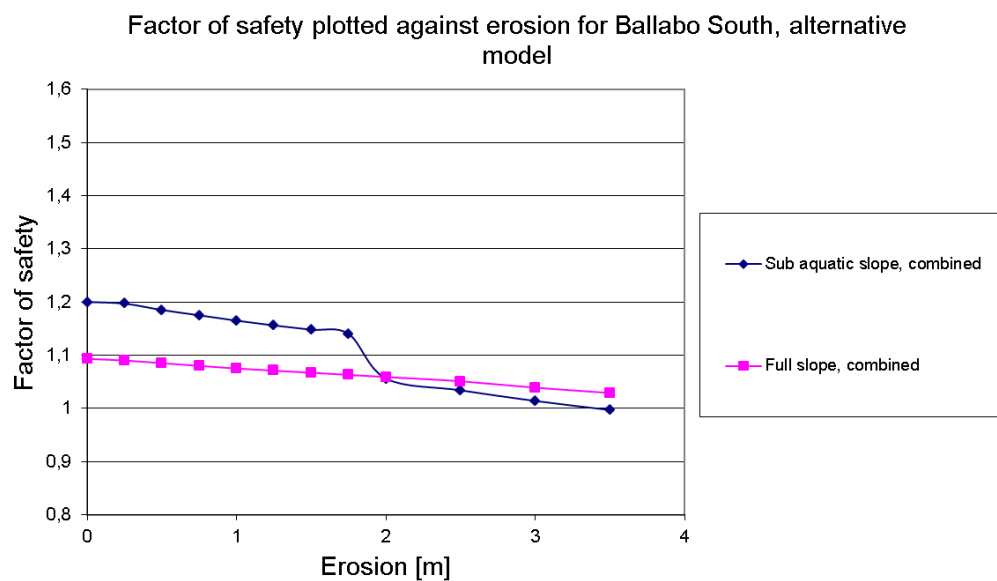


*Figure 48 Plot of the factor of safety against erosion for the Ballabo South slope, alternative model, with erosion of assumed old slide mass.*

### 9.2.2 Ballabo South: current erosion

In this model the erosion is defined as only occurring in the deepest part of the river section, corresponding to the assumed current erosion conditions. Comparing Figure 50 to Figure 43, erosion can be seen to have been taken place in the far left of the profile.

*Table 13 Results from slope stability calculations for the Ballabo South slope with current erosion conditions.*

	Sub aquatic slope	Full slope
Erosion [m]	$F_k$	$F_k$
0.00	1.093	-
0.50	1.094	-
1.00	1.094	-
1.50	1.094	-
2.00	1.094	2.234
2.5	1.094	1.832
3.0	1.094	1.559
4	1.094	1.365

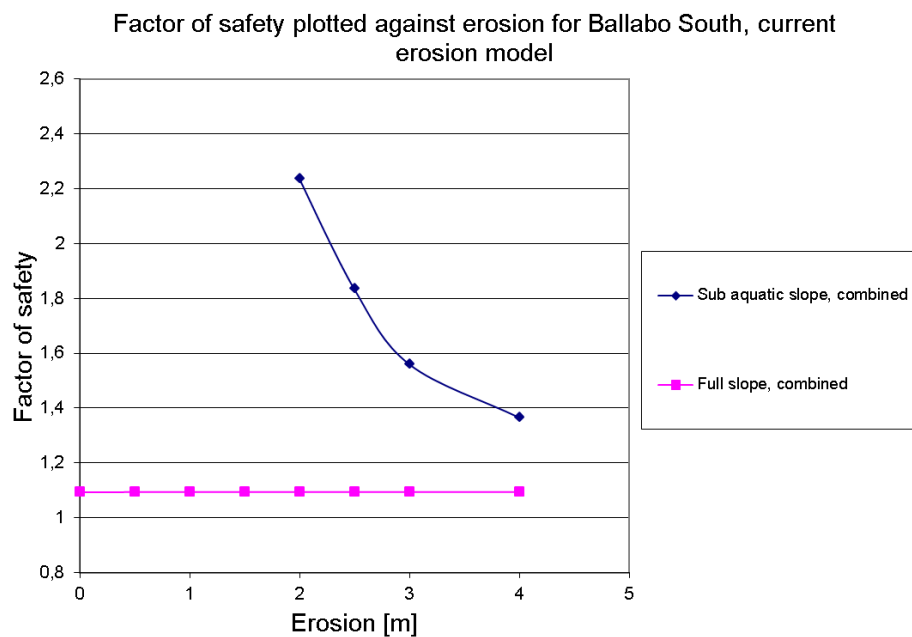


*Figure 49 Plot of the factor of safety against erosion for the Ballabo South slope for current erosion conditions.*

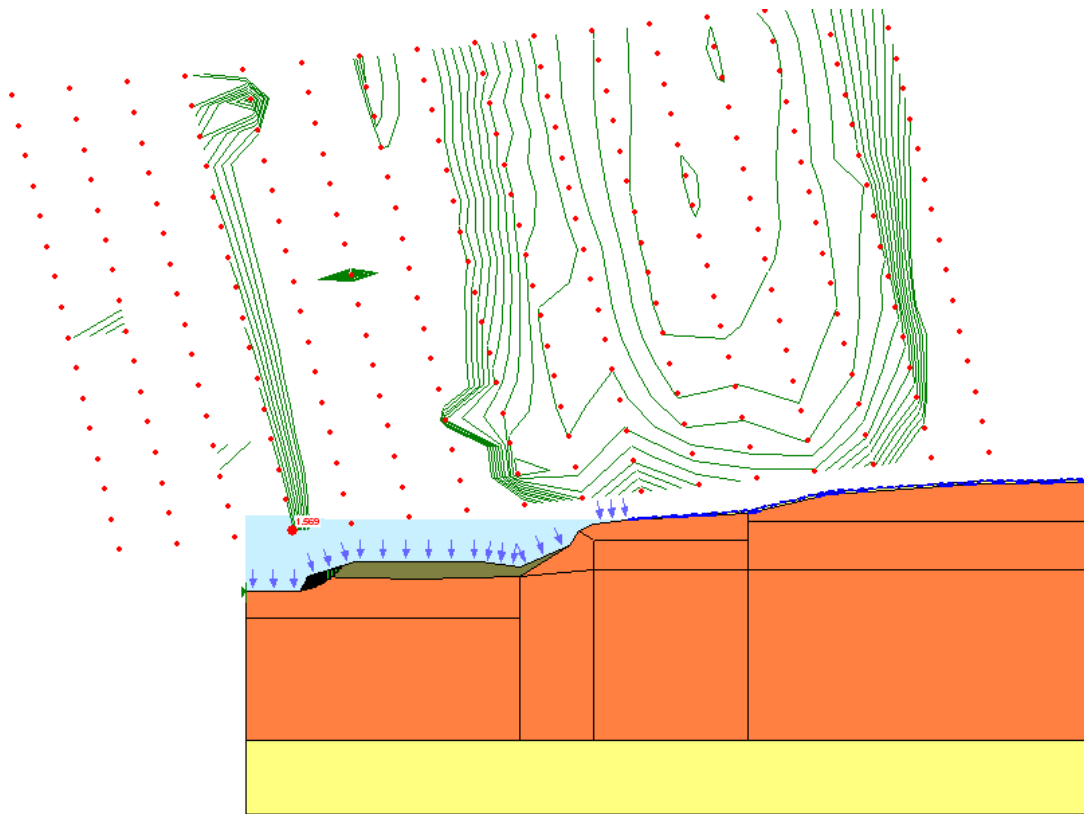


*Figure 50 The assumed current erosion situation. In this screen shot 3 m have been eroded at the far left of the slope profile.*

### 9.2.3 Ballabo North

In the table below the values are shown going from a lower factor of safety to a higher factor of safety as the erosion parameter increases. This is because the erosion is modelled in a “reversed mode”, where it has been tracked backwards; see Chapter 8, Section 8.2.3.1. In Figure 51 the results are plotted in the same manner as in the previous cases for convenience.

*Table 14 Results from slope stability calculations for the Ballabo North slope.*

	Full slope		Sub aquatic slope
Erosion backtracking [m]	$F_k$	$F_c$	$F_k$
0.00 (current state)	0.971	1.028	1.051
0.40	0.980	1.036	1.070
0.80	0.996	1.046	1.117
1.20	1.012	1.054	1.154
1.60	1.028	1.065	1.167
2.00	1.038	1.075	1.208
2.40	1.049	1.086	1.243

Factor of safety plotted against erosion for Ballabo North

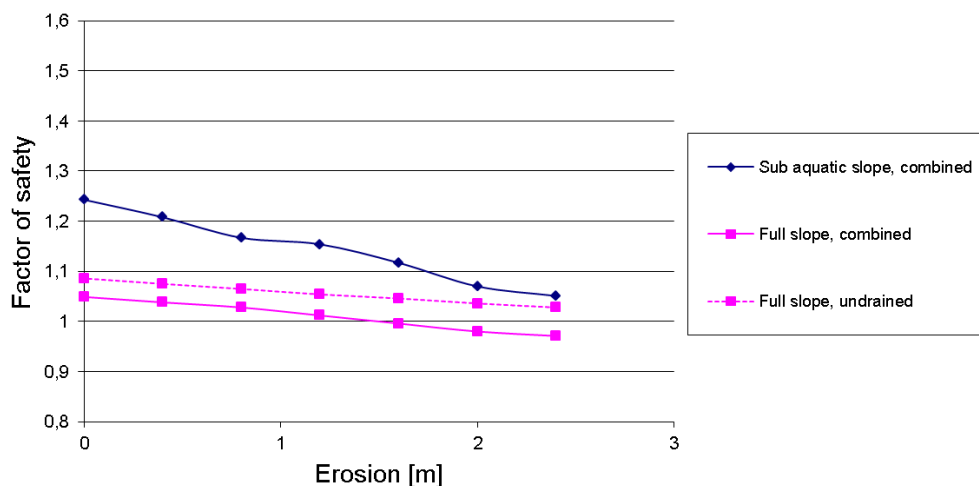


*Figure 51 Plot of the factor of safety against backtracked erosion for the Ballabo North slope, meaning the current state of the slope is at an erosion of 2.40 m in this plot.*

#### 9.2.4 Comments

The results from stability calculations of the Ballabo slopes compare very well with the results from the official investigations. Andersson et al (1999) attained results from a section just north of the old Ballabo landslide with both a combined and undrained factor of safety very close to 1.0. These values should be compared with the full slope factors of safety for the Ballabo North slope;  $F_k = 0.971$  and  $F_c = 1.028$ . In the official investigation they also carried out calculations for a slope south of the Ballabo landslide mass where they got an undrained factor of safety using Janbus direct method of 1.1 for the full slope. For the subaquatic slope they got  $F_c = 1.6$  and  $F_k = 1.3$ . This also compares well with the results from Ballabo South in this study. The length and depth of the critical slip surfaces for the full slopes are also very much in agreement with the official investigation.

The slopes from the official investigation do not correspond directly to the south and north slopes in this study because the slope profiles are not drawn along the exact same coordinates and some changes in bathymetry could be expected to have taken place since the official investigation. The agreements between the results do however indicate that Ballabo North and South are modelled realistically in Slope/W.

Another important note is that the calculations carried out have not taken any possible anisotropic effects into account. Calculations performed in the official Ballabo investigation to determine the effect of anisotropy resulted in an increase of both undrained and combined factor of safety with about 7 %.

## 10 Final conclusions and summary of results

This chapter sums up the results from all the previous chapters, tying them together into a theory on how river erosion, landslides and slope development in Göta River are related to each other based on the studies made in this thesis.

### 10.1 Characterization of erosion

Based on the topographic and geophysical datasets examined in this thesis work, as well as literature studies, it has been possible to establish that the bottom erosion occurring along Göta River is very localized, unevenly distributed over the bottom section and can be characterized as four different main processes:

- Corassion along trenches, which seems to be the most dominant form of bottom erosion, and has a significant impact on the slope stability as these trenches often form along the slope toes of the river banks. This erosion has a vertical progress, and does not significantly progress horizontally into the river bank, although this erosion at some point causes either a small or large slope failure which in turn affects the slopes geometry horizontally. A good example of this is the Agnesberg study in Chapter 8. This erosion can also occur in the middle of a river section, but in that case has very little or no direct effect on the river banks slope stability (for a river section width typical width). These trenches in which corrosion occurs can sometime be hard to define, but they range from very narrow, less than 1m, up to what can be regarded as the whole deep lane in the river.
- Erosion of old landslide soil masses, as can be seen in the modelling of the Ballabo South slope in Chapter 8. Old landslide soil masses erode relatively quickly due to their low strength, and this type of erosion is likely to occur both because of direct fluvial shear and corassion processes. The rate of old landslide soil mass erosion can be expected to occur at a rate that is decreasing with time due to the fluvial shear stress depending on the cross section area of the river which increases with erosion and thus causing less flow and shear. The deeper soil in an old landslide soil mass should in theory also be more resistant to erosion than the upper layers due to compaction and consolidation.
- Erosion of deep holes, which has been observed at several places, takes the form of depressions or holes that clearly breaks with the surrounding bottom topography. One such case is the Ballabo North slope in Chapter 8, where a relatively large depression has been formed in the bottom. This thesis hasn't studied the details and reasons of these processes, but it is most likely due to local weak spots in the soil and a specific type of whirling water flow such as eversion, see Chapter 2.
- Anthropogenic erosion, which can be described as any erosion taking place that has to do more directly with human activities. In the case of Göta River this is mainly erosion related to the ship traffic, but could also be caused by construction and other infrastructure developments. It is hard to assess how much bottom erosion is caused by ships, but there are clearly some cases as

seen in Figures 12 and 13 in Chapter 5 where erosion seems to be caused by propeller induced flows. When it comes to the erosion caused by ship waves, it has clearly been established in previous studies such as Sundborg and Norrman (1963), Hultén et al (2006) and Althage (2010) that they are the most significant cause of erosion of the river banks.

The most common erosion processes taking place and having the most critical effect on the slope stability are corassion along the slope toe and wave erosion on the river banks. Conceptual drawings of the main erosion processes found in this study are presented in the figures below:

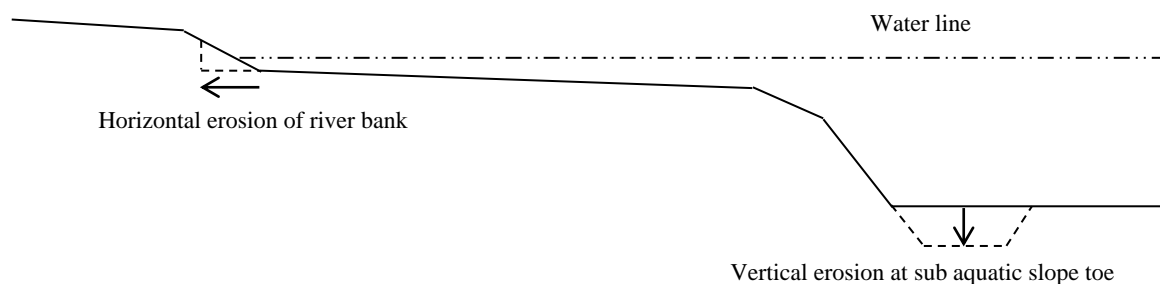


*Figure 52 Corassion along bottom trench and erosion of river bank.*

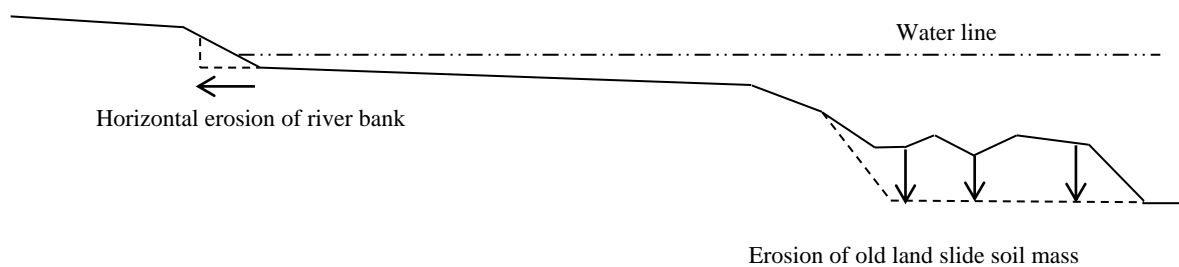


*Figure 53 Erosion of old landslide soil mass and erosion of river bank.*

The vertical erosion at the slope toe in Figure 52 above is mainly caused by corassion, but when looking at a section through a local deep hole that has been eroded the geometry will look similar if the deep hole is located close to the slope toe.

These results should not be regarded as true for the whole river, only as the results from work within the scope of this thesis. However, some previous assumptions with regard to the geometric characteristics of the erosion in Göta River does not seem to apply to the areas studied in this thesis, and there is some cause to believe that those assumptions might be invalid for most parts of the river as well. These previous assumptions are that most of the subaquatic river bed is subjected to fluvial erosion, and in particular that the sub aquatic slopes are most subjected to this (Hultén et al, 2006; Hultén et al 2007). No observations have been made in this study that suggests that there is any significant direct, or fluvial, horizontal erosion of the sub aquatic slopes taking place.

The horizontal erosion of the river bank has not been studied in this thesis, mainly due to the fact that there is no bathymetric data from 2003 near the shorelines of the river.



Furthermore large parts of the river shore is today well protected against this type of erosion, and for most parts the land up from the shore is relatively flat, especially in the southern parts of the river. This makes horizontal erosion of the river bank much less critical with regard to landslides.

## 10.2 Quantification of erosion

The analysis and quantification of erosion in Göta River in this study has been made by comparing the difference in river bathymetry between 2003 and 2006. This is different from the most recent methods used to quantify the same, and the results also differ somewhat from those previous studies (Sundborg & Norrman, 1963; Larsson et al, 2006).

In the previous studies the erosion rates have been estimated by studying water turbidity and the amount of suspended soil particles at the river mouth of Göta River. This method results in rather accurate estimations of the amount of soil that is transported by the river over a certain time period. Further estimations can then be made of how much of this transported material originates from the river bed of Göta River, and how much originates from the main river reservoir Lake Vänern, tributaries and precipitation runoff etc. Larsson et al (2006), based on such estimations, suggested possible erosion rates of 2-3 m at the river shore and 0.5-1 m along the bottom over the next 100 years. These values were of course proposed as a form of average or general value for the whole river, with the acknowledgment that local variations could be substantial. This is of course a consequence of quantifying erosion through the measurement of transported soil, as this method only gives the net amount of the total transported soil mass at the river mouth and very little information on the detailed distribution of eroded material along the river.

The case studies in this thesis have shown that the erosion processes are indeed highly localized, and that even in parts of the river where there seem to be significant on-going erosion, the erosion still only occurs on a relatively small percentage of the river bottom at that section. As a result of this, the real erosion rates in most cases where there is significant on-going erosion would be expected to be much larger than the rough estimations by Larsson et al (2006). Values from the river bathymetry comparisons in these case studies also confirm that this most likely is the case, see table below.

*Table 15 Erosion rates for case studies.*

Case study	Type of erosion	Approximate erosion rate
Agnesberg	Along trench	1-5 cm/year.
Old Ballabo Landslide	Landslide soil mass	15-20 cm/year
Ballabo South	Along trench	3-5 cm/year

This thesis thus can be seen as a complement to previous studies on the subject, providing a more detailed description of both the geometric characteristics and the quantity of erosion, which is possible to do only with reliable bathymetry data.

It should however be noted that the erosion rates presented in the table above should be used within the right context. Those erosion rates are most likely not constant, and it should also not be forgotten that bottom erosion also is related to the rate of post glacial land uplift. As has been shown in this thesis as well, the erosion will, if continuous, at some point cause a small or large landslide due to the decrease in slope stability with the erosion, see Section 10.3 below. And as seem to be the case, a large landslide significantly affects the erosion rates both up- and downstream of the landslide.

### 10.3 Erosion and the slope stability factor of safety

Using the established characteristics of the erosion of cohesive sediments in Göta River described in Section 10.1 above, case studies were made on two areas along Göta River. The aim of these case studies was to model a number of different slopes as well as the specific bottom erosion they were subjected to, and plot how the slope stability factor of safety varied as a function of the progress of the specific erosion. These calculations were carried out using the software Slope/W and both undrained and combined soil strength models were used in the calculations, see Chapter 3. Due to the characteristics of the slope profiles, the slope stability factor of safety has also been calculated separately for slip surfaces completely below the water line, subaquatic slopes, and for slip surfaces reaching further back on land, full slopes. In many real cases such as in the Agnesberg landslide (see Chapter 8), large landslides reaching all the way back up on land, are triggered by smaller subaquatic landslides.

The slopes in the case studies, for which slope stability calculations were carried out, all differ from one another when it comes to both geometry and soil properties as well as the erosion processes they are subjected to. Therefore it is difficult, and perhaps even dangerous, to make general conclusions about how the factor of safety varies with erosion and time. It is however possible to use these values as realistic examples which can be compared with other studies, as well as give an approximate magnitude of how the factor of safety value can change with erosion for similar slopes and geological and river conditions.

The graphs below show how the factor of safety varies with erosion for the full and subaquatic slopes in the case studies. For *Agnesberg 1* and *2* as well as *Ballabo North* the erosion was modelled as vertical erosion at subaquatic slope toe, and for *Ballabo South* the erosion was modelled as erosion of an old land slide soil mass.

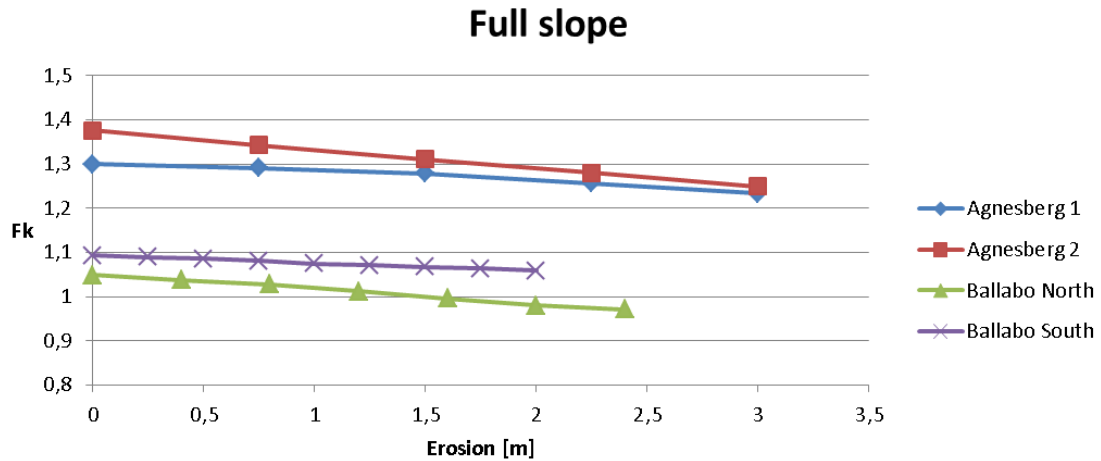


Figure 54 The combined factor of safety for the full slopes plotted as functions of erosion for the different case studies.

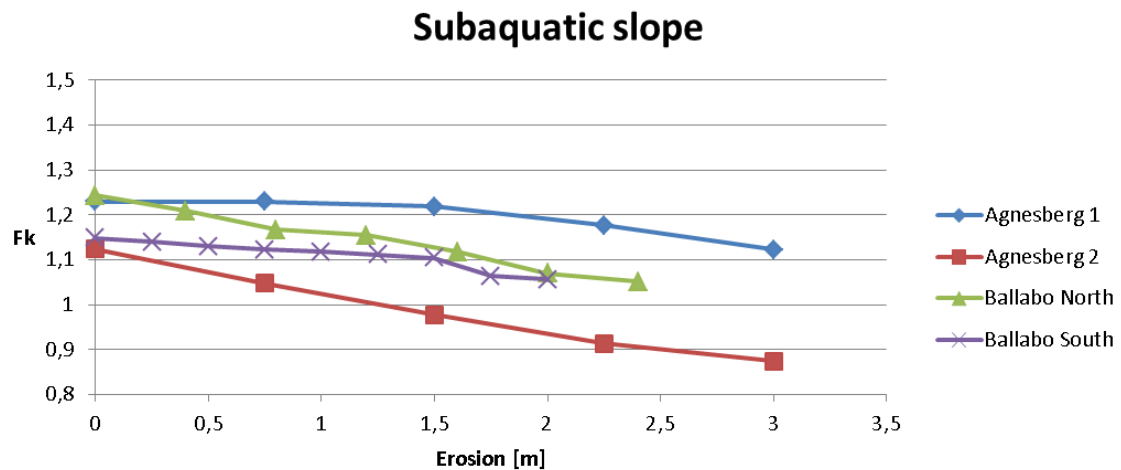


Figure 55 The combined factor of safety for the subaquatic slopes plotted as functions of erosion for the different case studies.

One thing that becomes apparent while watching the plots of the factor of safety is that the decrease of the factor of safety with erosion for the full slopes looks very similar. Despite the slopes and erosion being different and having different starting values of the factor of safety they all have similar curves. They are all near straight lines, with a relatively low gradient varying approximately between  $-0.02x$  to  $-0.04x$  where  $x$  is erosion in metres, see Table 16. This suggests that even though the modelled erosion appears rather different between the cases, it is from a full slope point of view in fact quite similar: soil eroding vertically downwards at the toe of the slope. As the geology and geometry of the slopes however is different, it might suggest something of a very linear decrease of the factor of safety for all kinds of full slopes subjected to vertical bottom erosion.

*Table 16 The combined factor of safety for the full slopes expressed as a function of erosion for the case studies.*

<b>Full slope</b>	<b>Approximation of <math>F_k</math> for full slopes as a function of <math>x</math> (erosion in metres)</b>
Agnesberg 1	$F_k = 1.305 - 0.0223 \cdot x$
Agnesberg 2	$F_k = 1.375 - 0.0423 \cdot x$
Ballabo North	$F_k = 1.0515 - 0.0341 \cdot x$
Ballabo South	$F_k = 1.093 - 0.0173 \cdot x$

The results for the sub aquatic slopes are more varying, showing several different types of curves. This would of course be expected as the erosion has a proportionally larger impact on the geometry of the sub aquatic slope compared to the full slope. An important note is that both the subaquatic and full slope can have the most critical factor of safety, and that the subaquatic factor of safety due to its more varying curve can go from being the least critical to the most critical with erosion or vice versa.

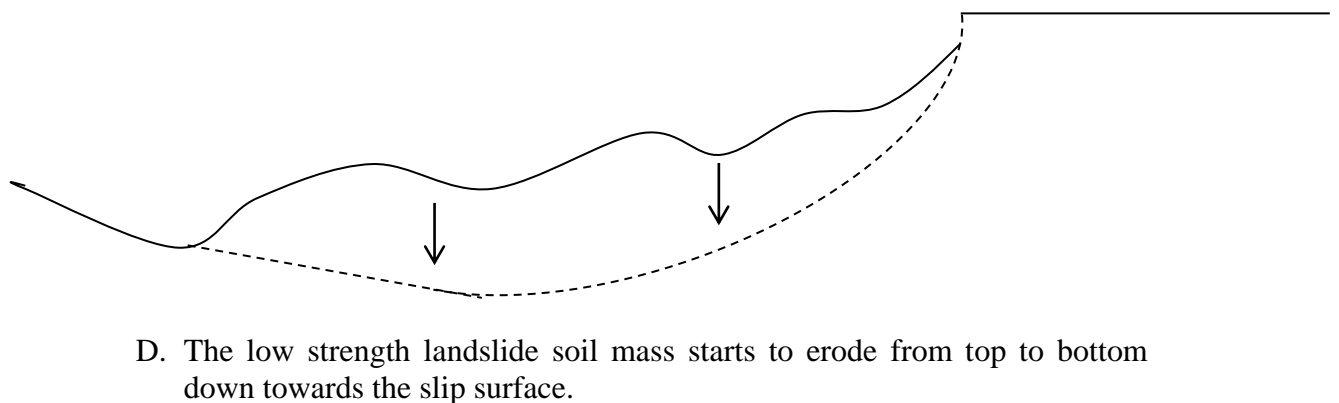
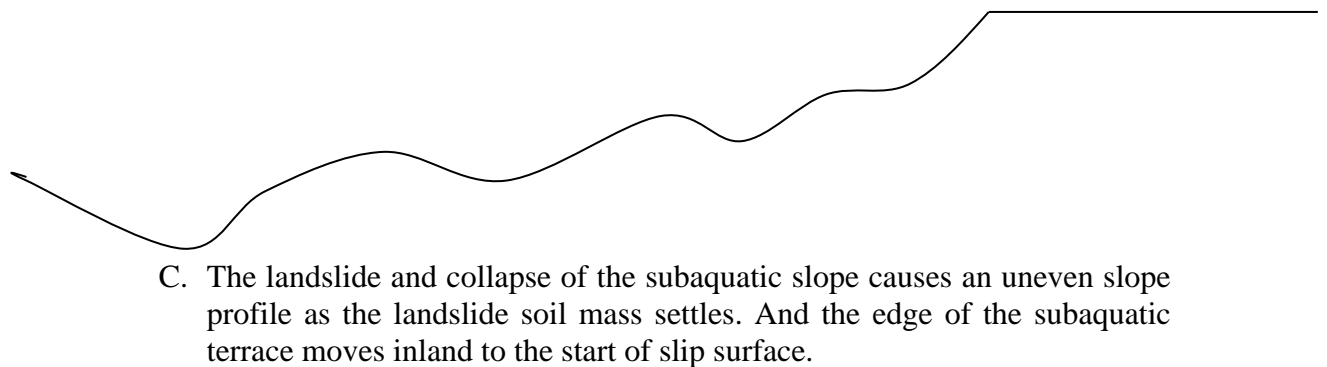
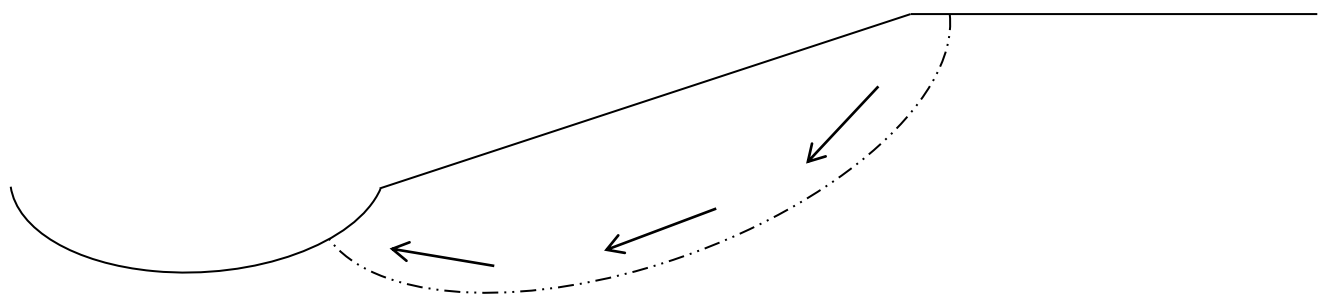
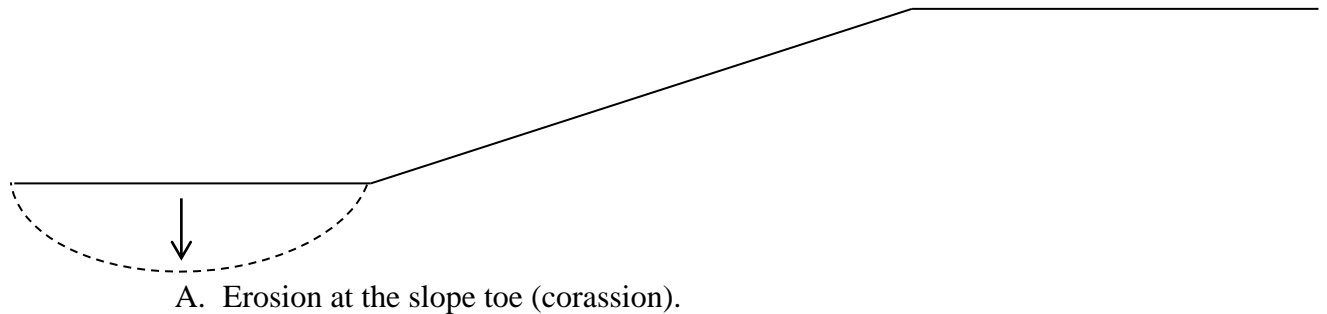
## **10.4 Slope profiles and geomorphology**

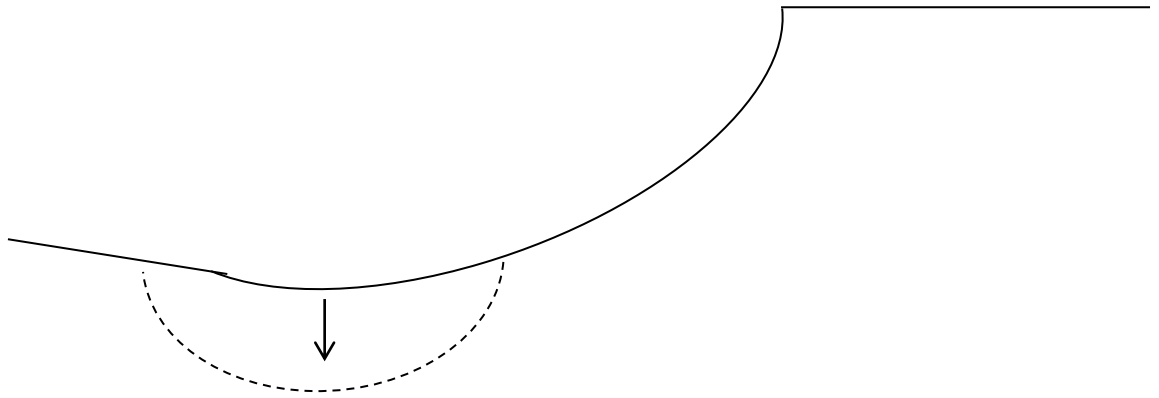
It is shown through previous literature and studies of Göta River as well as through direct observations in this thesis that there is on-going erosion in the river, and what the main characteristics of this erosion are. The implementation of the results from these erosion studies into slope stability models has shown how erosion lowers the factor of safety and might be a significant cause for both past and future landslides. Previous documented and studied landslides, together with observations of bathymetric data, also shows that landslides of different sizes and types frequently occur along the river.

Based on this it is possible to form a general theory on how some of the different slope geometries that are found in the river relate to bottom erosion and landslide processes (see chapter 4 for slope profiles).

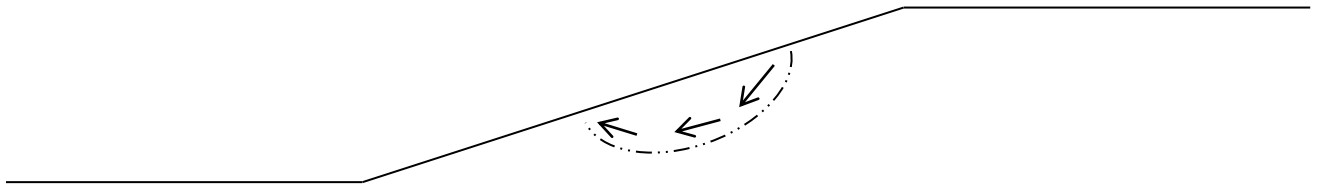
### 10.4.1 General theory on development of slope profiles

Below a theory is presented of how some of the most characteristic slope profiles, as described in chapter 3, could have developed as a result of erosion and landslides.

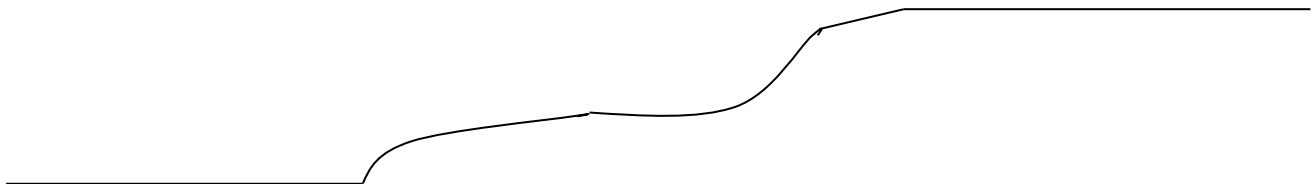




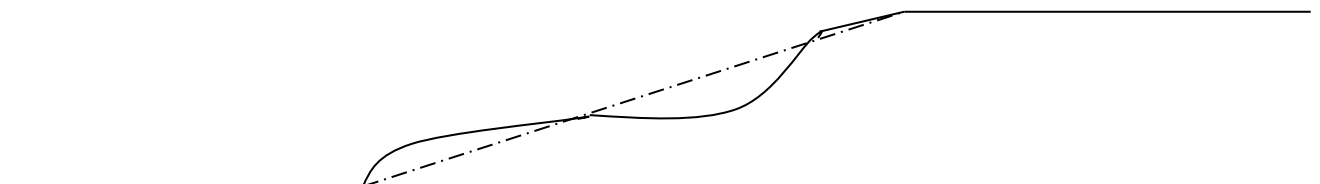
- E. Eventually the soil mass from the landslide has eroded, causing a profile that is aligned with the landslide slip surface (unless there has not already been another slope failure before all of the landslide soil mass has eroded). This is due the fact that the landslide soil mass has a much lower shear strength than the soil below the slip surface. After this stage, the process begins again with erosion along the slope toe.



- F. One of the observations in the study of the bathymetric data sets (chapter 3), is what appears to be a small landslide in the middle of a slope, caused by unknown reasons. A concept of this is drawn above.



- G. This type of minor landslide, where the subaquatic slope only partly collapses, would cause a profile which could be described as having double subaquatic terraces.



- H. A double terrace profile shown together with a dashed line representing the original, pre-landslide profile.

These geomorphologic processes as presented in this theory are of course very general in nature, and there are naturally many geometric variations of different sizes in the real cases where also other processes would be expected to be involved. The theory is however based on a large number of observations at different geographic locations along the river which does show these reoccurring slope profile types. Adding to this the more detailed case studies of old known landslides, as well as the observation of the minor mid-slope landslide, and on-going erosion processes there clearly seem to be a connection between the different slope types similar to what is presented in this theory.

It is difficult to put a timescale on these processes as it would vary very much depending on local conditions and size of geometries. But as an example based on the erosion rates observed in the case studies, the geomorphologic process from A to E above would take place at a magnitude of 100 years. Some of the observations particularly in the north of the river also suggest that the erosion process in A can go on for a very long time before a slope failure occurs, creating very deep and near vertical canyons.

Another possible effect, strengthening the creation of deep and near vertical canyons in the river bottom is soil creep. Lindskog (1983) measured soil movement in some parts of the river with high and steep river banks as high as 3 cm per year, with the movements appearing to be parallel to the slope surface. This could for example mean that in some cases where vertical erosion occurring at the bottom, there might also be soil movements at about the same rate, squeezing the slopes in towards the centre of the river. These soil movements could potentially also offset any fluvial erosion of subaquatic slopes, again strengthening the theory about the subaquatic slopes being very unaffected by direct erosion. Overall very little is known about the effects of this type of soil movement on slope stability and geomorphology.

With regard to time it is however possible to say that because of the quicker erosion rates of a landslide soil mass, the state at which most slopes would be expected to be in at any given moment is A and E. This very much coincides with observations of slope profiles in the river where the number of slope profile samples corresponding to state C is about 10-25 %.

In chapter 3 one of the distinctions between the different slope profiles is the length of the subaquatic terrace. This length is mainly caused by the horizontal erosion of the river bank, and is something that varies for each individual slope regardless of the type of slope profile as described in this theory.

It should also be noted that many of the slope profiles in the northern part of the river also are affected by the rise of water level caused by the various dam constructions in Göta River. This has resulted in areas of the river where horizontal erosion of the river bank also has caused slope profiles with the appearance of double subaquatic terraces.

## **10.5 Comparison to similar study in Italy 2009**

As mentioned in the beginning of this report there is a limited amount of this type of studies available, where river erosion has been characterized and applied geometrically onto slope profiles for the analysis of slope stability. The access to such large and accurate bathymetric datasets to perform this kind of analysis has been very interesting and advantageous indeed. One very article that was found during the

literature review carried out in this thesis work that touches on the same topic was Scesi and Gattinoni (2009). In their study they compared bathymetric values along slope profiles in the Trebbia River in Northern Italy to examine the relationship between river dynamics and slope stability to be able to predict related geohazards. Figure 56 below show one of these profiles, or cross sections, and the bathymetric values from the years 1992 and 2003. Even though the geology of the Trebbia River valley consists of a different geology, principally consisting of different types of sandstone and other soft bedrock very close to the surface, the similarities between the cross sections in Figure 56 below and for example Figure 23 in Chapter 8, Section 8.2, in this thesis (the cross sections of N\_Agnesberg\_2) are very striking. Both of the cases show distinct ridges in the middle of the river bed, with trenches on both sides, and with significant erosion in the trenches and very little or no erosion on the centre ridge. Scesi and Gattinoni (2009) also concludes that the deep fluvial erosion at the slope toe in the long run will trigger instability phenomena, although this in Trebbia River would result in rock slides rather than clay landslides.

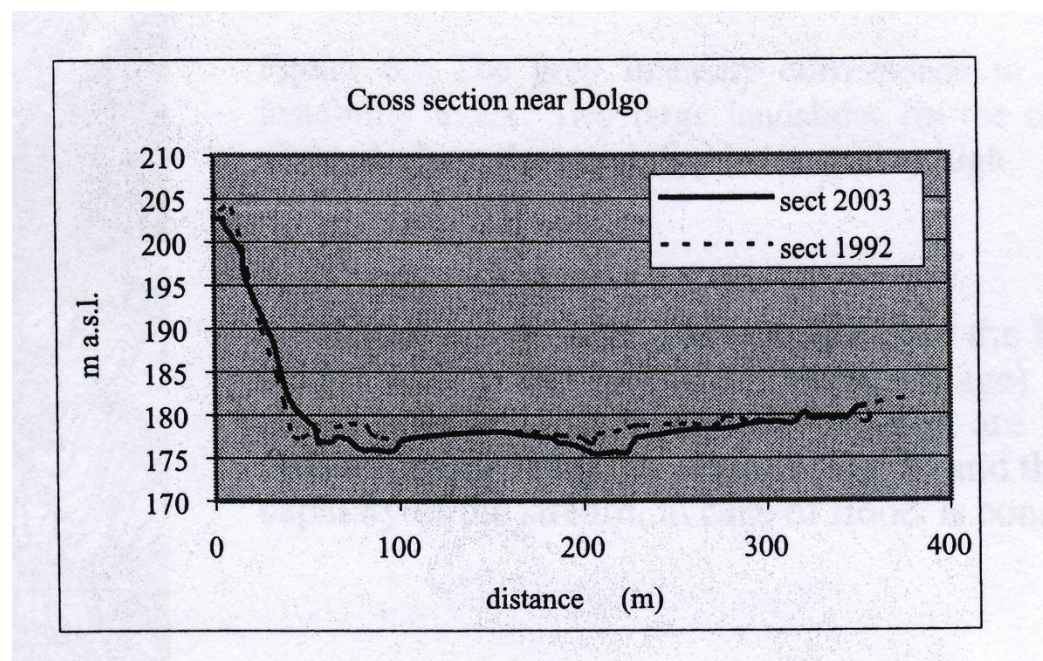


Figure 56 Comparison of bathymetric data along a slope profile between the years 2003 and 2009 in the Val Trebia River (Scesi and Gattinoni, 2009).

Although this is only one comparison, the fact that the geology and hydraulic setting of the river in Italy is fundamentally different could be an indication that the river bed erosion characterized in this thesis is not limited only to the geological settings of Göta River but is more general in nature.



# 11 Discussion

The work carried out in this thesis has perhaps raised more questions than it has answered, but a number of interesting observations have been made and some conclusions have been possible to derive from these results.

## 11.1 Erosion and GIS

This thesis has clearly shown that it is possible to use bathymetry data of this type and quality to analyse and determine how erosion and sedimentation processes. In particular when combined with other data such as backscatter, side scan etc. It has however also shown that it isn't as straight forward as one might expect, and comparing two bathymetric datasets of the same area but from different points in time needs a more in depth analysis than just taking the resulting values from a subtraction of one of the datasets from the other. This is especially the case when dealing with such a large dataset as this, covering almost 200 km of river. One has to have an insight into the geology and geomorphologic processes to be able to interpret and use the bathymetric datasets effectively and accurately.

Some of the most interesting observations of the erosion in this thesis are that the dominant erosion processes indeed seem to be corassion along trenches in the bottom. And in the other cases where clay is eroding directly due to the hydraulic shear stress, it is most likely only when the clay is very soft and loose as is the case for an old landslide mass. This casts some doubt about the possibility to determine if the bottom is subjected to erosion or sedimentation by only looking at backscatter data classification.

There are also several observations of what seem to be sub aquatic landslides that have taken place sometime between 2003 and 2009. These observations show a soil mass that simply seems to have slid down the sub aquatic slope and settled on the bottom. If that is the case, it also put some doubt on a previous assumed notion raised in connection to the Agnesberg landslide that the soil mass of a small sub aquatic landslide almost immediately is eroded and suspended in the water greatly increasing the risk of further progressive landslides.

Another interesting feature which showed up during the study of erosion was the effects of a landslide on erosion. As seen in the case study of the Ballabo landslide and the surrounding slopes a possible effect of a landslide of that magnitude is that it lowers the erosion upstream and downstream. In such a landslide where a considerable soil mass slides into the river and settles on the bottom it slows the water flow directly ahead and below it, reducing the shear stress which in turn reduces the fluvial erosion rate, especially downstream. Most of the erosion might be caused by corassion where a continuous flow of grinding soil particles, larger than clay, erodes the cohesive river bed along trenches. A landslide in such an area would effectively cut of such a process, which is dependent on this grinding material being carried and transported along the surface of the river bottom.

The great use of GIS when it comes to this type of study has however clearly been demonstrated, even though the use of GIS in this case has been rather basic. This is of course noted in the on-going work carried out at SGI, where GIS solutions and infrastructure have been under a rapid development during the last years. It promises well for the future when more and more databases will be available and integrated.

The study of erosion and sedimentation processes would for example be much helped if all bathymetric measurements continuously is stored in such a way that they are accessible to use in a GIS. And from a point of view from this kind of research, it would of course be very valuable to establish a national bathymetry database based on multibeam echo soundings. In the same way as the entire country is being scanned by LIDAR to create a national database of the land topography.

## **11.2 Slope stability calculations**

This thesis has touched on many fields and areas ranging from GIS, erosion, geology and geotechnical engineering, but the primary objective have been to study slope stability and how the factor of safety varies with erosion. Although further work and slope stability calculations would have been desirable, there are some interesting bits in the final results of the slope stability vs. erosion calculations, such as the similarities between the gradient of the decrease of the factor of safety for the full slopes.

In the results from the Ballabo calculations an interesting observation is also that a threshold value appears to exist for the erosion where the factor of safety suddenly decreases very rapidly for a sub aquatic slope. In that case the threshold also means that the sub aquatic slope suddenly becomes more critical than the full slope, and again pointing out that awareness of both the sub aquatic slope and full slope is important. This shows the importance of being aware of the simple fact that there are both a sub aquatic slope and a full slope that one has to take into consideration when performing geotechnical evaluations of these types of slopes. Not least when it comes to predictions of how the slope stability might change with time due to changes in climate etc. Changes of the factor of safety for a sub aquatic slope do not follow the corresponding change for a full slope.

## **11.3 Preventive measures**

It is clearly shown that erosion will be a cause for concern in the coming century, when it comes to slope stability along Göta River. This notion of course nothing new, but it has through the case study in this thesis shown very specifically what the effects might be even without taking other matters into consideration such as an increased pore pressure or increase of river flow.

Practically this means that preventive measures will likely have to be undertaken to prevent this type of erosion from undermining the slope stability. This is neither a new notion or a new idea, the on-going extensive Göta River commission at SGI will result in many specifics with regard to this, and as is described in Chapter 8 about Agnesberg many measures has already been taken.

These measures consisted of placing geosynthetics, rocks and other reinforcements along the bottom of Agnesberg stretching hundreds of meters in both north and south direction. Based on the work in this thesis, and in particular the study of erosion, one alternative possibility and approach to bottom erosion protection might be to sort of mimic the effects of the old Ballabo landslide. Particularly in Göta River south of Lilla Edet the dominating type of bottom erosion seem to occur along trenches through where coarse material is transported and causes corrosion of the clay. Because of the nature of this type of erosion it should be very sensitive to disturbances

of those established trenches and pathways, which seems to be the case after the Ballabo landslide, which effectively seem to have cut off the erosion processes downstream. The idea would be that placing some form of erosion protection at points along a stretch instead of a continuous placement of material along the stretch might give a very good result preventing erosion. The measurements in these points could be anything from sheet pile walls to gravel or rock. The idea is that the effect would be a decrease or total stop of corrosion in between these points, and the key issue is that the costs would be much less than placing a continuous protection along the same stretch. The effects of these two types of measurements are of course different and one is not perhaps intended to replace the other, but it is an idea of a concept that could perhaps save money and be viable as more and more detailed data of the river bottom becomes available.

## 11.4 Quantification of erosion

As noticed this thesis spans many fields, and it would have been possible to spend many hours working on any one of these fields with regard to the subject of this thesis. So a natural suggestion for future work would be just that.

When it comes to the study of erosion by using bathymetry and other data in GIS, there is room for much more detailed analysis and evaluations of uncertainties in the data but perhaps even more so for statistical analysis of the features in the data. But also to analyse different correlations both between geological features and between GIS data using more rigorous statistical methods would give a more complete understanding.

It would also be desirable to have more quantity, i.e. to simply do more of the same. Performing more studies of specific slopes in the same manner as was done with the Agnseberg and Ballabo slopes in this thesis. Although the results in this thesis showed some tendencies in how the factor of safety varies with erosion, it is of great interest to have the results from many more cases, something which there simply was no time for within the scope of this master thesis project. The study of other rivers and water bodies would of course also be a necessity for more general results with regard to erosion and slope stability.

When it comes to erosion many tries have been made to quantify erosion through bathymetry measurements, not least by Sundborg and Norrman in the 1960:s. They even went as far as marking sections along the river where they had performed echo soundings with bronze plates so they could be used as references for future work. The ball seems to have been picked up and lost repeatedly over the decades since, with no coherent plan to continue or follow up these types of investigations in a structured and organized manner. As a consequence the work and research on erosion now being undertaken in the Göta River project in some ways have had to start from the beginning again, outlining new plans for the future that are very similar to the plans already outlined 50 years ago.

There is also a large archive of photographic material that was part of Sundborg and Norrmans investigation stored at the Institution of Geography at Uppsala University. These photographs were taken with the purpose of using photogrammetric methods to quantify the erosion of the bank slopes as well as mass calculations of potential landslides. The camera locations were carefully marked with iron nails in the terrain along with documentation about the camera angles. New technology has of course

made much of this obsolete, but it shows the importance of not letting current work be readily available for analysis in the future.

Therefore one important recommendation when it comes to the continued research on erosion in Göta River, or any other location where similar studies is or will be conducted, is that great length is taken to create a framework and documentation that ensures that the “ball” is not dropped in the future. This framework should include measures to keep data updated with regards to data formats so it always can be easily accessed and understood in the future. The advancements of computers and geographical information systems and databases have of course made this task much more manageable, and it should be fully utilized.

## 12 References

- Althage, J. (2010). *Ship-Induced Waves and Sediment Transport in Göta River, Sweden*. M.Sc. Thesis. Department of Building and Environmental Technology, Lund University, Lund.
- Andersson, H., Ottosson, E., Sällfors, G. (1999): *Skredet i Ballabo, Västerlanda*. Statens geotekniska institut, Rapport 57, Linköping.
- Andersson, M., Lundström, K., Rankka, W., Rydell, B. (2008): *Erosion och sedimenttransport i vattendrag*. Statens geotekniska institut, Varia 592, Linköping.
- Drobic, A. (2011): *Impact on the East Ormo Tower's stability due to the increase in wind load*. M.Sc. Thesis. Department of Civil and Environmental Engineering, Chalmers University of Technology, Göteborg.
- Geography Department of Lord Wandsworth College (2011).
- GEO-SLOPE International Ltd (2008): *Stability Modeling with SLOPE/W 2007- An Engineering Methodology, Fourth Edition*, GEO-SLOPE International Ltd, Calgary, Alberta, Canada.
- Göta älvs Vattenvårdförbund (2006): *Fakta om Göta älv- En beskrivning av Göta älv och dess omgivning 2005*. Göta älvs Vattenvårdsförbund, Göteborg.
- Hedvall, T. (2008): *Terrängmodellering Göta Älv*. Vattenfall Power Consultant AB, Göteborg.
- Hultén, C., Andersson-Sköld, Y., Ottosson, E., Edstam, T., Johansson, Å. (2007): Case studies of landslide risk due to climate change in Sweden. *Landslide and Climate Change*, Taylor & Francis Group, London, 2007, pp. 149-157.
- Hultén, C., Edstam, T., Arvidsson, O., Nilsson, G. (2006): *Geotekniska förutsättningar för ökad tappning från Väneren till Göta älv*. Statens geotekniska institut, Varia 565, Linköping, Sweden, 2006
- IVA Skredkommissionen (1995): *Anvisningar för släntstabilitetsutredningar*, Ingenjörsvetenskapsakademien, Rapport 3:95, Linköping.
- Jenssen, L., Tesaker, E. (2009): *Veileder for dimensjonering av erosjonssikringer av stein*. Norges vassdrags- og energidirektorat, Veileder nr 4, Oslo, November 2009.
- Klingberg, F., Påsse, T., Levander, J. (2006): *K43. Bottenförhållanden och geologisk utveckling i Göta älv*. Sveriges Geologiska Undersökning, Göteborg.
- Klingberg, F. (2010): *Bottenförhållanden i Göta Älv: SGU-rapport 2010:7*. Sveriges Geologiska Undersökning, Göteborg.
- Larsson, R., Ottosson, E., Sällfors, G. (1994): *Agnesbergsskredet*. Statens geotekniska institut, Rapport 44, Linköping.
- Lawrence, W. G. (1995): *Soil Freeze-Thaw Effects on Bank Erodibility and Stability*. US Army Corps of Engineers, Cold Regions Research & Engineering Laboratory, Hanover, New Hampshire, USA.
- Lindskog, G. (1983): Brief report of the investigation of the slope stability along the river in Göta River valley. Statens Geotekniska Institut, Linköping.
- Marin Miljöanalys AB (2009): *Rapport Sjömätning; Göta älv, Nordre älv. SGI U304-0909*. Marin Miljöanalys AB 09-12-22, Göteborg.

Marin Miljöanalys AB (2010): *Rapport Ytgeologi; Göta älv, Nordre älv. SGI U304-0909*. Marin Miljöanalys AB 09-12-22, Göteborg.

Marin Mätteknik AB (2004): *Sjömätning i Göta älv*. Marin Mätteknik AB, Statens Geotekniska Institut- Projekt nr: 41005, Göteborg.

Rankka, K., Rydell, B. (2005): *Erosion och översvämningar- Underlag för handlingsplan för att förutse och förebygga naturolyckor i Sverige vid förändrat klimat- Deluppdrag 2*. Statens geotekniska institut, Varia 560:2, Linköping.

Sandebring, H., Ottosson, E. (1994). *Agnesbergsskredet. Skredförebyggande åtgärder. Agnesbergsutredningen*. Statens geotekniska institut, Rapport 44, Linköping.

Scesi, L., Gattinoni, P. (2009): Study of the interactions between rivers dynamic and slope stability for geohazard prediction: A case in Val Trebbia (Northern Italy). *International symposium on prediction and simulation methods for geohazard mitigation*, Kyoto, 25-27 May, 2009, pp 241-246.

SGI (2011). *Comission Göta River*. <

[http://www.swedgeo.se/templates/SGIStandardPage\\_\\_\\_\\_1400.aspx?epslanguage=EN](http://www.swedgeo.se/templates/SGIStandardPage____1400.aspx?epslanguage=EN)> Available 03.10.2011.

Sundborg, Å., Norrman, J. (1963): *Göta Älv hydrologi och morfologi- med särskild hänsyn till erosionsprocesserna*. Statens Geologiska Undersökning, Avhandlingar och uppsatser I 4:0 Nr 43, Stockholm, 1963.

Sällfors, G. (1994). *Slänters Stabilitet*. Kurslitteratur L:32, Department of Civil and Environmental Engineering, Chalmers University of Technology, Göteborg

Williams, D.R., Romeril, P.M., Mitchel, R.J. (1979): Riverbank erosion and recession in the Ottawa area. *Canadian Geotechnical Journal*, Vol. 16, No. 4, 1979, pp. 641-650.

### **Verbal and written communication:**

Persson, H. (member of the erosion expert group at SGI) & Tengbert, H. (Sjöfartsverket) (2010). Telephone and e-mail correspondence and discussions with regard to the 2003 and 2009 bathymetry data.

Persson, H. (member of the erosion expert group at SGI) (2011). Discussions with regard to the hydraulic shear stress dataset and general discussions with regard to the work in this thesis.

### **Figures:**

Geography Department of Lord Wandsworth College (2011). *Hjulström curve*. <  
[http://dlgb.files.wordpress.com/2008/09/hjulstrom\\_curve\\_task.jpg](http://dlgb.files.wordpress.com/2008/09/hjulstrom_curve_task.jpg) > Available 03.10.2011.

SGI (2011). *Vad är ett ras?*. <

[http://www.swedgeo.se/templates/SGIStandardPage\\_\\_\\_\\_763.aspx?epslanguage=S](http://www.swedgeo.se/templates/SGIStandardPage____763.aspx?epslanguage=S)  
V > Available 03.10.2011.

Slope/W (2011). Daniel Millet; generated using the software 'Slope/W 2007'. Göteborg.

All additional figures in this report that are not otherwise referenced are created by the author of this thesis Daniel Millet.

**Maps:**

Agnesberg, Sweden (2011). Scale undetermined; Daniel Millet; “using ‘Google Maps’”. < <http://maps.google.com/maps?q=agnesberg&oe=utf-8&rls=org.mozilla:sv-SE:official&client=firefox-a&um=1&ie=UTF-8&hl=en&sa=N&tab=wl> > (2011.10.03).

ArcGIS (2011). Scales undetermined; Daniel Millet; “using ‘ArcView’ and internal databases at SGI, including wms © bakgrundskartor Lantmäteriet (10.2010-06.2011).